AD-A080 588 SRI INTERNATIONAL MENLO PARK CA F/G 1/2
DEVELOPMENT OF WIND SHEAR MODELS AND DETERMINATION OF WIND SHEA--ETC(U)
JAN 78 D W ELLIS, M G KEENAN DOT-FA75WA-3650
UNCLASSIFIED FAA-RD-79-119 NL

| OF |
AD A080588

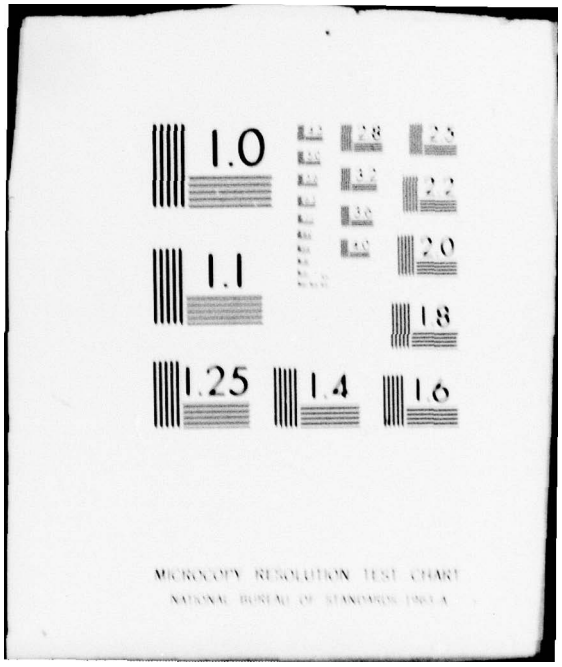
1.0
1.1
1.25
1.4
1.6
2.8
2.5
2.2
2.0
1.8
MICROCOPY RESOLUTION TEST CHART
NATIONAL BUREAU OF STANDARDS 1963-A

Report No. FAA-RD-79-119

LEVEL II

DEVELOPMENT OF WIND SHEAR MODELS AND DETERMINATION OF WIND SHEAR HAZARDS

ALL-WEATHER LANDING SYSTEMS, ENGINEERING SERVICES SUPPORT PROJECT, TASK 2

D. W. Ellis, M. G. Keenan

SRI INTERNATIONAL, MENLO PARK, CALIFORNIA 94025

January 1978

Interim Report

Document is available to the U.S. public through the National Technical Information Service, Springfield, Virginia 22161.

Prepared for

U.S. DEPARTMENT OF TRANSPORTATION
FEDERAL AVIATION ADMINISTRATION
Systems Research & Development Service
Washington, D.C. 20590

NOTICE

This document is disseminated under the sponsorship of the Department of Transportation in the interest of information exchange. The United States Government assumes no liability for its contents or use thereof.

1. Report No.	2. Government Accession No.	3. Recipient's Catalog No.
FAA-RD-79-119		

4. Title and Subtitle
DEVELOPMENT OF WIND SHEAR MODELS AND DETERMINATION OF WIND SHEAR HAZARDS

5. Report Date
January 1978

6. Performing Organization Code

8. Performing Organization Report No.
SRI Project 4364

7. Author(s)
D. W. Ellis, M. G. Keenan

9. Performing Organization Name and Address
SRI International
333 Ravenswood Avenue
Menlo Park, California 94025

10. Work Unit No. (TRAIS)

11. Contract or Grant No.
DOT-FA75WA-3650

13. Type of Report and Period Covered
Interim Report.
April [redacted] — November [redacted] 1977

12. Sponsoring Agency Name and Address
U. S. Department of Transportation
Federal Aviation Administration
Systems Research and Development Service
Washington D.C. 20590

14. Sponsoring Agency Code
FAA/ARD-743

15. Supplementary Notes
Prepared on ALL-WEATHER LANDING SYSTEMS, Engineering Services Support, Project 4364, Phase 2

16. Abstract

This report documents work concerned with the specification of a large set of wind profiles for use in piloted simulator tests concerning low-level wind shear encountered during approach, landing, takeoff, and climbout. In addition, candidate standard wind profiles for use in training and system qualification are recommended.

Measured and mathematically modeled wind data represented as a function of both aircraft altitude and distance are "flown" with a fast-time computer model piloted by an idealized controller. The wind models and the runway position relative to each wind field are systematically varied to produce a number of different wind profiles. Based on aeronautical system performance in the computer, relative comparisons of wind profile severity are made, potentially hazardous wind profiles are identified, and their relative severity is designated as "low," "moderate," or "high" for purposes of piloted simulator tests. Piloted simulation results are used to verify the severity ratings. Effects of wind shear on aircraft are illustrated using simplified examples and then correlated with wind profile characteristics. Wind profile design techniques and implementation methods are discussed, and a set of candidate standard wind profiles is recommended.

The results of the wind shear hazard determination work indicate that the severity of a wind shear encounter is highly dependent on the position and alignment of the approach path with respect to the wind field and on the timing of the encounter. Another conclusion is that both wind shear in the vertical wind component and wind shear in the longitudinal wind component can produce a hazardous condition. High severity wind shear is also found to be hazardous on takeoff.

17. Key Words	18. Distribution Statement
Wind shear, Aircraft safety, Aircraft weather, Thunderstorm gust front, Frontal wind shear, Aircraft approach and landing	Document is available to the U.S. Public through the National Technical Information Service, Springfield, Virginia, 22161.

19. Security Classif. (of this report)	20. Security Classif. (of this page)	21. No. of Pages	22. Price
UNCLASSIFIED	UNCLASSIFIED	95	

Form DOT F 1700.7 (8-72) Reproduction of completed page authorized

410 281

METRIC CONVERSION FACTORS

Approximate Conversions to Metric Measures

Symbol	When You Know	Multiply by	To Find	Symbol
		LENGTH		
in	inches	*2.5	centimeters	cm
ft	feet	30	centimeters	cm
yd	yards	0.9	meters	m
mi	miles	1.6	kilometers	km
		AREA		
in^2	square inches	6.5	square centimeters	cm^2
ft^2	square feet	0.09	square meters	m^2
yd^2	square yards	0.8	square meters	m^2
mi^2	square miles	2.6	square kilometers	km^2
	acres	0.4	hectares	ha
		MASS (weight)		
oz	ounces	28	grams	g
lb	pounds	0.45	kilograms	kg
	short tons (2000 lb)	0.9	tonnes	t
		VOLUME		
tsp	teaspoons	5	milliliters	ml
Tbsp	tablespoons	15	milliliters	ml
fl oz	fluid ounces	30	milliliters	ml
c	cups	0.24	liters	l
pt	pints	0.47	liters	l
qt	quarts	0.95	liters	l
gal	gallons	3.8	liters	l
ft^3	cubic feet	0.03	cubic meters	m^3
yd^3	cubic yards	0.76	cubic meters	m^3
		TEMPERATURE (exact)		
°F	Fahrenheit temperature	5/9 (after subtracting 32)	Celsius temperature	°C

*1 in = 2.54 (exactly). For other exact conversions and more detailed tables, see NBS Misc. Publ. 286, Units of Weights and Measures, Price $2.25, SD Catalog No. C13.10:286.

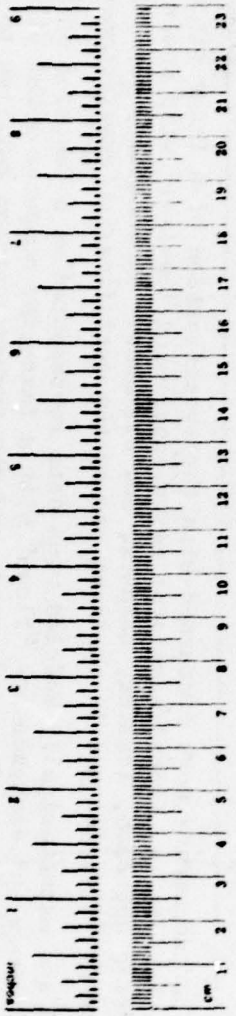

Approximate Conversions from Metric Measures

Symbol	When You Know	Multiply by	To Find	Symbol
		LENGTH		
mm	millimeters	0.04	inches	in
cm	centimeters	0.4	inches	in
m	meters	3.3	feet	ft
m	meters	1.1	yards	yd
km	kilometers	0.6	miles	mi
		AREA		
cm^2	square centimeters	0.16	square inches	in^2
m^2	square meters	1.2	square yards	yd^2
km^2	square kilometers	0.4	square miles	mi^2
ha	hectares (10,000 m^2)	2.5	acres	
		MASS (weight)		
g	grams	0.035	ounces	oz
kg	kilograms	2.2	pounds	lb
t	tonnes (1000 kg)	1.1	short tons	
		VOLUME		
ml	milliliters	0.03	fluid ounces	fl oz
l	liters	2.1	pints	pt
l	liters	1.06	quarts	qt
l	liters	0.26	gallons	gal
m^3	cubic meters	35	cubic feet	ft^3
m^3	cubic meters	1.3	cubic yards	yd^3
		TEMPERATURE (exact)		
°C	Celsius temperature	9/5 (then add 32)	Fahrenheit temperature	°F

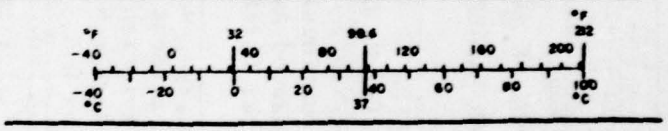

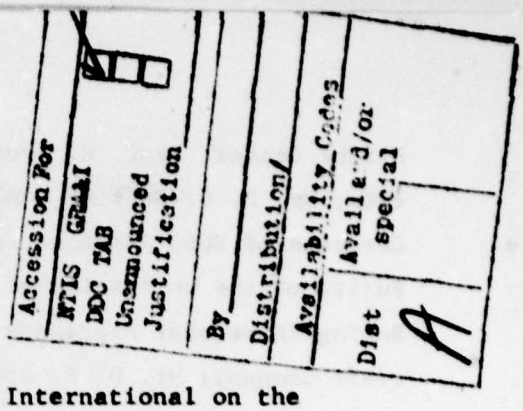

PREFACE

This interim report describes the work of SRI International on the development of wind shear models and the determination of wind shear hazards as a part of Task 2 of the All-Weather Landing Systems Engineering Support contract (DOT FA75WA-3650). Phases 1 and 2 of Task 2 began a series of piloted aircraft simulator experiments in which candidate aiding concepts for coping with low-level wind shear were evaluated using four different wind profiles representing four respective meteorological wind conditions. One objective of this subtask on wind models and hazard definition was to develop an expanded set of wind profiles for use in next-stage Task 2 piloted simulations using B-727 and DC-10 aircraft models. Another objective was to develop a representative set of candidate standard profiles with sufficient severity to provide for system qualification. The sponsoring organizations for this project are FAA Wind Shear Program Office and ARD-740; the Technical Monitor is Mr. W. J. Cox.

The authors are grateful to the many people who have contributed to this study. While a complete list of contributors would be too lengthy, we wish to thank Mr. W. J. Cox, Lt. Col. L. W. Wood and Mr. H. W. Schlickenmaier of the FAA for many helpful discussions and creative suggestions; Mr. J. D. McDonnell and Mr. P. L. Jernigan of Douglas Aircraft Company for data on the DC-10 aircraft and information on aircraft simulation design; Mr. J. W. Kerrigan and Mr. M. Hazen of Boeing Commercial Aircraft Company for data on the B-727 aircraft; and Mr. J. L. Foster and Mr. L. Miller of Collins Radio Group, Rockwell International, for information of flight control systems.

Most of the wind data used in this project were contributed by other researchers and meteorologists. We appreciate the effort entailed in supplying this information and enjoyed many informative discussions regarding specific meteorological conditions. We especially thank the following contributors: Mr. D. W. Camp and Dr. G. H. Fichtl of NASA Marshall Space

Flight Center; Prof. W. Frost of the University of Tennessee Space Institute, Mr. R. C. Goff of NOAA National Severe Storms Laboratory and Dr. F. Caracena of NOAA Atmospheric Physics and Chemistry Laboratory; Prof. T. Fujita of the University of Chicago; Dr. A. Roosme and Mr. N. M. Barr of Boeing Commercial Airplance Company, Mr. W. A. Stephens of Douglas Aircraft Company; Mr. D. F. Sowa, Northwest Airlines; and Mr. F. G. Coons of the FAA. Mr. W. Viezee, Senior Research Meteorologist, of SRI contributed several of the wind models and much helpful advice.

CONTENTS

CONTENTS (Con't)

ILLUSTRATIONS

TABLES

TABLES (Con't)

I INTRODUCTION

A. Program Objectives and Approach

Wind shear may be described as a change in wind magnitude or direction over a relatively small space; for example, a change in a headwind from 30 knots at 300-feet altitude to 10 knots at 150 feet. Complex and rapidly changing wind conditions close to the ground create significant hazards to low-level flights. Wind shear has been cited as a contributory factor in aviation accidents, thus the effects of wind shear on aircraft approach, landing, and takeoff have been the subject of several studies and experiments.

The work documented in this report is part of Task 2 of the All-Weather Landing Systems Engineering Support contract (DOT FA75WA-3650) for the FAA. The objectives of this subtask were (1) to specify wind profiles for piloted simulator tests incorporating wind shear, and (2) to recommend candidate standard wind profiles with sufficient severity to provide for system qualification.

The project began by identifying and specifying meteorological wind conditions in the terminal area environment that were known to produce significant wind shear. Wind profiles based on these conditions were then generated and "flown" on a general-purpose computing facility in fast time, using B-727 and DC-10 aerodynamic models with an idealized controller as pilot. The runway position relative to the wind field and, where applicable, the wind model parameterization were systematically varied to produce a number of different wind profiles. Relative comparisons of wind profile severity were made on the basis of aeronautical system performance in the computer, and the results correlated with the wind profile characteristics. Emphasis was placed on defining how and to what extent the aeronautical system was affected by wind shear, and then relating these findings to "real world" wind conditions. The results of the work were checked against the results of the subsequent B-727 piloted simulator

tests. The analysis method is described schematically in Figure 1.

Initial stages of this project included the specification of candidate wind profiles from both measured and mathematical models of selected meteorological conditions. This task relied heavily on previous work and the support of a number of contributors. A list of the wind data contributors is given in the Preface to this report.

B. Organization of Report

This report is divided into seven sections. Section II defines the meteorological phenomena that are considered to produce the wind shears evaluated in this project. Section III describes the computer model design. Section IV uses the computer model with simplified wind encounters to illustrate some of the observed effects of wind shear on aircraft. Section V describes the techniques used to measure aeronautical system performance, assess the relative wind shear severity, and specify the wind profiles used in the piloted simulations. Section VI is dedicated to the specification of candidate standard profiles. Section VII states our conclusions and recommendations, although throughout the report we have tried to state our results in context with the discussions within each section.

Wind profiles resulting from this work, various technical details, and supporting documents are given in Appendices A through D.

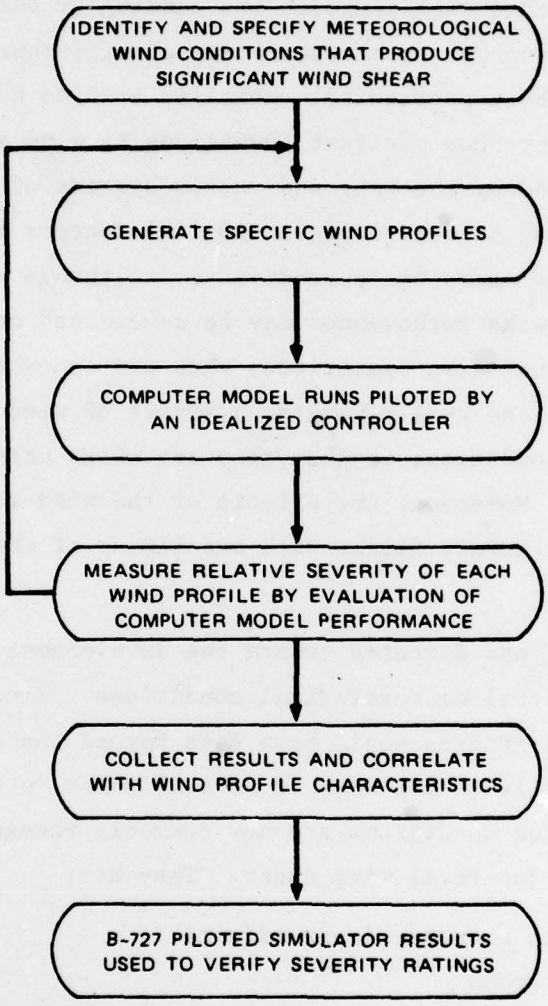

FIGURE 1 ANALYSIS METHOD

II SOURCES OF WIND SHEAR IN THE TERMINAL AREA

Wind shear encountered during approach and landing or during takeoff and climbout may result from one or a combination of different causes. Wind disturbances caused by topographical anomalies such as buildings, trees, mountains, or valleys can manifest themselves as wind shear. Wind shear may also be generated by the wake and vortex systems of other aircraft. And, wind shear may be due to meteorological factors arising from local weather phenomena or atmospheric conditions. Although wind shears caused by topography and wake turbulences may be severe and certainly impose constraints on terminal area operations, they are somewhat predictable. On the other hand, the really hazardous aspect of wind shears arising from meteorological conditions is that they are often neither predictable nor easy to detect. Moreover, the effects of the wind shear may be highly dependent on the aircraft flight path and timing of the wind shear encounter.

Work on this project was directed toward the development of a set of wind profiles based on actual meteorological conditions. Since engagement in lengthy meteorological studies would have been beyond the scope of the study, SRI has drawn heavily on the work of several other investigators. Three broad classes of wind conditions are now commonly recognized as significant producers of low-level wind shear. They are:

(1) Atmospheric boundary layer effects

(2) Frontal systems

(3) Thunderstorms

In the following paragraphs, a brief summary of the principal features of each class will be given, followed by some specific examples of profiles considered for evaluation in this study.

A. Atmospheric Boundary Layer Effects

The atmospheric boundary layer is usually defined as the region below 3,300 feet (1,000 m). Within this region the winds are influenced by solar heating and surface friction. In daylight, solar heating of the ground results in the transfer of thermal energy to the air adjacent to the ground, making it more buoyant. The buoyancy forces act to move parcels of air vertically (turbulent mixing). The mean wind speed at any given altitude in a turbulent environment will depend on the amount of air transferred to that altitude from regions having differing wind speeds. Mixing, therefore, affects the shear rate by modifying the mean wind variation with altitude. At night the reverse takes place; i.e., thermal energy is transferred from air to the cooler ground, resulting in negative buoyancy forces. Under negative buoyancy forces little or no mixing occurs, and the boundary layer tends to become stratified. Strong shears are often associated with this condition because the various layers tend to move independently, with stronger winds occurring in the top layers that are relatively decoupled from any surface retarding forces.

In the region between 500 and 3,300 feet (150 and 1,000 m), a transition occurs between the surface wind and the winds aloft. The latter are influenced by synoptic scale pressure, temperature gradients, and Coriolis forces. Since the winds aloft are not generally aligned with the surface winds, a turning of the wind vector commonly occurs in this region. The amount of turning varies, but in most cases can be between 10 and 50 degrees.

A frequently used boundary layer mathematical model has the following general form:[1*]

$$W_u = \frac{U^*}{k} \left[\ln\left(\frac{Z}{Z_o}\right) + \Psi\left(\frac{Z}{L}\right)\right] \quad ; \tag{1}$$

$$W_v = 0 \quad ; \tag{2}$$

$$W_w = 0 \quad ; \tag{3}$$

[1*] Superscripts denote references listed at the end of the report.

where W_u, W_v, and W_w = the wind velocity components

U^* = surface friction velocity

k = Von Karman's constant, ≈ 0.4

Z = altitude above reference level

Z_o = surface roughness length

L = Monin-Obuhov stability length

ψ = empiricially derived function of Z/L

Boundary layer winds can be broken down into the following categories:

(1) Unstable--Unstable winds are usually associated with daytime conditions (hot afternoons). Heat conducted from ground to air causes much turbulence and mixing. Winds tend to be more uniform with altitude; wind shears are mild.

(2) Neutral--Neutral winds occur in daytime when the thermal energy transfer to air from ground is moderate. Vertical movement resulting from buoyancy forces is small compared with the horizontal movement. Moderate mixing and turbulence are typical. Wind speed and shear rates are greater than those for unstable winds.

(3) Stable--Stable winds are usually associated with nighttime conditions. Heat transferred to ground from air results in negative buoyancy forces and very little mixing. Inversion layers may occur below 1,000 feet; shear rates are higher than those for neutral and unstable winds.

(4) Very stable--Very stable winds result from stable conditions in which layers become decoupled. Frictional retardation of the wind is so low that a high-speed wind (nighttime low-level jet) commonly occurs just above the

inversion layer. This condition is characterized by potentially large shear rates.

Examples from the above categories are shown in Figure 2. In Figure 2(a) values of wind as a function of altitude were computed from Equation 1. Identical values of surface roughness (Z_o) and surface friction velocity (U*) were used to illustrate the differences in unstable, neutral, and stable cases over relatively smooth terrain, such as grass or prairie land. The function $\Psi(\frac{Z}{L})$ varies with the stability length L. Values of L

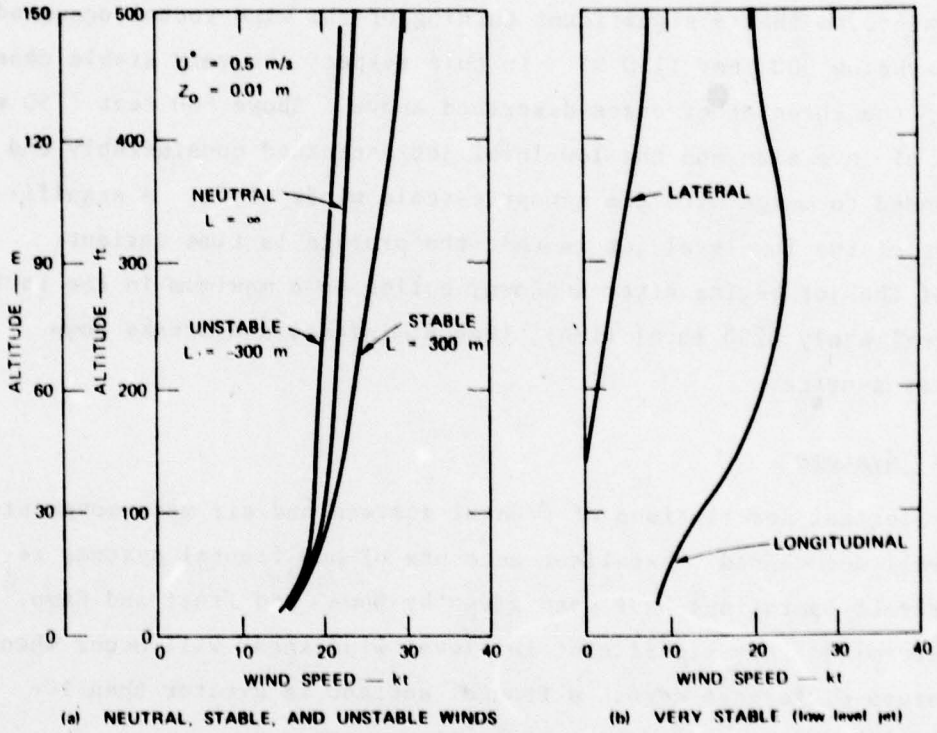

FIGURE 2 WIND PROFILES FROM ATMOSPHERIC BOUNDARY LAYER EFFECTS

are normally such that $\frac{Z}{L}$ and $\Psi(\frac{Z}{L})$ take on small negative values for the unstable case and small positive values for the stable case. In the neutral case $L = \infty$ and $\Psi(\frac{Z}{L}) = 0$, reducing Equation 1 to a simple logarithmic function. It should be noted that a wide range of values of the parameters L, U*, and Z_o can be realized; thus the wind profiles shown in the figure

are examples from a wide range of possible wind profiles.* The significant features of boundary layer wind shears are: (1) wind speed variation with altitude above 500 feet (150 m) is small, and (2) the stable atmosphere has greater shear rates than the neutral atmosphere over similar terrain.

An example of a very stable wind condition or low-level jet is shown in Figure 2(b). This graph of lateral and longitudinal winds was derived from Cedar Hill Tower measurements.[2] The profile shown here is typical of a moderate low-level jet occurring at night and shows a maximum wind at an altitude of about 330 feet (100 m). It is evident from the graph that the crosswind component has a different altitude dependence than the longitudinal component, so that a significant turning of the wind vector occurred at altitudes below 500 feet (150 m). In this respect the very stable case differs from the three other cases described above. Above 500 feet (150 m) the effects of inversion and the low-level jet decreased considerably and the wind tended to merge with the synoptic-scale winds aloft. A significant feature of the low-level jet is that the profile is time variant. Formation of the jet begins after sundown, builds to a maximum in the early hours (approximately 0200 local time), then diminishes and breaks down shortly after sunrise.

B. Frontal Systems

Meteorological descriptions of frontal surface and air mass movements have been well documented. Excellent accounts of how frontal systems relate to aircraft operations have been given by Sowa[3] and Frost and Camp.[4] Sowa has determined that significant low-level wind shear will occur when the temperature difference across a frontal surface is greater than 10-degrees F or the front is moving at 30 knots or more.

Due to the characteristically sloping frontal surface, wind direction changes will occur as a function of altitude and distance. Advancing cold fronts tend to incline backward away from the warm air mass; thus a directional wind shear may exist above a point on the surface for as long

*A comprehensive computer program that permits calculation of these profiles has been developed by W. Frost of U. Tennessee Space Institute.

as three hours after passage of the cold front. Warm fronts incline forward toward the direction of the cooler air mass; thus directional shear above a given point will precede passage of a warm front by as much as six hours and will cease when the front has passed. For aircraft attempting to land these effects can produce a variety of wind shear profiles, depending on the runway alignment and position relative to the front.

An example of a cold front creating wind shear in a landing situation is shown in Figure 3.* Paths A and B represent 3-degree glide paths through the wind field. The runway lies in the plane of the figure with the glide path intercept point (GPIP) for each path just outside the illustrated portion of the wind field. Wind profiles along paths A and B are shown in Figure 4. These profiles define quantitatively details that are qualitatively illustrated by the streamlines in Figure 3. For path A tailwind-to-headwind shear occurs from 500- to 300-feet altitude; for path B the shear occurs at lower altitudes. Although the two wind profiles came from the same wind field, they vary greatly from one another because they were measured along different flight paths.

By varying the runway alignment and the location of the GPIP relative to known wind fields, such as the one in Figure 3, a number of wind profiles are possible. We used this method to generate several shears for evaluation. Frontal shear data were obtained from aircraft accident reports (NTSB) and other sources.

C. Thunderstorms

The dynamic nature of thunderstorms makes this class of wind profiles the most difficult to predict and to model. Much effort has been devoted to gaining a better understanding of thunderstorm mechanics by several organizations, notably, National Oceanic and Atmospheric Administration (NOAA), National Severe Storms Laboratory (NSSL), National Aeronautics and Space Administration (NASA), and the University of Chicago Department of Geophysical Sciences.

---

*Basic wind field data for Figure 3 are from Goff.[5]

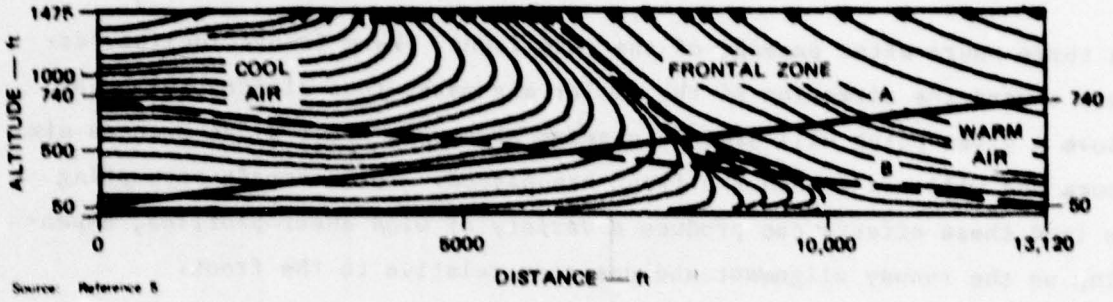

Source: Reference 5

FIGURE 3 FRONTAL WIND FIELD

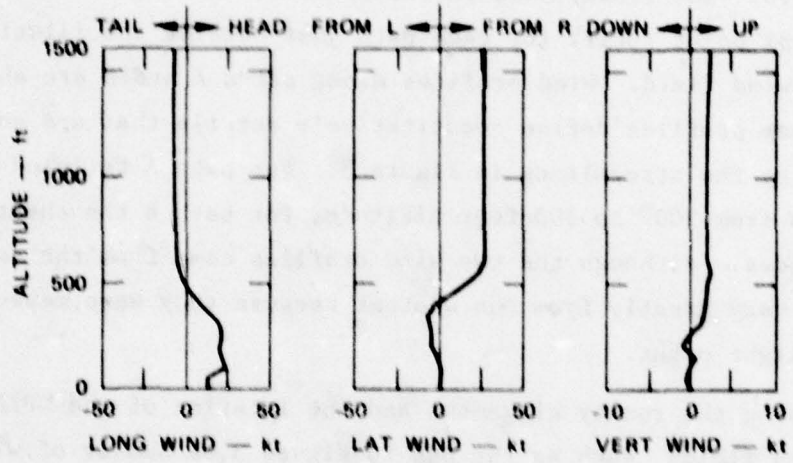

PROFILE A

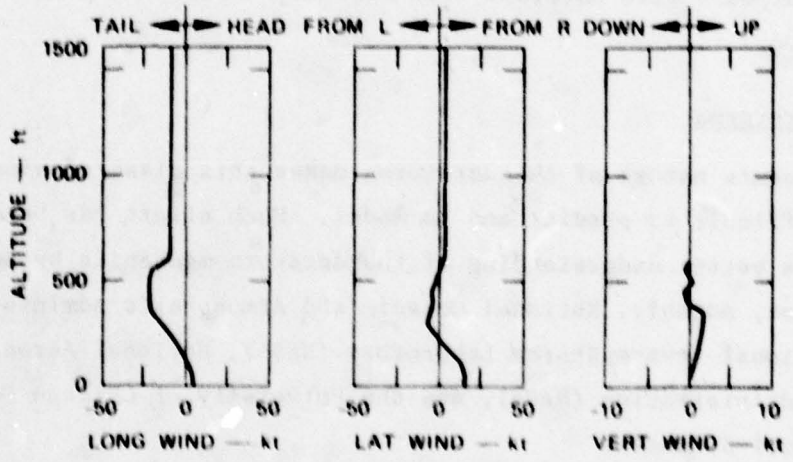

PROFILE B

FIGURE 4 FRONTAL WIND PROFILES

A considerable amount of data has been gathered from tall towers, such as the NSSL tower at Norman, Oklahoma, that have been instrumented to measure wind speed and direction, temperature, pressure, and vertical winds. Additional data have been obtained from ground sensors, Doppler radar, and aircraft and satellite pictures. These data clearly show that the structure of thunderstorms undergoes continual changes in stages that can be broadly defined as formative, mature, dissipating, and final. Common to all stages are updraft, downdraft, outflow, and gust-front activity, all of which constitute a potential hazard to landing operations. Fujita and Caracena[6] have investigated three aviation accidents resulting from encounters with very intense downdraft/outflow activity during the passage of thunderstorm cells in the vicinity of airports.

In a typical mature thunderstorm cell moist air cooled by evaporation descends until it is forced outward (outflow) by the ground. This outflow tends to be concentrated in the direction of cell movement. The rapidly moving cool air, slowed somewhat by drag at the surface, constitutes a small-scale cold front, commonly called a "gust front." The gust front advances at speeds up to 40 mph and can precede the storm center by as much as 10 miles. Warm air ahead of this gust front is forced to rise above the frontal surface, which is inclined toward the cooler air mass at about 45- to 75-degrees. The storm cell is replenished by warm dry air entering from the sides at tropospheric level. In a small percentage of storms an additional source of air is supplied from the stratosphere above the anvil top, causing very intense downdrafts in the cell known as "downbursts."[6,7]

Thunderstorms produce moving, dynamically changing wind fields of complex form. Strong updraft/downdraft shears and headwind/tailwind shears are inherent in their wind field and often occur simultaneously. Although the speed of movement of the storm cell is small enough to be considered stationary relative to the speed of a landing aircraft, it is sufficiently fast to present an entirely different set of wind parameters to each aircraft in a landing sequence.[7] The time of encounter must be considered a crucial factor in evaluating encounters with thunderstorm wind shear. Other important factors include runway orientation

and position of the GPIP relative to the storm center, the number of cells in the vicinity, and the maturity and intensity of each cell.

A wind field from a thunderstorm in its mature stage[5] is shown in Figure 5. A complex downdraft is located at a distance of about 3,000 feet. The cold air outflow from this downdraft proceeds outward to the cool-warm air boundary (gust front) at about 16,000 feet. The sloping front and warm air updraft described earlier are also evident in the figure. To illustrate the wind profile variation with distance, glide paths A and B are superimposed with the GPIP at a distance of 2,500 and and 9,000 feet, respectively. Figure 6 shows profiles of wind along these paths. Profile A shows the tailwind-to-headwind shear caused by traversing the gust front at about 650-feet altitude. Coinciding with this is the increase in updraft strength, which peaks at just above 500-feet altitude. Thereafter, a more or less steady headwind with a very slight downdraft is encountered by the aircraft down to about 150 feet. At that level the outflow diminishes to nearly zero as the aircraft approaches the GPIP near the downdraft center. This reverse shear (headwind-to-tailwind) of 20 knots in the last 150 feet of altitude would create a hazardous situation. On the other hand, Profile B illustrates a less hazardous situation in which the aircraft penetrates the wind field about one-half minute earlier, encounters an increasing headwind shear of 20 knots from 500- to 100-feet altitude after crossing the gust front, and completes the last 100 feet of approach with no further shear. Only slight wind shears in the vertical wind component are encountered and these are above 250 feet.

Several profiles such as the one described above were generated for evaluation by varying the GPIP and runway orientation (0- or 180-degrees) relative to selected wind fields. Sources of wind field data included Goff (NSSL),[5] Frost,[4] Fujita,[7] and the Douglas Aircraft Company. (The latter two were based on accident data at Kennedy Airport, June 24, 1975 and at Philadelphia International, June 23, 1976.)

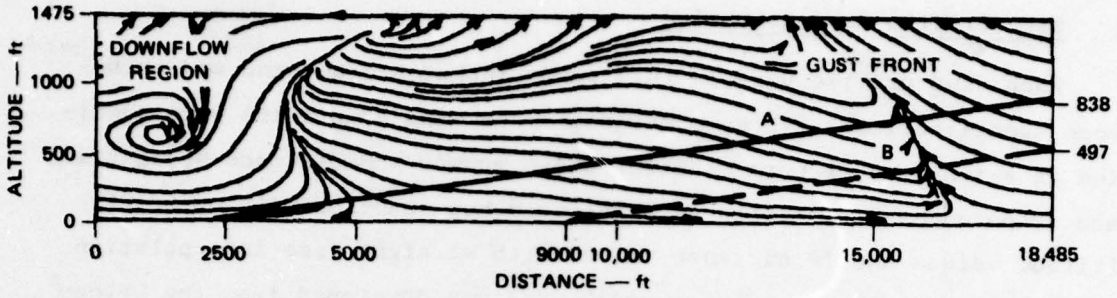

FIGURE 5 THUNDERSTORM WIND FIELD

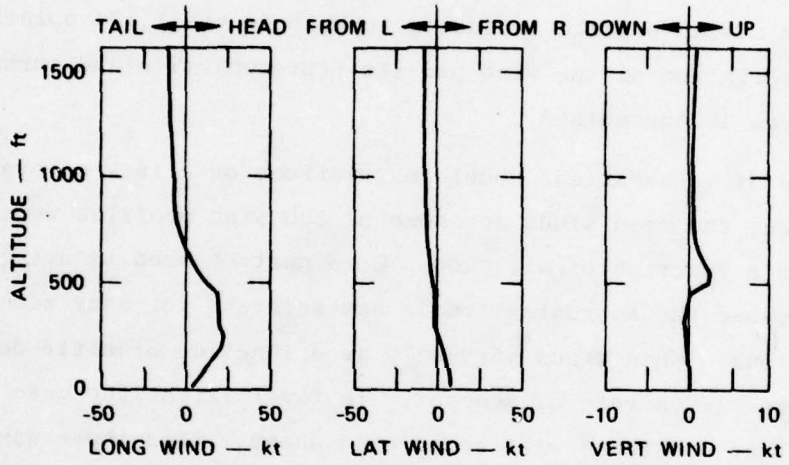

PROFILE A

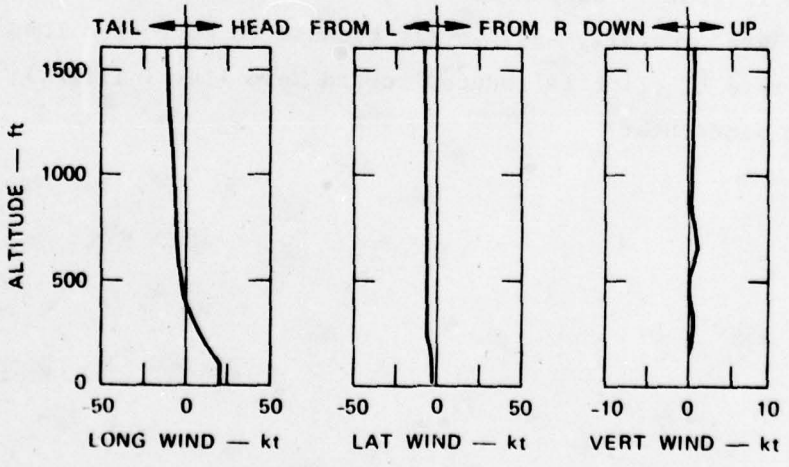

PROFILE B

FIGURE 6 THUNDERSTORM WIND PROFILES

D. Wind Profile Representation

Each wind profile used in this study included mean wind and turbulence specifications. Three orthogonal mean wind components were specified as a function of both altitude above runway and distance along track. Each component was specified as a table lookup function with up to 21 altitude values and 16 distance values with straight-line interpolation between points. The turbulence model used was developed from the Dryden[8] spectra. Six turbulence parameters (3-rms intensities and 3-scale lengths) were specified as a function of altitude using a table lookup function with up to 21 altitude values. The maximum amount of total storage required for a wind profile including turbulence was 1,134 points. A detailed description of the wind profile representation and turbulence model is given in Appendix A.

Because of mathematical model restrictions or a lack of available measured data, the mean winds for some of the wind profiles were specified only as a function of altitude. Care must be used in using these profiles because the approximation is not accurate for many meteorological wind conditions. When winds vary only as a function of altitude, wind shear will vary with rate of descent. In level flight the mean wind will remain constant and there will be no wind shear. When these wind profiles are flown on approach, wind shear will be lessened if a flatter flight path is flown. During takeoff, winds varying only as a function of altitude are generally easy to fly because to correct a loss in air speed, the rate of climb is reduced toward zero (level flight), where there is no wind shear.

III COMPUTER MODEL DESIGN

The computer model was implemented on a general purpose digital computer in the Aviation Systems Laboratory at SRI International. The model was encoded as a collection of FORTRAN IV subroutines that ran in either real time or fast time. Control inputs and test conditions were entered interactively via an alphanumeric display terminal. Results were available in the form of graphic display by key parameters, printouts of performance measures, and detailed plotted data.

A. Aircraft Models

The equations of motion for a rigid-body aircraft were written in 3 degrees of freedom, which included horizontal, vertical, and pitching motion. For each flight configuration of the aircraft modeled, a set of dynamic stability derivatives was incorporated. After the initial conditions were set, the equations of motion were integrated numerically with respect to time, using fourth-order Runge-Kutta approximation. A detailed description of the equations of motion and the assumptions used in deriving them appears in Appendix B.

The engine model (also described in Appendix B) consisted of a simple first-order lag for spool-up and spool-down times where a time constant was adjusted to approximate that of the engine under test.

B. Control System Model

Autocoupled approaches were flown using a pitch attitude controller similar to that provided by an autopilot and a thrust controller based on maintaining a reference airspeed. The pitch control algorithm (Figure 7) contained the following feedback terms: pitch, pitch rate, vertical offset from glide slope. The thrust control algorithm (Figure 8) contained airspeed as the feedback parameter. The control laws were optimized to give good performance and stability margin over all test conditions.

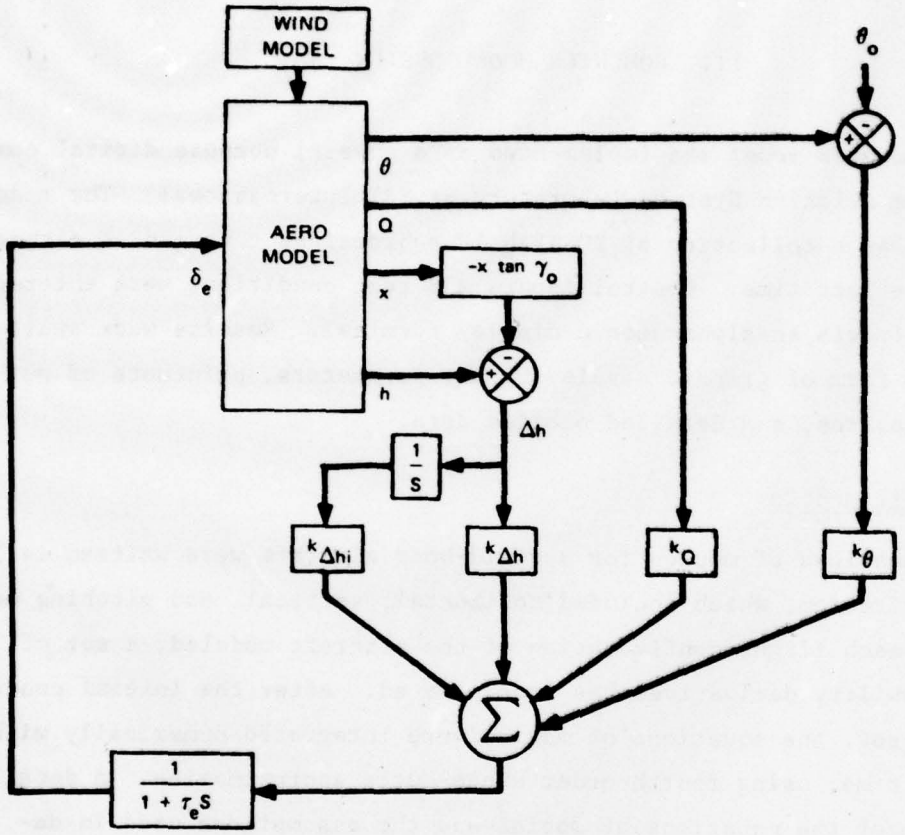

θ = PITCH ALTITUDE

θ_o = REFERENCE PITCH ATTITUDE

Q = PITCH RATE

x = DISTANCE

h = HEIGHT ABOVE RUNWAY

γ_o = REFERENCE APPROACH ANGLE

Δh = HEIGHT ERROR FROM GLIDE SLOPE

δ_e = ELEVATOR DEFLECTION FROM TRIM

S = LAPLACE TRANSFORM VARIABLE

τ_e = CONTROL SYSTEMS DELAY TIME CONSTANT

$k_{\Delta hi}$, $k_{\Delta h}$, k_Q, k_θ = FEEDBACK PARAMETER GAINS

FIGURE 7 PITCH ATTITUDE CONTROL SYSTEM MODEL

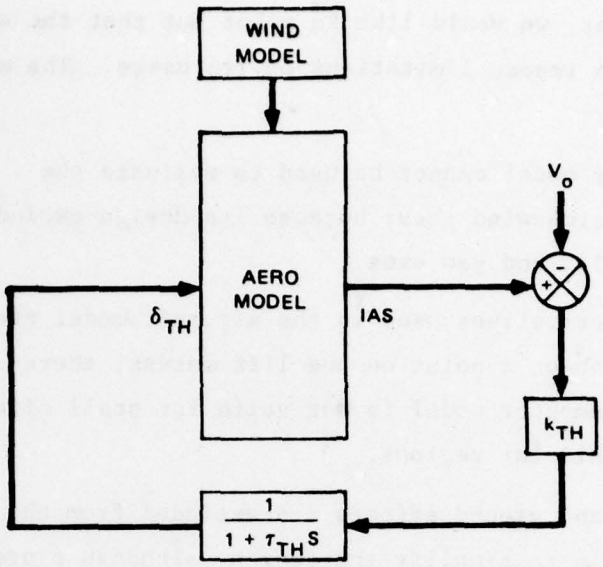

IAS = AIRSPEED
V_o = REFERENCE AIRSPEED
δ_{TH} = THRUST CONTROL DEFLECTION FROM TRIM
S = LAPLACE TRANSFORM VARIABLE
τ_{TH} = ENGINE AND CONTROL SYSTEMS DELAY TIME CONSTANT
k_{TH} = GAIN

FIGURE 8 THRUST CONTROL SYSTEM MODEL

Therefore, a separate set of gains and time constants was used for each aircraft configuration modeled.

Takeoff runs were handled in much the same manner as approach runs with the exception that vertical offset from glide slope was not included as a pitch control term. Initial conditions were set for the nominal thrust, airspeed, and pitch attitude for climbout just after takeoff. Each run then began, using fixed thrust, with pitch attitude managed by its controller. Since the flight configuration used was for a gear-up (clean) airplane, ground roll was computed manually.

C. Limitations of Computer Model Design

The computer model design was kept as simple as possible while satisfying the project requirements. The realism of the computer runs exceeded

our expections, however, we would like to point out that the assumptions used in the derivation impose limitations on its usage. The more important restrictions are:

(1) The computer model cannot be used to evaluate the effects of crosswind shear because its design excludes lateral, roll, and yaw axes.

(2) Stability derivatives used in the aircraft model are linearized about a point on the lift curves; therefore, the computer model is not valid for stall effects or other nonlinear regions.

(3) Flare laws and ground effects are excluded from the model primarily to simplify the design, although a previous study[1] cites ground effects as having negligible effect on performance results.

(4) There is no explicit pilot model. Although one could have been included, we feel that inclusion of a pilot model would be inconsistent in view of the other simplications (e.g., the lack of a flare law). Moreover, in wind shear environments, there is a large variation in responses among pilots.

D. Verification of Computer Model Design

After each computer run, plots of the aircraft state parameters and control deflections were examined. The plots were consistent with known characteristics of the aeronautical system. Over all the wind profiles tested under approach conditions, the minimum and maximum values of angle of attack α attained were 5 degrees and 16 degrees (see Figure 9). Pitch attitude θ ranged from 1.5 to 18.5 degrees. Airspeed remained above stall and below the limits imposed by flap setting. Other aircraft state parameters and control deflections remained within operational limits.

It is certain that there was some error in the computer model since a single set of aerodynamic stability derivatives for each flight configuration was used over the range of α and airspeed. However, as illustrated

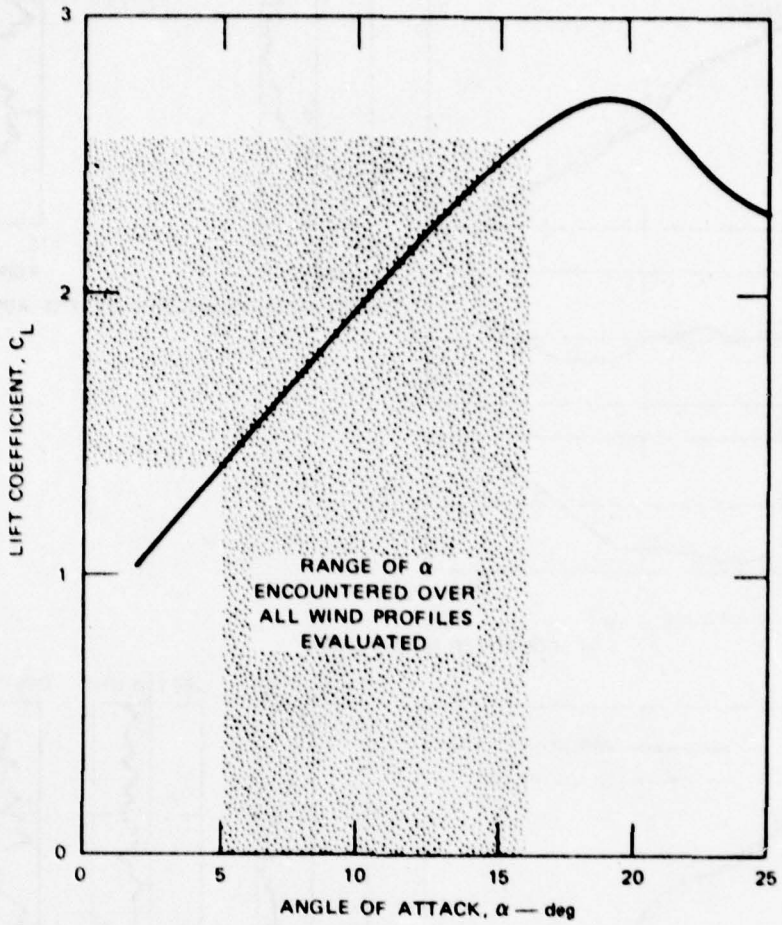

FIGURE 9 RANGE OF α ENCOUNTERED DURING COMPUTER MODEL APPROACH RUNS

in Figure 9, the non-linear region was avoided. We believe the accuracy of the computer model is entirely adequate for this study. As a further check, we compared the computer model runs with some of the Task 2, Phase 2, piloted simulator runs using a full, non-linear, 6 degree-of-freedom, motion base simulator located at Douglas Aircraft Company in Long Beach. The aircraft model was a DC-10-10. In Figure 10, a computer model run (a) is compared with one of the Phase 2 piloted simulator runs (b). The aircraft position, airspeed, and ground speed traces are nearly the same in both runs. The piloted run is typical of the better approaches in the series. Many of the piloted runs showed poorer performance.

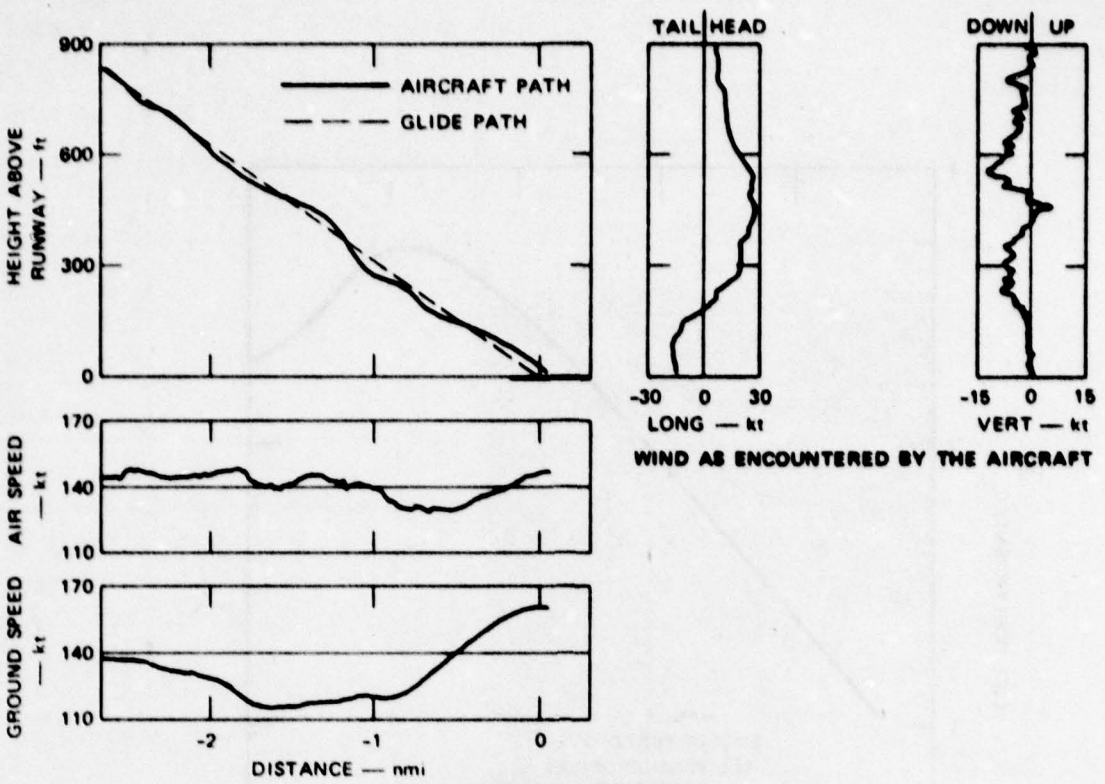

(a) COMPUTER MODEL RUN

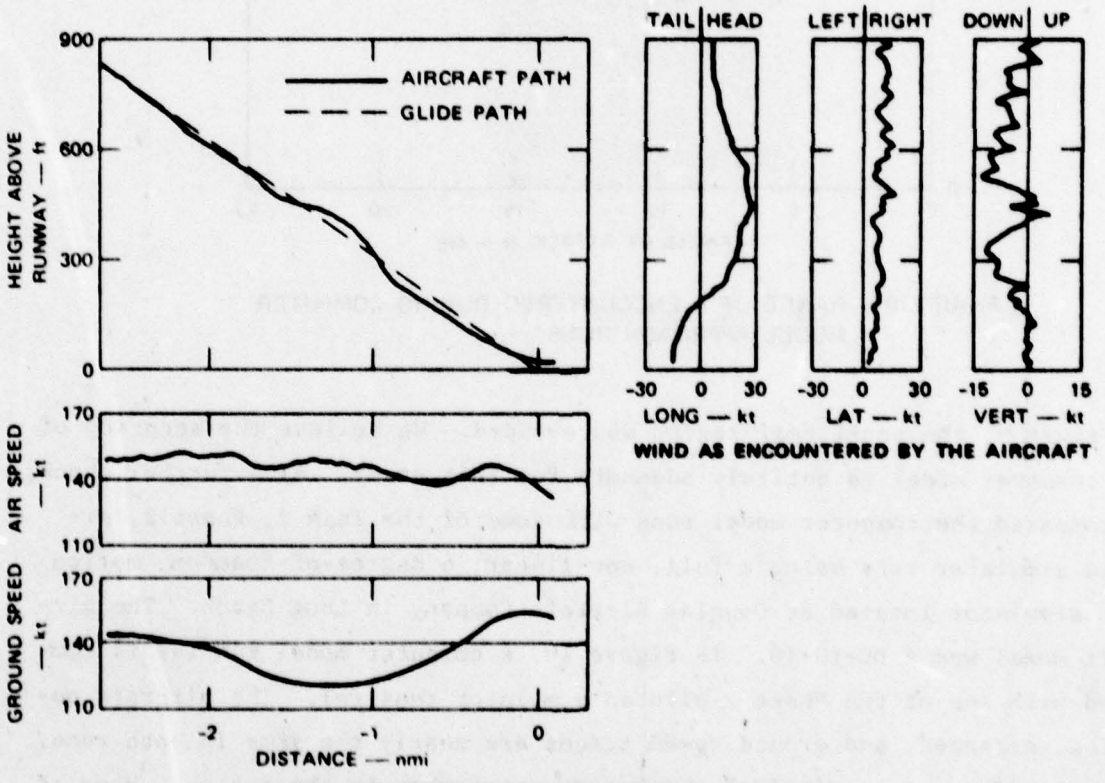

(b) DC-10 PILOTED SIMULATION, PHASE 2, RUN NO. 52

FIGURE 10 COMPARISON OF COMPUTER MODEL RUN WITH PILOTED SIMULATOR RUN

IV EFFECTS OF WIND SHEAR ON AIRCRAFT

It is not surprising that the behavior of complex aeronautical systems in equally complex wind fields is not simple. To identify wind shear characteristics that are hazardous to low-level flight and then to assess their effects on the behavior of the aircraft in a complex environment, it is helpful to consider the problem first from a simplified viewpoint. Figures 11 through 14 show sudden headwind, tailwind, updraft, and downdraft encounters. Although the winds appear as step inputs in the figures, they are actually applied as steep ramps over a short period of time since a true step change in wind velocity over zero time would require infinite acceleration. The following paragraphs discuss certain features of these step changes in detail. The concepts developed may then be applied to the wind profiles examined in Sections V and VI.

A. Direction of Shear, Longitudinal Wind Component

Shearing of the longitudinal wind component (longitudinal wind shear) may be characterized by its direction. A headwind that changes to a tailwind may be said to be in the headwind-to-tailwind direction or simply a headwind-tailwind shear. Other examples of headwind-tailwind shears are a decreasing headwind or an increasing tailwind. In a similar manner, tailwind-headwind shears include a tailwind changing to a headwind, an increasing headwind, and a decreasing tailwind.

Figure 11 shows a response to a sudden 20-knot headwind (tailwind-headwind shear) applied at an altitude of 750 feet above the runway and subsequently removed (headwind-tailwind shear) at an altitude of 300 feet. At 750 feet (Point A on the graph) the airspeed suddenly increased. Although the thrust controller reduced thrust to compensate, the response time of the engines and the inertia of the moving aircraft were such that the groundspeed of the aircraft changed much more slowly than airspeed. A condition of excess lift was present and the aircraft rose above glide path. The aircraft was pitched downward by the pitch controller and

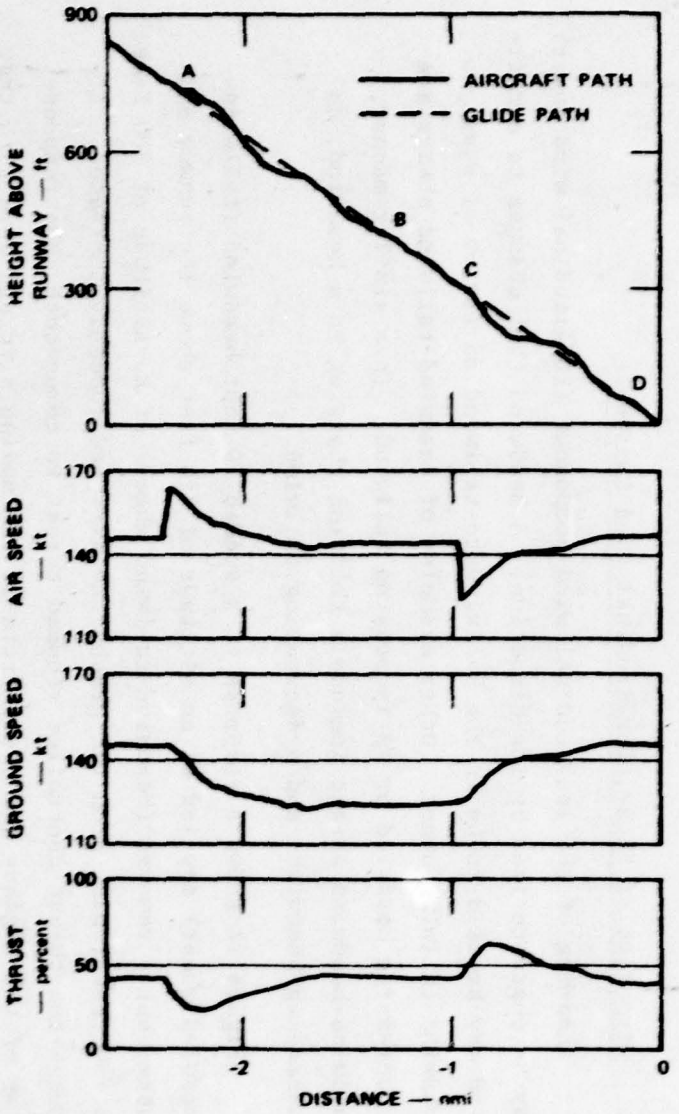

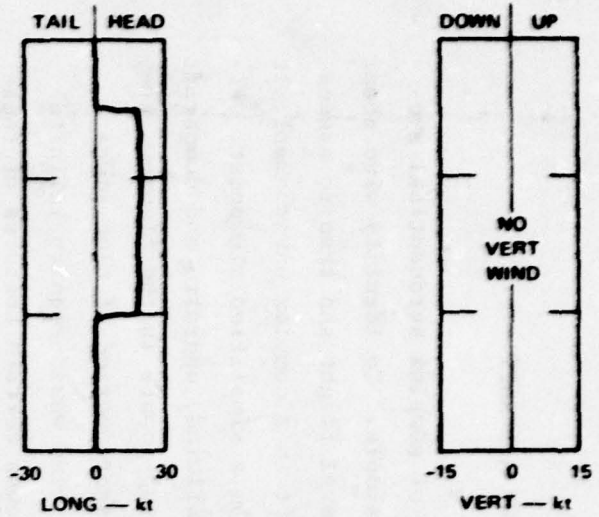

WIND AS ENCOUNTERED BY THE AIRCRAFT

FIGURE 11 SUDDEN HEADWIND ENCOUNTER

with the help of the thrust controller, eventually became stabilized on the glide path at the proper airspeed. At Point B the ground speed was 20 knots lower than the reference speed because of the 20-knot headwind. Note that there were some oscillations and overshoot as the aircraft recaptured the glide path. These traits are present in most aircraft/controller systems when a sudden displacement occurs. The plot of the piloted wind shear simulation shown earlier in Figure 10 is an example of this type of shear condition.

At Point C in Figure 11 the headwind was suddenly removed. Since the aircraft and control systems cannot respond instantaneously, a condition of insufficient lift sent the aircraft below the glide slope. This headwind-tailwind shear (C) contains the additional hazard of rapid airspeed loss and increase in angle of attack.

In Figure 12 a sudden 20-knot tailwind was applied at an altitude of 750 feet above the runway and then removed at 300-feet altitude. The response of the aircraft was exactly what would be expected after an examination of the 20-knot sudden headwind case. At the onset of the tailwind (headwind-tailwind shear) a loss of lift occurred with a sharp drop in airspeed. The aircraft fell below the glide slope. Because of the tailwind, the ground speed increased to 20 knots above the reference speed. When the tailwind was suddenly removed (tailwind-headwind shear), airspeed increased sharply with an increase in lift, thus pushing the aircraft above glide slope.

The step wind response (Figures 11 and 12) show that the departures from glide slope were approximately the same for both headwind-tailwind and tailwind-headwind wind shear. This suggests that, if a pilot can keep from stalling his aircraft, he may expect a headwind-tailwind shear to push him low with about the same effectiveness that an equal tailwind-headwind shear would tend to push him high. Headwind-tailwind shears may contain the hazards of airspeed loss and increases in flight path angle, or excessively high ground speed. Because of these hazards, we conclude that, with all other factors being equal, headwind-tailwind shears are potentially more hazardous than tailwind-headwind shears.

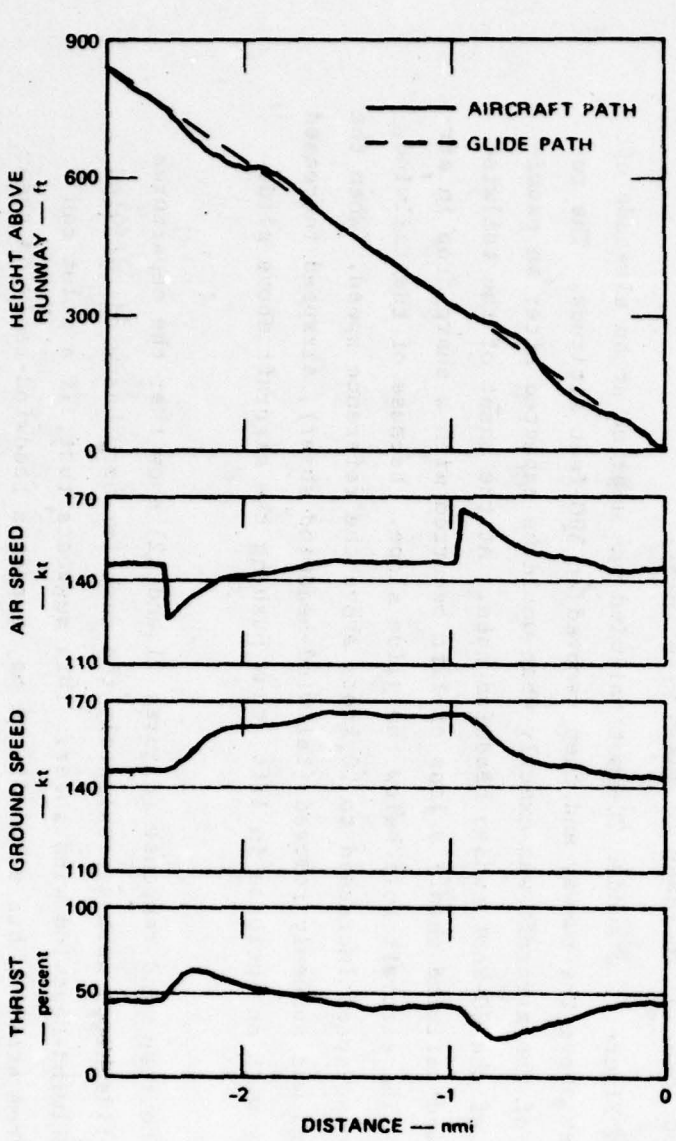

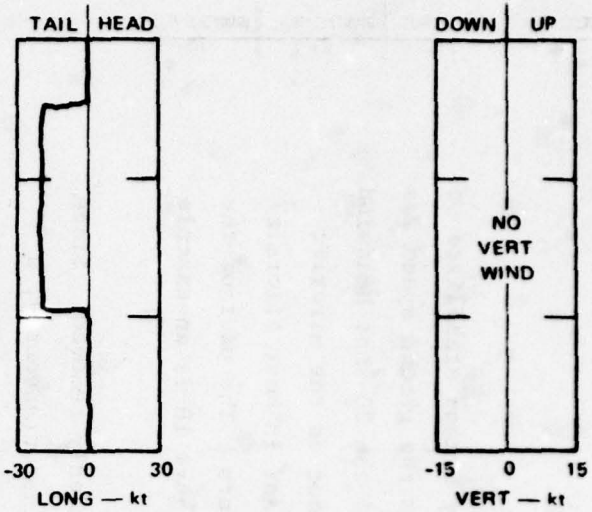

WIND AS ENCOUNTERED BY THE AIRCRAFT

FIGURE 12 SUDDEN TAILWIND ENCOUNTER

B. Direction of Shear, Vertical Wind Component

A response of an aircraft to a sudden 7-knot updraft is shown in Figure 13. At 750-feet altitude above runway, an updraft encounter (downdraft-updraft wind shear) caused a condition of excess lift that forced the aircraft above the glide slope. Since the change in airspeed was small, the thrust controller commanded only a small change in thrust over the duration of the updraft. To maintain the glide path, the pitch controller corrected the excess lift condition by pitching down. Initially, the downdraft-updraft wind shear caused an increase in angle of attack that subsequently lowered as the aircraft accelerated upward and then pitched downward. This pitch-down attitude was maintained over the duration of the updraft. When the updraft was removed (updraft-downdraft wind shear), the aircraft dipped below the glide path. Removal of the updraft caused a momentary decrease in angle of attack until the aircraft resumed its normal pitch attitude.

Similar results were obtained when the aircraft was subjected to a sudden 7-knot downdraft (Figure 14). Since the change in airspeed was small, responses to flight path disturbances due to vertical wind changes were mostly through changes in pitch attitude. The updraft-downdraft wind shear forced the aircraft below the glide path with a momentary decrease in angle of attack. The pitch-up maneuver immediately followed. During the downdraft, the aircraft climb capability was reduced. The downdraft-updraft wind shear then forced the aircraft above the glide path accompanied by a momentary increase in angle of attack.

Glide path deviations were about the same for both updraft-downdraft and downdraft-updraft wind shears. This suggests that, if the aircraft does not stall, a pilot can expect an updraft-downdraft shear to push him below glide path with about the same effectiveness that a downdraft-updraft would push him above glide path. A steady downdraft reduces the climb capability of the aircraft.

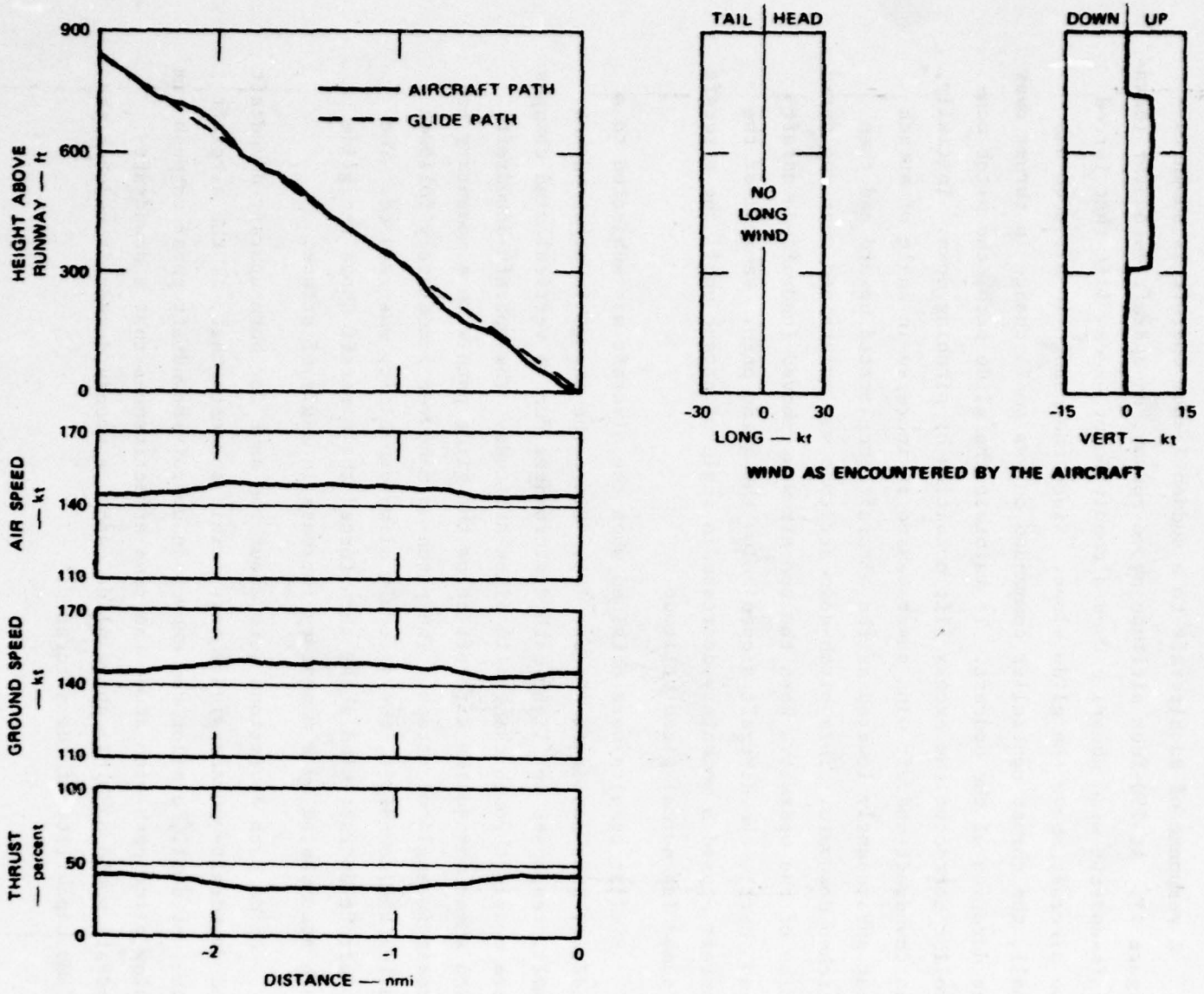

FIGURE 13 SUDDEN UPDRAFT ENCOUNTER

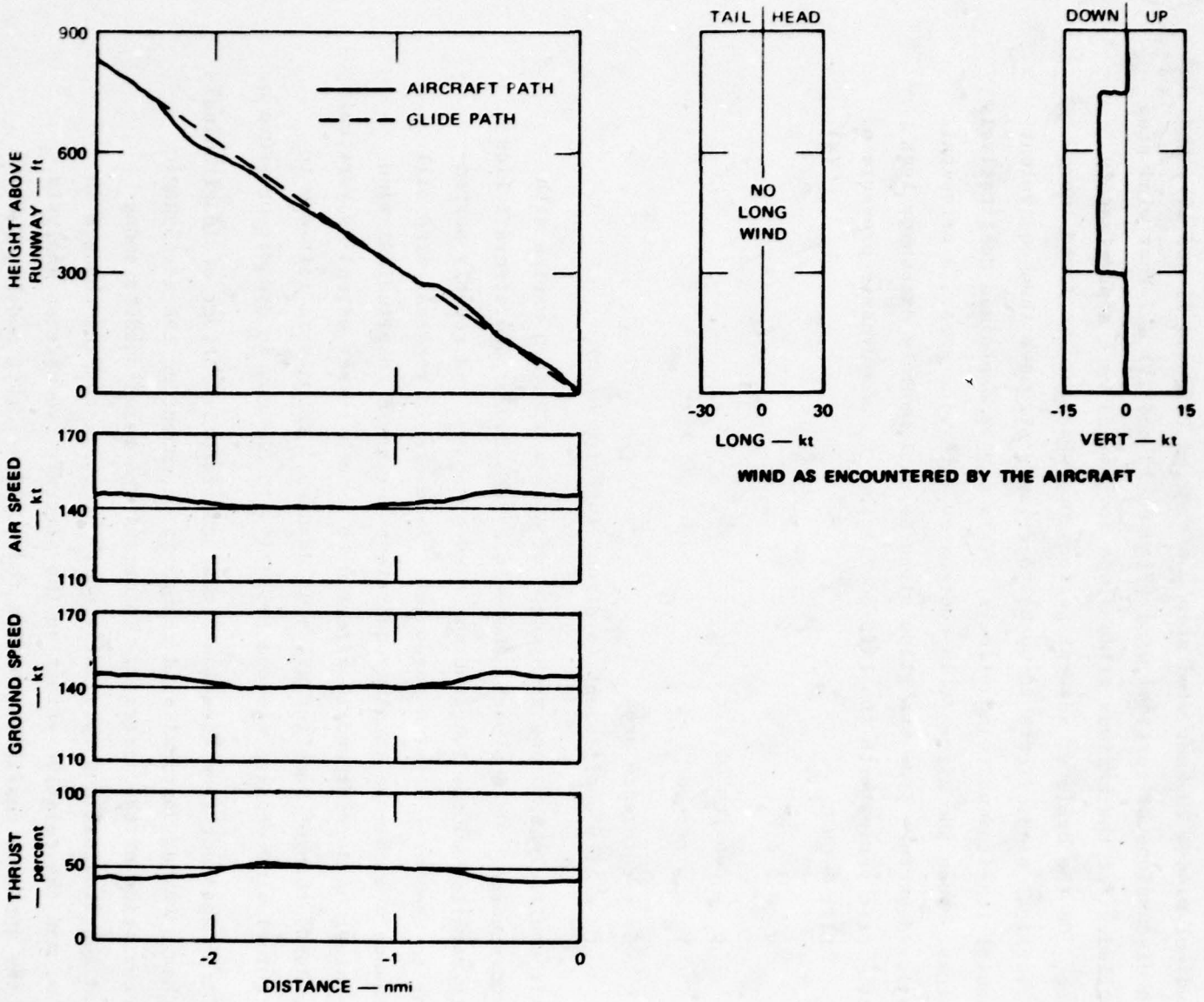

FIGURE 14 SUDDEN DOWNDRAFT ENCOUNTER

C. Comparison of Longitudinal Wind Effects with Vertical Wind Effects

The reader has probably noticed that in the above discussions of longitudinal wind a 20-knot wind step was applied (Figures 11 and 12), and that in discussions of vertical wind (Figures 13 and 14) a 7-knot wind step was applied. Yet the maximum glide slope deviations were approximately the same. On the basis of several performance measures, we found incremental vertical wind effects to be 2½ to 3 times stronger than equivalent incremental longitudinal wind effects. This may be explained qualitatively as follows. When the aircraft is confronted with wind shear, a principal reason for departure from the glide slope is an immediate excess or lack of lift. Lift varies with the lift coefficient C_L and dynamic pressure q.

$$\text{Lift} \approx qS\,C_L \qquad (4)$$

where $q = \frac{1}{2}\rho V_a^2$

ρ = density of air

V_a = airspeed

S = reference area

C_L = lift coefficient (a direct function of α).

The lift coefficient varies with angle of attack α, and q varies with airspeed squared. On approach, the velocity vector of the aircraft lies roughly parallel to the longitudinal wind component and roughly perpendicular to the vertical wind component. A change in vertical wind will thus change α much more than an equivalent change in longitudinal wind. On the other hand, airspeed is affected to a much lesser extent by vertical wind changes than by longitudinal wind changes. Changes in lift due to longitudinal wind changes are due primarily to changes in dynamic pressure q.

It is apparent from Equation 4 that the relative effect of longitudinal wind change versus vertical wind change is dependent on the aerodynamic characteristics of the aircraft. To detail the relationships among applied longitudinal and vertical winds, the corresponding changes in q and α, and the relative effect on the aircraft, we made an analysis using the approach configuration for the DC-10 aircraft model. The instantaneous changes in α and q for various-sized increments of longitudinal

and vertical wind are plotted in Figure 15. The change in α is greater for vertical wind increments than for longitudinal wind increments, and the change in q is dominated by longitudinal wind. The effects of the changes in q and α are reflected by the instantaneous accelerations acting on the aircraft (see Figure 16). The vertical accelerations produced by up- or down-draft shear are well over twice the vertical accelerations produced by an equal shear of the longitudinal wind component. Although this analysis applied only to the instantaneous situation, the results are substantially in agreement with the computer model runs.

D. Reversals in Wind Shear Direction

A wind shear in one direction may be followed shortly by a wind shear in the opposite direction. For example, in Figure 11, the tailwind-headwind shear at 750-feet altitude was followed by a headwind-tailwind shear at 300 feet, and in Figure 13, a downdraft-updraft shear at 750-feet altitude was followed by an updraft-downdraft shear at 300 feet.

The timing of the reversal in wind shear direction greatly affects the performance of the aircraft. If the tailwind-headwind wind shear in Figure 11 had occurred at a lower altitude, the aircraft would not have had time to recover from the first wind shear before encountering the wind shear reversal. The potential severity of this occurrence is illustrated in Figure 17, where the tailwind-headwind shear has been lowered to 400-feet altitude. Even though the magnitude of the headwind is the same, the aircraft is affected more adversely.

E. Geometrical Factors

The reader may recall from Section II that, in general, the wind profile viewed from a 3-degree glide path varies greatly with the positioning of the runway within the wind field. When the aircraft deviates from the glide path, its position within the wind field dictates that it will encounter winds that are not the same as those it would have received had it remained on the glide path. The situation is complicated further by the fact that the outcome of the approach is influenced by the height of the wind shear encounter and the timing of the reversals in wind shear direc-

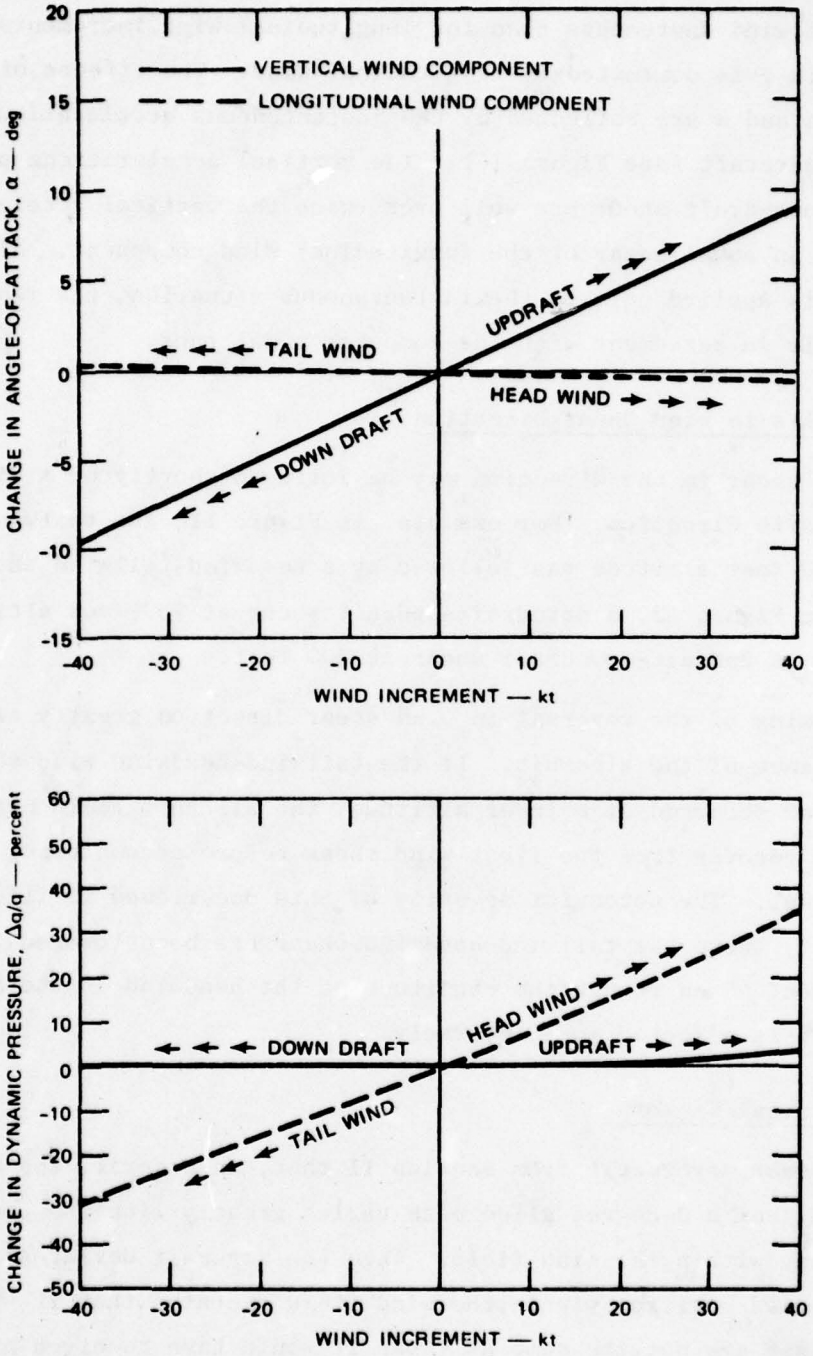

FIGURE 15 EFFECT OF SUDDEN WIND ON INSTANTANEOUS ANGLE-OF-ATTACK AND DYNAMIC PRESSURE

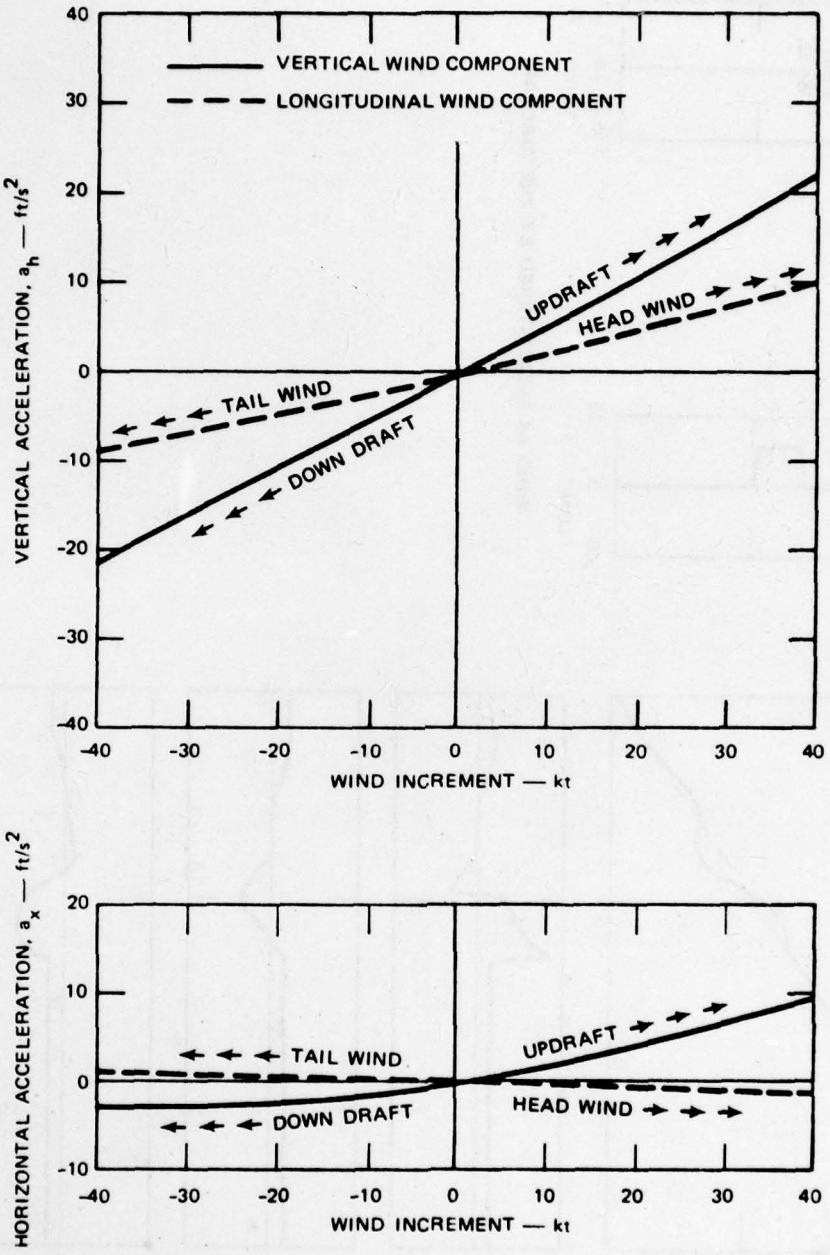

FIGURE 16 EFFECT OF SUDDEN WIND ON INSTANTANEOUS AIRCRAFT ACCELERATION

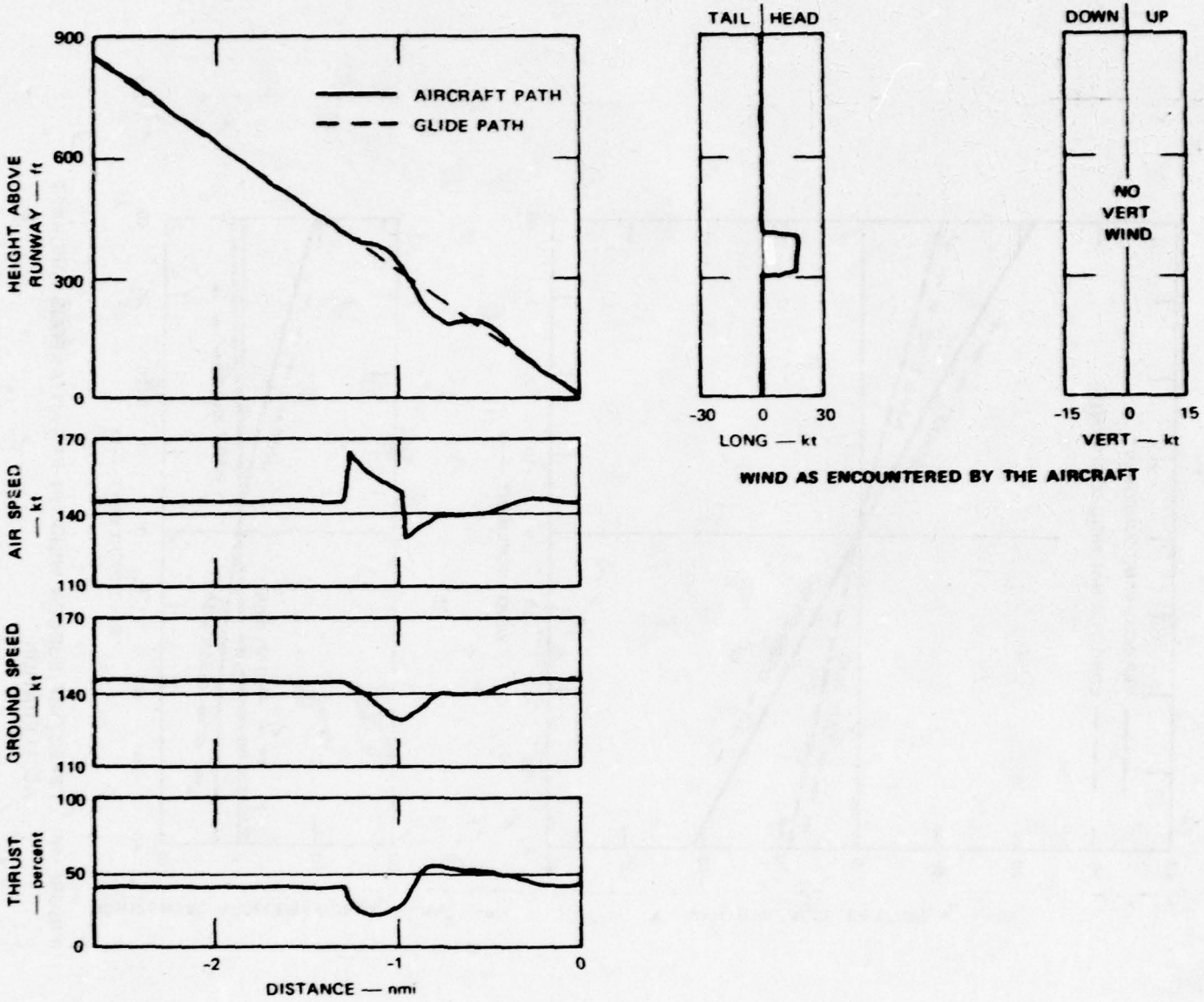

FIGURE 17 POTENTIAL HAZARD OF REVERSALS IN WIND SHEAR DIRECTION

tion. Wind shears occurring at low altitudes do not allow much time for recovery. Severe wind shears occurring at a higher altitude may force a long landing because of overshoot during recovery.

V SPECIFICATION OF WIND PROFILES FOR PILOTED SIMULATION TESTS

To obtain an expanded set of wind profiles for this project, approximately 50 wind fields representative of actual meteorological conditions were collected and put into two-dimensional tabular form. Each wind field was read into the computer and "flown" using the computer model described in Section III. B-727 and DC-10 aerodynamic models were flown. Through translation of the runway position within the wind field and rotation of the runway by 180 degrees, several wind profiles were examined from each wind field. Wind shear severities were compared by observing their effects on the performance of the computer model. Potentially hazardous wind profiles were identified, and their relative severity was designated as "low," "moderate," or "high" for purposes of the B-727 and DC-10 piloted simulator wind shear tests. Approximately 20 representative wind profiles were assembled from which the winds for each piloted simulation exercise were selected.

A. Performance Measures

To assess the effects of wind shear, performance criteria must be established. Due to the complexity of the aeronautical system and the variety of operational requirements, measurement of a single parameter is not an adequate measure of total system performance. For example, a measurement of longitudinal displacement at touchdown would not indicate whether the airspeed was safely managed or whether obstacles beneath the approach path were avoided. Several measures must be combined.

This project used landing outcome, approach outcome, path following and airspeed management performance criteria. Since the computer model did not contain lateral axes, we did not evaluate the effects of crosswinds; however, lateral winds were included in the results by adding maximum rate of lateral wind shear to the performance measures. Rankings of wind profile severity were found to be largely independent of the exact

choice of performance measures if the measures were reasonable and if several of them were used. A detailed listing of the performance measures is given in Table 1.

Table 1

PERFORMANCE CRITERIA

Criteria	Measured by
Landing outcome	Longitudinal displacement from GPIP at touchdown
Approach outcome	Vertical displacement from glide slope at 100 feet
Path following	Maximum displacement below glide slope over the 750-feet to 50-feet flight path segment; and by MEA* over the same segment
Airspeed management	Airspeed error (high and low value) over the 750-feet to 50-feet flight path segment
Crosswind severity	Maximum rate of lateral wind shear

*MEA is the maneuver equation average,[10,11] a measure of glide slope tracking error defined as the mean value of the function of f over the flight path segment where:

$$f = \begin{cases} |\Delta H + 3.5 \ \dot{\Delta h} - 3.5 \ \dot{\theta}| & \text{for } h \leq 180 \text{ ft} \\ \frac{16}{0.089H} \ |\Delta H + 3.5 \ \dot{\Delta h} - 3.5 \ \dot{\theta}| & \text{for } h > 180 \text{ ft} \end{cases}$$

where

h = height above runway in ft
ΔH = vertical offset from glide slope in ft
$\dot{\Delta h}$ = rate of change in H in ft/sec
$\dot{\theta}$ = rate of change of pitch angle in deg/sec

In general, a smaller value of MEA will indicate better performance.

B. Scoring of Candidate Wind Profiles

The relative severity of each wind profile was measured by ranking it against the other wind profiles; thus absolute measurement of perfor-

mance as it pertains to the operational environment was not required. The ranking procedure used equal weighting among the performance measures with the rationale being that in the isolated case where a particular performance measure failed as a general indicator of wind profile severity, its value would be outweighed by the value of the other measures.

The ranking procedure is applied to the wind profiles used in the B-727 piloted simulator tests in Tables 2 and 3. Table 2 shows a tabulation of the raw values of each performance measure for each of the 12 wind profiles. Based on the raw values obtained for each measure, a ranking of severity is established running from 1 to 12, with 12 being the most severe (Table 3). The total score is determined using an equally weighted summation of the individual rankings divided by the number of measures (i.e., simply an average). The wind profiles are rearranged on the basis of their total score in Table 4. For plots of each wind profile the reader is referred to Appendix C.

Table 2

COMPUTER MODEL PERFORMANCE DATA, B-727 WIND PROFILES

WIND PROFILE	LONG DISP AT TD (FT)	VERT DISP AT 100 FT (FT)	MAX DISP BELOW GS (FT)	MEA	AIRSPEED ERROR (kts)	CROSS-WIND (RANK)
B1	156	1.1	4.2	6.06	12.0	5
B2	62	1.8	8.0	3.96	11.0	2
B3	35	1.1	5.8	2.77	8.0	8
B4	103	0.8	4.6	5.71	10.3	7
B5	155	17.8	18.4	5.84	26.7	10
B6	64	8.8	10.0	4.28	14.9	11
B7	98	16.2	16.3	4.00	24.9	6
B8	262	7.3	13.0	7.37	18.1	9
B9	496	0.2	25.9	6.89	29.6	12
B10	300	32.6	66.2	12.00	42.6	1
B11	555	17.2	41.2	11.55	33.1	3
B12	197	13.3	26.0	7.83	30.3	4

Table 3

RANKING OF B-727 WIND PROFILES USING COMPUTER MODEL DATA

WIND PROFILE	LONG DISP AT TD	VERT DISP AT 100 FT	MAX DISP BELOW GS	MEA	AIRSPEED ERROR	CROSS-WIND	SCORE Σ/6
B1	7	3.5	1	7	4	5	4.6
B2	2	5	4	2	3	2	3
B3	1	3.5	2	1	1	8	2.8
B4	5	2	3	5	2	7	4
B5	6	11	8	6	8	10	8.1
B6	3	7	5	4	5	11	5.8
B7	4	9	7	3	7	6	6
B8	9	6	6	9	6	9	7.5
B9	11	1	9	8	9	12	8.3
B10	10	12	12	12	12	1	9.8
B11	12	10	11	11	11	3	9.6
B12	8	8	10	10	10	4	8.3

Table 4

COMPUTER MODEL SEVERITY RATINGS,
B-727 WIND PROFILES

SCORE	WIND PROFILE	SEVERITY
9.8	B10	HIGH
9.6	B11	
8.3	B12	
8.3	B9	
8.1	B5	MODERATE
7.5	B8	
6.0	B7	
5.8	B6	
4.6	B1	LOW
4.0	B4	
3.0	B2	
2.8	B3	

Although we have shown the determination of relative wind shear severity for only the winds used in the B-727 piloted simulator tests, the wind profiles used in the DC-10 simulator tests were rated using the same techniques. A description of the DC-10 wind profiles is also given in Appendix C.

C. Comparison of Severity Ratings with B-727 Piloted Simulation Results

After the B-727 piloted simulator tests had been completed, the wind profiles used were ranked a second time using the results of the simulation. The test results under baseline conditions were first averaged over all pilots. Scoring (Table 5) used five equally weighted performance measures that were similar to the measures used in the initial scoring. The severity ratings are compared with the computer-derived ratings in Table 6. Overall results were consistent; however, it is interesting to note that Wind Profiles B1, B5, and B11 showed slightly less severity than expected. These differences might be explained by the fact that these particular wind profiles were used in previous simulator tests in which some of the subject pilots had participated. Practice might have improved their performance on these profiles. Wind Profile B7 seems more severe than expected. It is difficult to speculate on this result since Wind Profile B7 is less severe but similar in shape to Wind Profile B9. However, all the above differences may be explained by statistical variation within the experimental data.

The results of the B-727 piloted simulator tests quantify to some extent the meaning of the severity classifications "low," "moderate," and "high." As shown in Table 6, for the low-severity wind shears, 82 percent of the approaches were within criteria limits under baseline conditions. For the moderate wind shears, 64 percent of the approaches were within limits, and for the high-severity shears, 54 percent of the approaches were within limits. The statistical significance of these data was tested using the Cochran Q test.[18] There were significantly ($p < .05$) more approaches within limits for the low-severity wind profiles than for either the moderate- or the high-severity wind profiles. The difference in approach performance between moderate- and high-severity

Table 5

RANKING OF WIND PROFILES USING B-727 PILOTED SIMULATION DATA

WIND PROFILE	LANDING OUTCOME	APPROACH OUTCOME	MAX DISP BELOW GS	AIRSPEED ERROR	RMS DEV FROM LOC	SCORE Σ/5
B1	1	6.5	2	4	5	3.7
B2	2	3	8	5	3	4.2
B3	3	3	1	1	1	1.8
B4	9	3	5	2	2	4.2
B5	5.5	8.5	10	6	4	6.8
B6	5.5	3	7	3	10	5.7
B7	5.5	10.5	6	11	12	9.0
B8	12	6.5	4	7	7	7.3
B9	11	8.5	3	8	11	8.3
B10	9	12	12	12	6	10.2
B11	9	3	9	9	8.5	7.7
B12	5.5	10.5	11	10	8.5	9.1

Table 6

COMPARISON OF COMPUTER MODEL RESULTS
WITH B-727 PILOTED SIMULATION RESULTS

COMPUTER MODEL RESULTS		PILOTED B-727 SIMULATION RESULTS	
RELATIVE SEVERITY	WIND-PROFILE RANKING	WIND-PROFILE RANKING	APPROACHES WITHIN LIMITS UNDER BASELINE CONDITIONS
HIGH	B10 B11 B12 B9	B10 B12 B7 B9	54% (WIND PROFILES B12, B9)
MODERATE	B5 B8 B7 B6	B11 B8 B5 B6	64% (WIND PROFILES B8, B5)
LOW	B1 B4 B2 B3	B4 B2 B1 B3	82% (WIND PROFILES B4, B1)

EXCEPT FOR SOME MINOR DIFFERENCES, WIND PROFILE 7 SEEMS MORE SEVERE THAN EXPECTED. PROFILE 7 IS SIMILAR IN SHAPE TO PROFILE 9.

wind profiles was not statistically significant, although the trend seems apparent from the data.

D. Wind Profiles for Takeoff

Takeoff wind profiles were flown using a DC-10 aircraft model configured for climbout at 407,000-pounds gross weight. Each run was initiated at runway level using fixed thrust with pitch attitude managed by the control algorithm described above in Section III C.

We did not establish specific performance measures for takeoff runs, nor did we make formal comparisons of wind profile severities. Of approximately 25 wind fields examined, four were found to produce wind profiles that caused the aircraft to experience a negative rate of climb. Three of these wind fields caused the aircraft to crash shortly after takeoff. Plots of aircraft altitude as a function of distance for typical takeoffs through severe wind shear are shown in Figure 18. The wind profile used (designated at T25B in Appendix C) contained a headwind-tailwind shear occurring in combination with a downdraft. The curves in Figure 18 exhibit varying performance for each of the three ground-roll distances. All three of the departure paths were flown with identical initial airspeed, thrust, and pitch angle, etc. The varied performance was due to the fact that the wind shear received by the aircraft was dependent on its position relative to the wind field. Displacements in distance of only a few thousand feet thus determined whether the takeoff was successful.

Because of mathematical model restrictions or a lack of available data, the mean winds for some of the wind profiles were specified only as a function of altitude above runway (they did not vary with distance). When this wind representation is used, the results must be interpreted with care because the approximation is not accurate for many meteorological conditions. When winds vary only as a function of altitude, wind shear will vary with the rate of climb. In level flight the mean wind will remain constant and there will be no wind shear. During takeoff, winds varying only as a function of altitude are generally easy to fly, since in order to correct a loss in airspeed, the rate of climb is reduced. Negative rate of climb was not observed on any of the wind profiles specified only as a function of altitude.

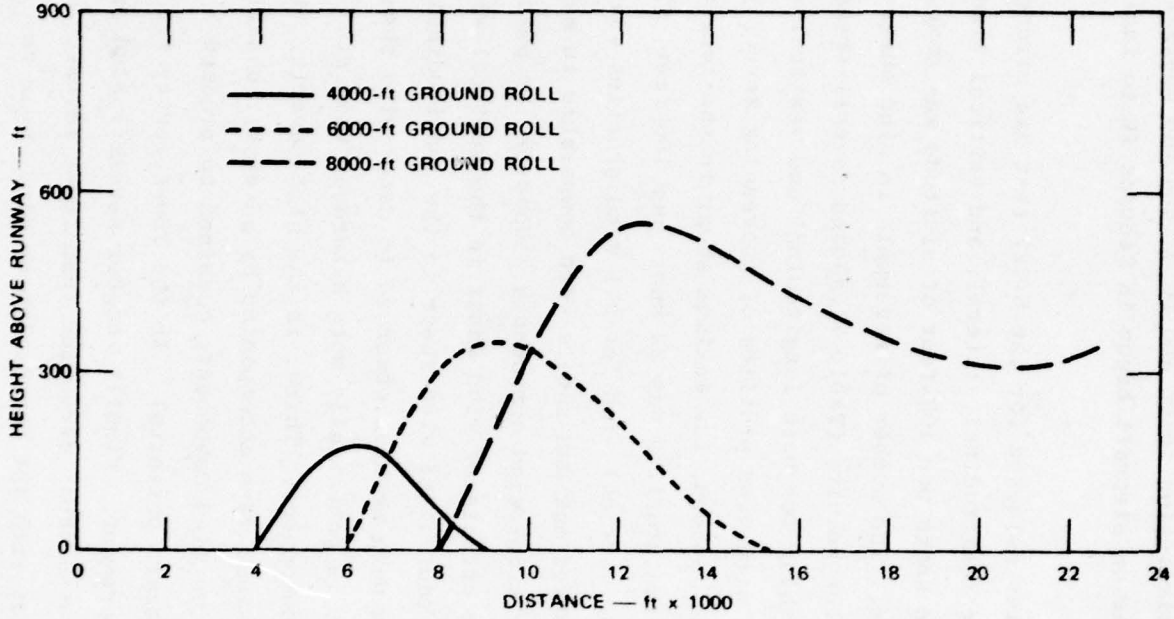

FIGURE 18 TAKEOFF FLIGHT PATHS IN SEVERE WIND SHEAR (computer model run, wind profile T25B)

E. Characteristics of Wind Profiles Used in Simulations

In this subsection wind profile characteristics are summarized, along with our observations of their relationship to wind profile severity. Our purpose is twofold: to document the wind profiles selected for use in the piloted simulation tests and to extend the analysis of the effects of wind shear on aircraft begun in Section IV to include these observations.

The wind profiles selected for the B-727 test are arranged by severity in Table 7. For longitudinal, lateral, and vertical wind components, the maximum shear in knots per 100-feet of altitude was computed along a 3-degree glide slope. The number of reversals in wind shear direction was also counted. The results (Table 7) showed several trends in the data. First, the maximum shear for both longitudinal and vertical wind components generally increased with wind profiles of increasing severity. This result was expected. Second, the maximum shear in the longitudinal wind component for all wind profiles was 22 knots per 100 feet, whereas the maximum shear in the vertical wind for all wind profiles was 23 knots per 100 feet. The observed maximum shears were comparable in magnitude for longitudinal and vertical wind components. However, we pointed out in Section IV that the effects of wind shear in the vertical wind component were stronger than equivalent wind shear in the longitudinal wind component. On the basis of the data we have observed to date, wind shear in the vertical wind component is potentially more hazardous than wind shear in the longitudinal wind component. Third, in the high-severity wind profiles, shearing vertical winds were accompanied by adversely shearing longitudinal winds. The two wind components combined to produce a complex wind shear with great hazard potential. In the low-severity wind profiles, no vertical wind was present. Finally, higher severity wind profiles included more reversals in wind shear direction than lower severity wind profiles. This is in agreement with the discussion on wind shear reversals given in Section IV and suggests that reversals tend to increase the potential severity of a wind profile.

The height and strength of the encounter is important to the detection

Table 7

CHARACTERISTICS OF WINDS USED IN B-727 SIMULATION--
MAXIMUM SHEAR AND REVERSALS

RELATIVE SEVERITY	WIND PROFILE	LONG WIND		LAT WIND		VERT WIND	
		MAXIMUM SHEAR (kt/100 ft)	NUMBER OF SHEAR REVERSALS	MAXIMUM SHEAR (kt/100 ft)	NUMBER OF SHEAR REVERSALS	MAXIMUM SHEAR (kt/100 ft)	NUMBER OF SHEAR REVERSALS
LOW	B1	13	0	12	0	— NO VERT WIND —	
	B2	11	1	— NO LAT WIND —			
	B3	8	1	8	1		
	B4	15	0	5	0		
MODERATE	B5	16	1	12	0	— NO VERT WIND —	
	B6	12	0	16	1		
	B7	10	1	5	0	3	1
	B8	20	0	14	1	3	1
HIGH	B9	22	1	18	1	4	0
	B10	21	1	— NO LAT WIND —		18	1
	B11	20	1	3	0	11	3
	B12	19	1	3	0	23	3

and avoidance of severe wind shear. To obtain an indication of wind shear magnitude as a function of altitude, we selected 12 representative wind profiles, computed the magnitude of wind shear in knots per 100 feet on a 3-degree glide slope for each, and averaged them together. The results (see Figure 19) showed that most of the wind shear activity occurred below an altitude of 400 feet, with the wind shear in the longitudinal wind component peaking at approximately 100-feet altitude.

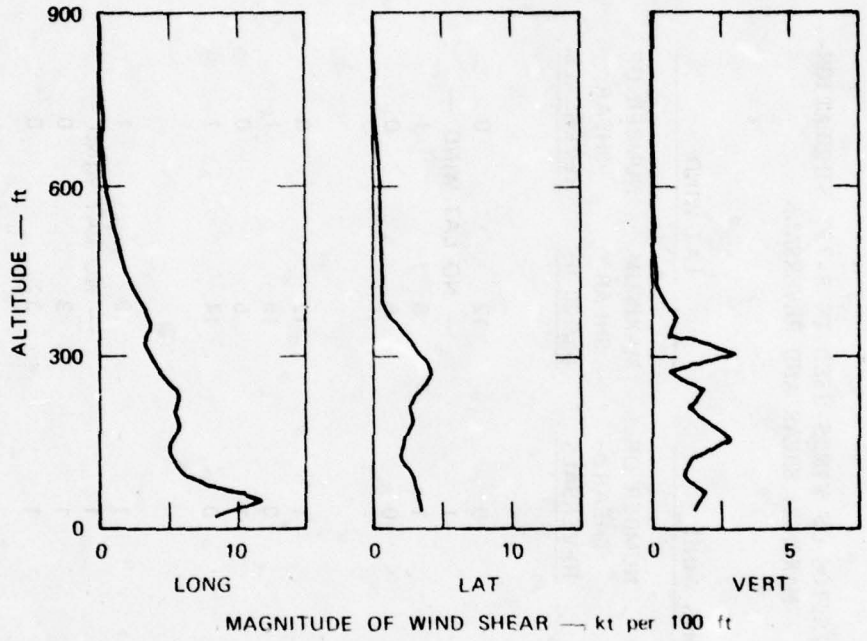

FIGURE 19 MAGNITUDE OF WIND SHEAR AS A FUNCTION OF ALTITUDE (averaged over 12 representative wind profiles)

VI CANDIDATE STANDARD WIND PROFILES

Recent research conducted by the FAA Wind Shear Program Office[9,13] and other organizations has demonstrated development of promising systems that will warn the pilot of potential wind shear hazard and will aid him in coping with variable winds should he inadvertently encounter a hazardous wind shear condition. It has also been demonstrated that pilots benefit from training in motion base simulators using wind models incorporating wind shear.

There is a need for a common standard against which promising techniques may be flown. The object would not be to fly through a set of wind profiles because in the operational environment there will likely be hazardous conditions that are not penetrable. Instead, it is emphasized that standard wind profiles be designed to demonstrate methods and systems that will enable the pilot to cope successfully with wind shear. Successful coping with wind shear includes the ability to detect the onset of wind shear and to safely avoid hazardous wind conditions. In addition, if the wind conditions are not hazardous but lie within the capabilities of the aircraft, the pilot should possess the methods and systems that will allow him to safely execute his flight plan in a confident and flexible manner. A set of standard profiles would thus be designed to include both very hazardous wind profiles that would best be avoided and relatively mild wind profiles that could be safely negotiated.

Standard wind profiles could also be used in pilot familiarization and training. Besides improving his techniques for detecting and coping with wind shear, the pilot would become more aware of the capabilities and handling qualities of his aircraft in a known wind shear environment.

A. Desired Features of Standard Wind Profiles

We have identified several useful features that standard wind profiles should have:

(1) Operational suitability--After successfully and consistently flying the wind profiles in the simulator, there should be a high level of confidence that the methods, systems, and pilots qualified will be able to safely cope with wind shear in the operational environment.

(2) Wide application--The wind profiles should apply to a sufficiently wide range of aircraft and flight control systems. It is obvious that all aircraft will not behave alike in wind shear and that wind shear effects will vary, depending on aircraft configuration and the control system used. Yet a separate wind shear specification for each aircraft configuration would be impractical.

(3) Wide range of severity--A wide range of wind profile severity must be available to represent both very hazardous wind profiles that should be avoided and mild wind profiles that can be negotiated safely. It would be helpful if the wind profiles were parameterized to allow adjustment of severity.

(4) Compatibility with flight simulators--Implementation of the wind profiles should be compatible with existing flight simulators. These machines have memory, computational, and input-output limits. Extensive hardware and software modifications are expensive.

(5) Compatibility with regulations--The design of the wind profiles should be compatible with FAA regulations, such as the airworthiness standards (FAR parts 23 and 25) defining aircraft performance limitations, stability, control, and handling requirements.

It is doubtful that all the above features could be fully implemented without compromise. Some trade-offs must be made. In addition, new and improved wind models are being developed, and therefore, the representation and implementation of a set of standard wind profiles should be designed to anticipate new developments.

B. Wind Profile Design Techniques

A set of standard wind profiles may be assembled by using either well-known, "actual" wind profiles derived from measurements, or abstractions of actual wind profiles, or wind profiles constructed from meteorological models. These techniques are compatible with one another provided that a common means of wind profile representation, such as a tabular arrangement or other common interface, is defined.

On the basis of the wind information received to date and our evaluations using the B-727 and DC-10 aircraft models, we feel that the current data base is adequate to specify a representative set of standard wind profiles for these aircraft. Specific recommendations are given in Appendix D. The advantage of using actual wind profiles is that the methods and systems qualified in the simulator are known to apply directly to the operational environment. This particular set of wind profiles proved useful in the piloted simulator tests and represents a wide but limited range of wind shear severity. The disadvantages of using wind profiles from measured data center on their lack of design flexibility. The choice of wind profiles is limited, and their severity is difficult to adjust.

Another design technique for generating a set of standard wind profiles is to represent measured wind data in a simplified, easily manipulated form. Wind shear severity can then be varied or specific wind profile features modified. The resulting wind profile would be an abstraction of the original wind profile. Normally, one thinks of wind profile shapes and features in terms of a history (expressed in terms of time, altitude, or distance) of the winds encountered by the aircraft on a typical flight path. An example would be a plot of wind as a function of altitude for a 2.8-degree glide slope, as shown in Figure 20. However, it is important to program winds as a function of both distance and altitude. When a wind profile is constructed or modified using the representation along a particular glide path (Figure 20), a method of transforming the result to a two-dimensional wind field representation is required. We asked ourselves how much the wind shear depended on distance as opposed to depending on height above the runway. For example, if the wind profile shown in Figure 20 were entirely dependent on distance, it could be represented by Table 8(a); alternatively, if it were entirely dependent on altitude, it could be represented by Table 8(b); or if it depended on both altitude and distance, Table 8(c) might be used. In the table the highlighted diagonal elements designate the wind encountered on the 2.8-degree glide path.

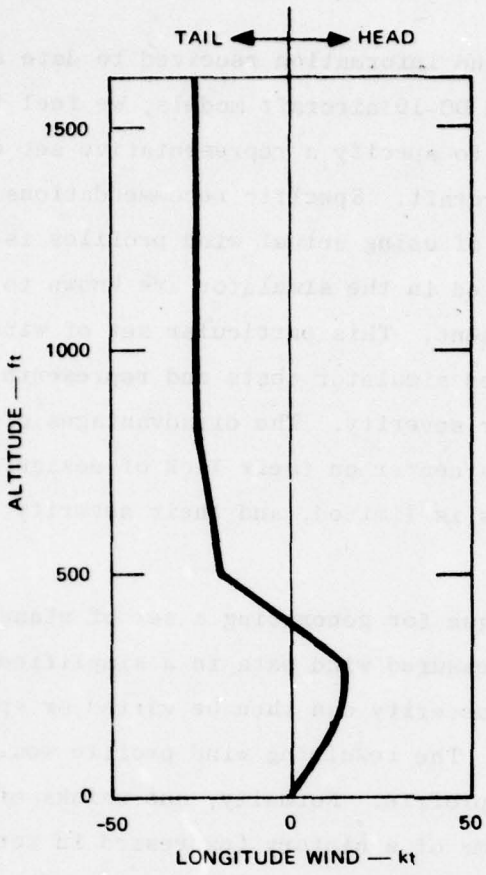

FIGURE 20 WIND PROFILE CONSTRUCTED FROM STRAIGHT LINE SEGMENTS ON A 2.8° GLIDE PATH

The tables were constructed using the following definition of distance factor $\bar{d}$.

$$u_{(h,x)} = \bar{d}u_{(x,x)} + (1-\bar{d})u_{(h,h)} \qquad (5)$$

where $u_{(h,x)}$ is an element of the wind table matrix U with indices h for altitude and x for distance. The specified flight path fills the diagonal elements of U. Given $\bar{d}$ the off-diagonal elements may be filled using equation (5). The distance factor $\bar{d}$ varies from 0.0 for wind dependent entirely on altitude, to 1.0 for wind dependent entirely on distance. Table 8(c) was computed using a distance factor of 0.5. Use of the distance factor offers a means for constructing artificial wind profiles.

Moreover, the idea can be extended to include definition of a distance factor matrix D containing elements $d_{(h,x)}$ relating the $u_{(h,x)}$ to the diagonal elements.

$$u_{(h,x)} = d_{(h,x)}u_{(x,x)} + (1-d_{(h,x)})u_{(h,h)} \qquad (6)$$

The distance factor matrix gives a means of examining existing wind profiles and suggests a method for choosing reasonable values of $\bar{d}$ for newly constructed wind profiles.

A survey was conducted using wind profiles from measured frontal system and thunderstorm data. The distance factor matrix D was computed for each wind profile, and the arithmetic mean $\bar{d}$ was then taken of the off-diagonal elements of D. For longitudinal, lateral, and vertical wind components, $\bar{d}$ ranged from 0.55 to 0.81, 0.50 to 0.84, and 0.41 to 0.72, respectively. The average $\bar{d}$ for all the wind profiles was 0.71 for the longitudinal wind component, 0.70 for the lateral component, and 0.54 for the vertical component. This showed that the measured wind profiles were highly dependent on distance.

Several wind profiles generated by methods similar to those described above were successfully constructed (or modified) and tested using the computer model. When wind profiles are so generated, meteorological credibility is traded for design flexibility; the constructed wind profiles do not necessarily obey the laws of fluid mechanics. However, it may be argued that a set of standard wind profiles should be directed toward exercising the aeronautical system under a set of systematically constructed test conditions. To precisely generate the test conditions in a direct and timely manner, some sacrifice in authenticity can be justified.

Parameterized mathematical models representing specific meteorological conditions offer both flexibility and realism for the construction of wind profiles. Wind models exist for unstable, neutral, and stable boundary layer meteorological conditions, but measured data are generally relied on for very stable conditions, frontal systems, and thunderstorms. Since frontal systems and thunderstorms are known producers of hazardous

Table 8

WIND TABLES REPRESENTING CONSTRUCTED WIND PROFILE

Height above runway (ft)	Distance to Glide Slope Intercept (ft x 1000)								
	16	14	12	10	8	6	4	2	0
800	-26.00	-24.00	-22.00	-20.00	-2.50	15.00	15.00	7.50	0.00
700	-26.00	-24.00	-22.00	-20.00	-2.50	15.00	15.00	7.50	0.00
600	-26.00	-24.00	-22.00	-20.00	-2.50	15.00	15.00	7.50	0.00
500	-26.00	-24.00	-22.00	-20.00	-2.50	15.00	15.00	7.50	0.00
400	-26.00	-24.00	-22.00	-20.00	-2.50	15.00	15.00	7.50	0.00
300	-26.00	-24.00	-22.00	-20.00	-2.50	15.00	15.00	7.50	0.00
200	-26.00	-24.00	-22.00	-20.00	-2.50	15.00	15.00	7.50	0.00
100	-26.00	-24.00	-22.00	-20.00	-2.50	15.00	15.00	7.50	0.00
0	-26.00	-24.00	-22.00	-20.00	-2.50	15.00	15.00	7.50	0.00

(a) Long. wind as a function of distance, $\bar{d} = 1$

Height above runway (ft)	Distance to Glide Slope Intercept (ft x 1000)								
	16	14	12	10	8	6	4	2	0
800	-26.00	-26.00	-26.00	-26.00	-26.00	-26.00	-26.00	-26.00	-26.00
700	-24.00	-24.00	-24.00	-24.00	-24.00	-24.00	-24.00	-24.00	-24.00
600	-22.00	-22.00	-22.00	-22.00	-22.00	-22.00	-22.00	-22.00	-22.00
500	-20.00	-20.00	-20.00	-20.00	-20.00	-20.00	-20.00	-20.00	-20.00
400	-2.50	-2.50	-2.50	-2.50	-2.50	-2.50	-2.50	-2.50	-2.50
300	15.00	15.00	15.00	15.00	15.00	15.00	15.00	15.00	15.00
200	15.00	15.00	15.00	15.00	15.00	15.00	15.00	15.00	15.00
100	7.50	7.50	7.50	7.50	7.50	7.50	7.50	7.50	7.50
0	0.00	0.00	0.00	0.00	0.00	0.00	0.00	0.00	0.00

(b) Long. wind as a function of altitude, $\bar{d} = 0$

Height above runway (ft)	Distance to Glide Slope Intercept (ft x 1000)								
	16	14	12	10	8	6	4	2	0
800	-26.00	-25.00	-24.00	-23.00	-14.25	-5.50	-5.50	-9.25	-13.00
700	-25.00	-24.00	-23.00	-22.00	-13.25	-4.50	-4.50	-8.25	-12.00
600	-24.00	-23.00	-22.00	-21.00	-12.25	-3.50	-3.50	-7.25	-11.00
500	-23.00	-22.00	-21.00	-20.00	-11.25	-2.50	-2.50	-6.25	-10.00
400	-14.25	-13.25	-12.25	-11.25	-2.50	6.25	6.25	2.50	-1.25
300	-5.50	-4.50	-3.50	-2.50	6.25	15.00	15.00	11.25	7.50
200	-5.50	-4.50	-3.50	-2.50	6.25	15.00	15.00	11.25	7.50
100	-9.25	-8.25	-7.25	-6.25	2.50	11.25	11.25	7.50	3.75
0	-13.00	-12.00	-11.00	-10.00	-1.25	7.50	7.50	3.75	0.00

(c) Long. wind as a function of distance and altitude, $\bar{d} = 0.5$

wind shear, models relating these conditions to aircraft operations are under development. For example, Sowa[4] has estimated wind shear from temperature and velocity differences across frontal systems, and Mitchell,[14] Caracena (NOAA), and Babcock (SRI) have independently investigated mathematical models of thunderstorm downdraft-outflow systems. The modeling of complete frontal systems and thunderstorms is a very complex problem, yet the modeling of individual wind profiles on aircraft approach or takeoff is feasible. An example is the 3-degree approach near a single downdraft-outflow cell shown in Figure 21. The wind velocities were computed in real time using the model proposed by Babcock. It is anticipated that the development of improved meteorological wind models at SRI and other research organizations will continue.

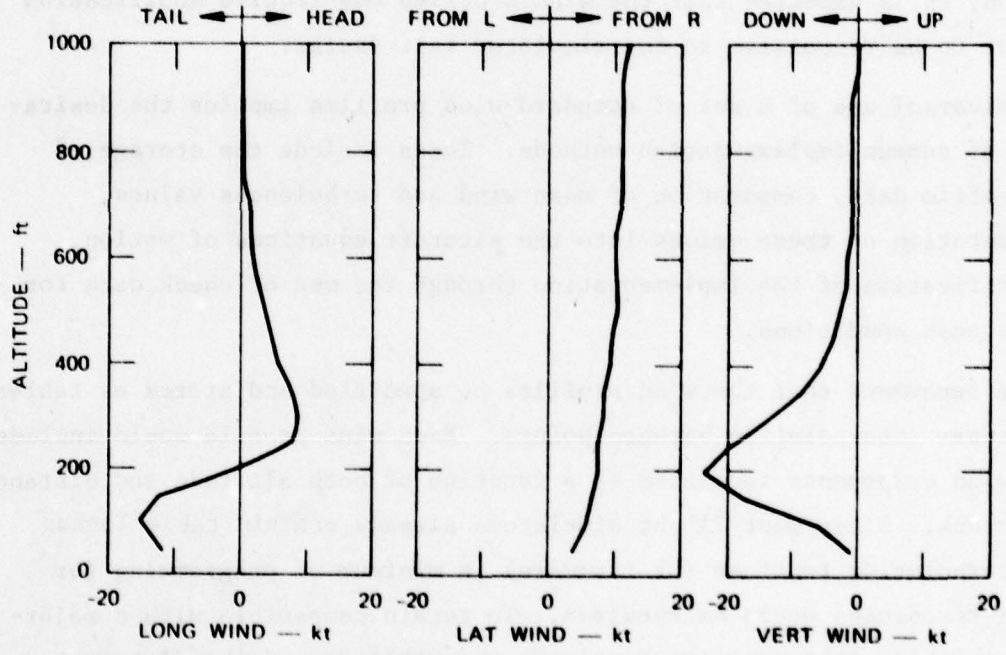

FIGURE 21 WIND PROFILE FROM SYMMETRICAL DOWNFLOW MODEL

C. Candidate Standard Wind Profiles

The wind profiles recommended for use as standard wind profiles (Appendix D) were derived from either measured data or well-known mathematical models. The wind shear severity represented ranges from sufficiently mild wind profiles, which can be safely negotiated, to hazardous wind profiles, which should be avoided. These wind profiles have proved useful in piloted DC-10 and B-727 simulator tests. Although we are confident of their suitability for these aircraft, use of these same wind profiles has not been fully verified for other aircraft. After the effects of wind shear on an increasing number of aircraft, flight configurations, and control systems have been evaluated, the addition or substitution of wind profiles of differing severity may be required. If necessary, the design techniques described in this section may be used to extend the range of wind shear severity. Further, for the purposes of system qualification, it is expected that the wind profiles may require modification in order to be responsive to the simulator test design.

Universal use of a set of standard wind profiles implies the desirability of common implementation methods. These include the storage of wind profile data, computation of mean wind and turbulences values, implementation of these values into the aircraft equations of motion, and verification of the implementation through the use of check data for various test conditions.

We recommend that the wind profiles be specified and stored as tables with linear interpolation between points. Each wind profile would include three wind components specified as a function of both altitude and distance along track. Since most flight simulators already contain table lookup and interpolation routines (or firmware), a minimum of programming (or machine resources) would be required. To remain compatible with a majority of existing interpolation routines, the altitude and the distance points should be equally spaced. An example of the tabular arrangement is shown in Table 9. In addition, we recommend that the implementation include provisions for the adjustment of aircraft position (distance) relative to the wind field so that the winds may be varied on approach and that the wind field may be repositioned for takeoff runs. This

Table 9

TABULAR REPRESENTATION FOR STANDARD WIND PROFILES
(Wind Profile T8A)

Height above runway (ft)	Distance (ft)																
	-15600	-14400	-13200	-12000	-10800	-9600	-8400	-7200	-6000	-4800	-3600	-2400	-1200	0	1200	2400	3600
900	-6.73	-6.73	-5.07	-2.37	-1.24	0.34	9.13	16.36	19.56	21.82	23.67	23.75	20.33	13.77	19.12	16.57	14.46
790	-6.10	-6.10	-4.60	-1.98	-0.44	1.49	9.30	16.80	19.95	21.74	23.46	23.03	18.60	14.26	17.74	16.30	14.81
680	-5.88	-5.88	-4.61	-2.04	0.35	2.99	8.71	16.86	20.61	22.42	23.88	23.24	18.94	15.32	15.94	15.78	14.08
570	-4.52	-4.52	-2.96	0.12	2.78	5.54	9.47	17.73	21.08	22.60	23.93	23.20	18.64	13.82	13.88	13.99	13.23
460	-3.07	-3.07	-1.31	2.04	4.80	7.84	11.04	18.47	21.13	22.33	23.69	23.16	18.42	12.27	11.70	12.38	12.55
350	-2.13	-2.13	-0.82	1.87	4.74	8.85	13.64	18.36	20.28	21.26	23.02	23.30	18.81	12.33	9.39	12.04	12.39
240	-1.56	-1.56	-0.18	2.81	6.14	10.14	14.51	18.99	20.33	21.05	22.89	23.01	17.99	11.75	7.12	10.89	11.87
130	-0.97	-0.97	0.56	3.95	7.68	11.41	15.14	19.44	20.48	20.95	22.75	22.55	16.84	11.02	5.28	9.62	11.20
20	-0.15	-0.15	1.44	4.92	8.69	12.45	16.22	19.13	20.32	20.66	22.31	21.93	15.60	10.32	4.38	8.52	10.41

Longitudinal Wind (kts)

Height above runway (ft)	Distance (ft)																
	-15600	-14400	-13200	-12000	-10800	-9600	-8400	-7200	-6000	-4800	-3600	-2400	-1200	0	1200	2400	3600
900	-7.92	-7.92	-7.65	-7.06	-6.34	-5.46	-4.23	-0.80	0.00	-0.44	0.04	1.57	1.99	-0.83	-2.97	-3.58	-3.12
790	-7.82	-7.82	-7.54	-6.90	-6.15	-5.37	-4.21	-0.79	-0.09	-0.64	0.06	2.08	2.93	0.74	-1.76	-2.65	-2.01
680	-7.62	-7.62	-7.37	-6.79	-6.10	-5.38	-4.34	-0.82	-0.40	-0.99	0.09	2.48	3.51	2.13	-0.21	-0.60	-0.69
570	-7.48	-7.48	-7.37	-7.06	-6.61	-5.97	-4.59	-1.44	-1.00	-1.32	0.04	2.59	3.81	2.89	0.63	0.14	0.07
460	-7.29	-7.29	-7.32	-7.32	-7.15	-6.58	-4.84	-2.22	-1.72	-1.64	-0.07	2.55	4.06	3.53	1.65	1.01	1.00
350	-6.97	-6.97	-7.07	-7.28	-7.36	-6.84	-4.98	-2.98	-2.50	-1.96	-0.27	2.33	4.40	4.28	3.54	3.08	2.72
240	-6.74	-6.74	-6.93	-7.29	-7.46	-6.99	-5.16	-3.50	-2.93	-2.11	-0.29	2.35	4.77	5.57	5.66	4.74	3.77
130	-6.53	-6.53	-6.77	-7.25	-7.54	-7.24	-5.38	-3.90	-3.31	-2.43	-0.43	2.48	5.24	6.81	7.28	6.11	4.61
20	-6.27	-6.27	-6.51	-7.06	-7.63	-7.75	-5.66	-4.16	-3.80	-3.20	-0.94	2.68	5.93	7.62	7.70	7.04	5.37

Lateral Wind (kts)

Height above runway (ft)	Distance (ft)																
	-15600	-14400	-13200	-12000	-10800	-9600	-8400	-7200	-6000	-4800	-3600	-2400	-1200	0	1200	2400	3600
900	0.49	0.49	0.63	0.92	1.36	2.50	5.12	1.61	0.09	-0.09	0.15	-0.42	-2.80	-5.41	0.73	-2.39	3.75
790	0.61	0.61	0.63	0.76	1.29	2.80	4.54	1.81	0.21	-0.12	0.05	-0.57	-2.76	-4.87	0.63	-2.13	3.07
680	1.11	1.11	0.84	0.63	1.20	2.01	3.88	0.89	-0.16	-0.24	-0.10	-0.66	-2.41	-3.19	0.60	-1.66	2.32
570	0.58	0.58	0.48	0.58	1.25	1.97	3.27	0.60	-0.21	-0.30	-0.32	-0.86	-2.23	-2.78	-0.13	-1.73	1.78
460	0.02	0.02	0.13	0.53	1.23	1.93	2.63	0.48	-0.19	-0.38	-0.56	-1.04	-2.01	-2.57	-0.72	-1.83	1.32
350	0.08	0.08	0.18	0.47	0.94	1.39	1.87	0.35	-0.25	-0.53	-0.80	-1.12	-1.56	-1.95	-0.51	-1.64	0.92
240	0.06	0.06	0.11	0.28	0.50	0.67	0.82	0.14	-0.17	-0.34	-0.50	-0.66	-0.86	-1.03	-0.22	-0.91	0.47
130	0.02	0.02	0.04	0.10	0.13	0.10	0.04	-0.02	-0.07	-0.12	-0.16	-0.20	-0.26	-0.27	-0.01	-0.26	0.13
20	0.00	0.00	0.01	0.01	0.02	0.02	0.01	-0.00	-0.01	-0.02	-0.02	-0.03	-0.04	-0.04	-0.00	-0.04	0.02

Vertical Wind (kts)

adjustment may be made by adding a selected number to the aircraft distance coordinate before it is used with the lookup tables. The surface winds for a given wind profile may be varied by adding a selected constant to the longitudinal wind component after the table lookup function. The accuracy of the meteorological model is only slightly affected by this "steady" movement of the wind field.

The turbulence models (Appendix A) developed from the Dryden[8] spectra are recommended because they are well known, reasonably simple to implement, and currently used in some simulators. Pilot comments in previous simulator studies that used this model were favorable. Each wind profile would include turbulence parameters with three rms intensities and three scale lengths, each specified as a function or altitude using a table lookup function of equally spaced points with linear interpolation between points.

VII CONCLUSIONS

In the following paragraphs, our major conclusions are summarized.

A. Quality of Computer Model Design

The method used in this project relied on a fast-time computer model that incorporated horizontal, vertical, and pitching motion (3 degrees of freedom), and used aircraft models flown with a pitch controller similar to that provided by an autopilot and a thrust controller to maintain a reference airspeed. The model yielded consistant and reliable results that agreed substantially with piloted simulator results providing more comprehensive simulations.

The computer modeling techniques used have proved to be a valuable supplement to piloted simulator tests. In addition to providing comparisons of wind profile severity and data for case studies on the effects of wind shear, automated fast-time computer modeling enables evaluation and refinement of techniques for coping with wind shear before the techniques are committed to costly piloted simulator tests.

B. Effects of Wind Shear on Aircraft

Generally, the severity of wind shear encounters was found to be highly dependent on the position and alignment of the approach path with respect to the wind field and on the timing of the encounter. The effects of wind shear on aircraft were dependent on aircraft configuration, engine response, control systems, and control technique. Prediction of the outcome when an aircraft encounters low-level wind shear in a complex wind field is thus difficult from knowledge of the wind field alone.

Another conclusion was that the aircraft models tested were affected by wind shear in the vertical wind component as well as by wind shear in the longitudinal wind component. Yet for all wind profiles derived from measured data, the maximum shear (23 knots per 100 feet) was comparable

in magnitude for vertical and longitudinal wind components. Shearing vertical winds were often accompanied by shearing longitudinal winds. In the high-severity wind profiles, the two wind components combined adversely to produce complex wind shear possessing greater hazards; in the low-severity wind profiles, no shear in the vertical component was present. Higher severity profiles were also found to contain reversals in wind shear direction.

The height and strength of the encounter is important to the successful detection and avoidance of severe wind shear. Wind shears occurring at low altitudes (from 100 to 300 feet) do not allow much time for detection and recovery. Severe wind shears occurring at higher altitudes may force a long landing because of overshoot during recovery; however, they allow additional time for the pilot to execute a go-around.

Severe wind shear was also found to be hazardous on takeoff. The hazards of wind shear encountered on takeoff are different in some respects from those encountered on approach and landing. For example, the departure path is steeper, and the effects are more localized. Because of the steeper path and higher airspeeds, the time of exposure to potentially hazardous shear is lessened. Measurement and prediction of potentially hazardous wind shear may be easier over the shorter time frame. On the other hand, on takeoff there is generally less reserve thrust available for recovering from a loss of airspeed induced by wind shear.

C. Relating Wind Shear Severity to Weather Phenomena

Most of the wind profiles tested in this project were based on actual weather conditions. Of three broad classes of wind conditions (atmospheric boundary layer effects, frontal systems, and thunderstorms) the most severe wind shear encounters occurred in wind fields produced by thunderstorms. Such wind fields are of complex form in which the wind profiles encountered by the aircraft varied greatly with distance. Large wind shears in both vertical and longitudinal wind components were found and they often occurred simultaneously; reversals in wind shear direction were common. In spite of the fact that a given wind field contained hazardous wind profiles, about 80 percent of the flights through the wind field at various

GPIP positions resulted in safe passage; i.e., their outcome was not adversely affected. The timing and positioning of the wind shear encounters were hazardous to the aircraft in a comparatively small percentage of flights. The situation is complicated further because a thunderstorm system may contain several storm cells traveling at a rate sufficient to produce entirely different wind profiles to each aircraft in a landing sequence.

Wind profiles from frontal systems varied considerably in relative severity, but were generally lower in potential severity than wind profiles from thunderstorms. Less wind shear in the vertical wind component of frontal wind profiles was found, since frontal systems lack the downflow region found in thunderstorms. The frontal wind fields varied less with distance, were less dynamic, and more predictable than wind fields attributed to thunderstorms. It is noted, however, that frontal systems are potentially very hazardous to aircraft operations. For example, a frontal profile may have moderate, sustained rates of shear with reversals accompanied by little or no turbulence. Thus, a moderate or high severity wind profile may not be detected until it is too late to avoid or recover from the effects of wind shear.

Wind profiles arising from atmospheric boundary layer effects tested in this project ranked low in relative severity. The unstable, stable, and neutral categories of boundary layer winds contained no vertical wind component and no low-altitude reversals in wind shear direction. When constant surface friction velocity and surface roughness were assumed, the wind fields varied only as a function of altitude. The most hazardous category of boundary layer wind is the very stable case (low-level jet), which is characterized by potentially high shear rates and low-level reversals in wind shear direction. Although the low-level jet wind profiles tested ranked low-to-moderate in relative severity, potentially dangerous low-level jet winds are possible.

VIII RECOMMENDATIONS

The results of the hazard determination work support the following recommendations:

(1) In this project, the behavior of the aeronautical system in wind shear was examined for a single piloting technique, one control system design, and two aircraft models. To quantify more explicitly the meaning of the severity ratings and the scope of the candidate standard wind profiles, future research should be extended to include additional aircraft models, aircraft configurations, control system designs, and piloting techniques.

(2) Go-around procedures and go-around control techniques should be included with analysis of approach and landing in wind shear.

(3) Techniques for recognizing and coping with wind shear during takeoff and climbout should be developed.

(4) The potential hazards of crosswinds should be evaluated. Hazard determination of crosswinds may be accomplished using analysis techniques, a lateral axis computer model, a 6-degree-of-freedom model, or by examination of past piloted simulation results.

(5) The methods used to implement standard wind profiles into simulator aeronautical models should be specified to ensure a uniform implementation (implementations are known to vary among existing flight simulators). Procedures to systematically check the implementation should be designed. The wind profiles will then truly represent a standard.

(6) Development of improved wind models suitable for training and system qualification should be continued. A wind profile data base should be assembled and maintained to support further wind shear research and flight simulator training programs.

APPENDIX A

WIND PROFILE REPRESENTATION AND TURBULENCE MODEL FOR SIMULATOR TESTS

1. Mean Wind Specification

Each wind profile includes three wind components specified as a function of both altitude and distance along track. Each component is specified as a table lookup function with up to 21 altitude values and up to 16 distance values with straight-line interpolation between points. The altitude points are not equally spaced nor are they the same for each wind profile, although they are the same over all distance values of a given profile. The maximum amount of storage required for the mean wind values is 3 x 21 x 16 = 1008 points.

2. Turbulence Specification

Turbulence parameters are included with each wind shear profile. Six parameters (3 rms intensities and 3 scale lengths) are each specified as a function of altitude using a table lookup function with up to 21 altitude values. The maximum amount of storage required for the turbulence associated with a wind profile is 6 x 21 = 126 points. This brings the maximum total storage for a wind profile with turbulence to 1008 + 126 = 1134 points.

The turbulence models used are developed from the Dryden spectra[8]. Turbulence wind components are generated by feeding a random, white, zero-mean, unit-variance input into a filter F(s). Transfer functions are as follows:

Longitudinal $$F_u(s) = \sigma_u \sqrt{\frac{L_u}{\pi V_a}} \frac{1}{1 + \frac{L_u}{V_a} s} ;$$

$$\text{Lateral} \qquad F_v(s) = \sigma_v \sqrt{\frac{L_v}{2\pi V_a}} \; \frac{1 + \sqrt{3}\frac{L_v}{V_a}s}{\left(1 + \frac{L_v}{V_a}s\right)^2} \; ;$$

$$\text{Vertical} \qquad F_w(s) = \sigma_w \sqrt{\frac{L_w}{2\pi V_a}} \; \frac{1 + \sqrt{3}\frac{L_w}{V_a}s}{\left(1 + \frac{L_w}{V_a}s\right)^2} \; ;$$

where:

σ_u, σ_v, σ_w = rms intensities

L_u, L_v, L_w = scale lengths

V_a = true airspeed

s = Laplace transform variable.

3. Formatting Of Data Cards

Wind velocity components are given in knots and all distances and altitudes are given in feet. For an aircraft tracking the approach path a positive value of along-track wind indicates a headwind, a positive value of cross-track wind indicates a crosswind blowing from the right, and a positive value of vertical wind indicates an updraft condition. The wind components are given in a space-fixed orthogonal coordinate system originating where the glide path intercepts the runway (GPIP). Negative values of distance are on the approach side of GPIP.

Wind values as a function of altitude and distance are entered into wind tables using 80 character records in the following order and formats. The first record specifies the number of altitude (NH) and distance values (NX) for which wind components are defined. If the value of NX is 1, the winds are a function of altitude only. The two parameters may be read with a FORTRAN statement using the format (2(10x, I2)). The second record contains the value of the first (or only) distance

for which wind components will next be entered. The second record may be read using the format (10x, F10.2). Following this is a group (numbering NH) of input records with each record containing a discrete altitude and the respective along-track, cross-track, and vertical-wind values. These records may be read using the format (4(10x, F10.4)). Table A-1 shows an example of wind component inputs for a wind profile defined for 10 altitudes and 10 distances.

Table A-1

FORMAT OF MEAN WIND INPUTS

Record No.	Item	Character Field Position
1	No. of altitudes	11-12
	No. of distances	23-24
2	First distance value	11-20
3	First altitude	11-20
	Along track wind	31-40
	Cross track wind	51-60
	Vertical wind	71-80
4	Second altitude	11-20
	Along track wind	31-40
	Cross track wind	51-60
	Vertical wind	71-80
•	•	•
•	•	•
•	•	•
13	Last altitude	11-20
	Along track wind	31-40
	Cross track wind	51-60
	Vertical wind	
14	Second distance	11-20
15	First altitude	11-20
	Along track wind	31-40
	Cross track wind	51-60
	Vertical wind	71-80

After all altitudes have been read for the first distance, the next record will contain the second distance value (if any), again followed by records containing the altitude and wind component values. Records will follow

until all wind components have been read for all distances.

Turbulence parameters (sigmas in knots and scale lengths in feet) associated with each wind profile will follow the mean wind component records for a given wind profile description. The first record containing turbulence information gives the number of altitudes for which turbulence parameters are defined in columns 1 and 2 using the format (10x, I2). The following records each specify an altitude and its respective sigma values (along-track, cross-track, vertical) and scale lengths (along-track, cross-track, vertical) and may be read using a 7F10.2 format statement. The ordering of the turbulence parameters is given in Table A-2.

Table A-2

FORMAT OF TURBULENCE INPUTS

Record No.	Item	Character Field Position
1	No. of altitudes	11-12
2	First altitude	1-10
	σ_u along track	11-20
	σ_v cross track	21-30
	σ_w vertical	31-40
	L_u along track	41-50
	L_v cross track	51-60
	L_w vertical	61-70
•	•	•
•	•	•
•	•	•
11	Last altitude	1-10
	σ_u along track	11-20
	σ_v cross track	21-30
	σ_w vertical	31-40
	L_u along track	41-50
	L_v cross track	51-60
	L_w vertical	61-70

APPENDIX B

EQUATIONS OF MOTION

LIST OF SYMBOLS

Symbol	
$\bar{c}$	Mean aerodynamic (geometric) chord
$C_D = \frac{D}{\bar{q}S}$	Aircraft drag coefficient
C_{D_o}	Drag coefficient for zero angle of attack and zero elevator deflection
$C_{D_\alpha} = \frac{\partial C_D}{\partial \alpha}$	Variation of drag coefficient with angle of attack
$C_{D_{\delta_e}} = \frac{\partial C_D}{\partial \delta_e}$	Variation of drag coefficient with elevator angle
$C_L = \frac{L}{\bar{q}S}$	Aircraft lift coefficient
$C_M = \frac{M}{\bar{q}S}$	Aircraft pitching moment coefficient
D	Drag force
d_T	Moment arm of thrustline
g	Acceleration of gravity
h	Height above runway

LIST OF SYMBOLS (Con't)

Symbol	Definition
$H_I = \int_t \Delta h$	Integral with respect to time of height error from glide slope
I_y	Aircraft moment of inertia
L	Lift force
M	Pitching moment
m	Aircraft mass
Q	Aircraft pitch rate
$\bar{q}$	Dynamic pressure
S	Reference surface area
T	Thrust force
T_o	Equilibrium thrust
u_T	Normalized thrust change
t	Time
V_a	Airspeed
V_o	Approach airspeed reference
V_{ex}, V_{eh}	Ground-referenced components of aircraft velocity

LIST OF SYMBOLS (Con't)

Symbol	Definition
V_{wx}, V_{wh}	Components of wind velocity
x	Longitudinal displacement
Δh	Height error from glide slope
ρ	Air density
θ	Pitch attitude angle
θ_o	Reference pitch attitude
γ	Ground-referenced flight path angle
γ_o	Reference flight path
γ_a	Air-referenced flight path angle
α	Angle of attack
δ_e	Elevator deflection
δ_T	Angle of thrustline with respect to fuselage reference line

EQUATIONS OF MOTION

Derivation of the aircraft equations of motion includes the following assumptions:

(1) The earth is considered an inertial frame.

(2) The aircraft is a rigid body confined to move in the X-Z plane with no lateral forces acting on it.

(3) Air density, acceleration of gravity, aircraft mass, and aircraft mass distribution are constants.

The aircraft is initially in equilibrium flight with no linear or angular accelerations, and no angular rates. The axis system and nomenclature used are defined in Figure B-1. The following angular and velocity relationships are required:

$$V_a = \sqrt{(V_{ex} - V_{wx})^2 + (V_{eh} - V_{wh})^2}$$

$$\gamma_a = \arctan\left(\frac{V_{eh} - V_{wh}}{V_{ex} - V_{wx}}\right)$$

$$\alpha = \theta - \gamma_a$$

The following equations may be derived by summing forces and moments and applying Newton's second law:

$$m\dot{V}_{ex} = T \cos(\theta + \delta_T) - D \cos\gamma_a - L \sin\gamma_a \qquad \text{(B-1)}$$

$$m\dot{V}_{eh} = T \sin(\theta + \delta_T) - D \sin\gamma_a + L \cos\gamma_a - mg \qquad \text{(B-2)}$$

$$I_y\dot{Q} = Td_T + \bar{c}F_A. \qquad \text{(B-3)}$$

where

$$T = T_o[1 + u_T] \ ,$$

$$D = \bar{q}SC_D \ ,$$

$$L = \bar{q}SC_L \ ,$$

$$F_A = \bar{q}SC_M \ ,$$

$$\bar{q} = \tfrac{1}{2}\rho V_a^2 \ .$$

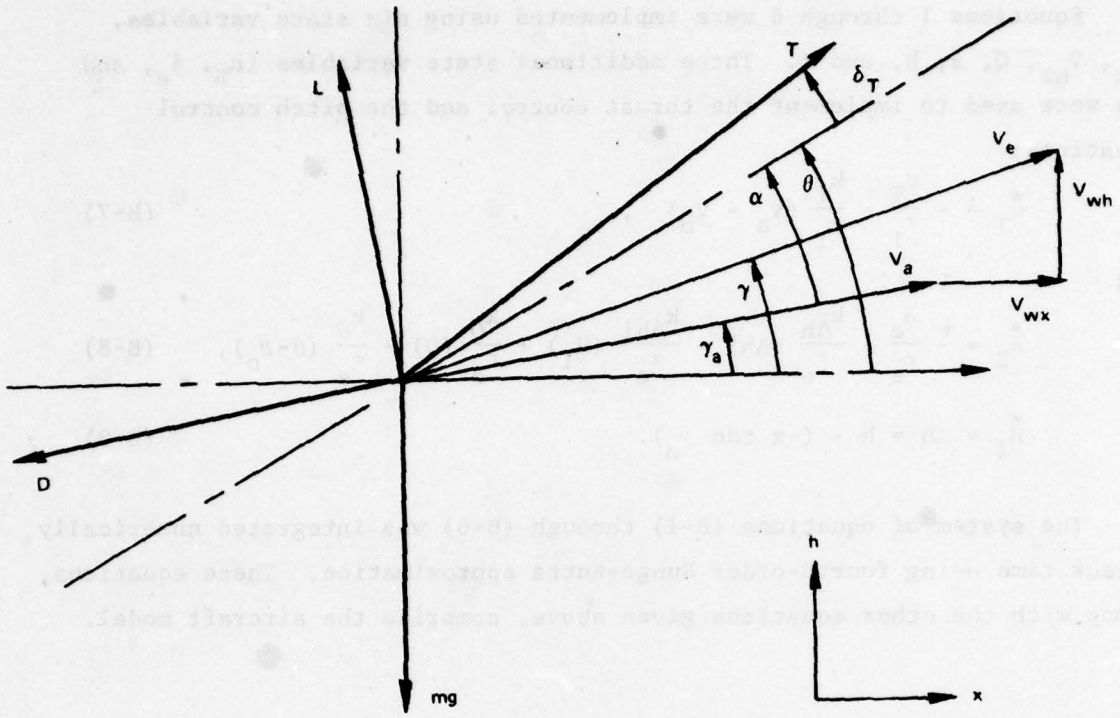

FIGURE B-1 AIRCRAFT MODEL FORCE AND VELOCITY RELATIONSHIPS

The aerodynamic coefficients C_D, C_L, and C_M are functions of a number of variables, and their expressions vary for different aircraft and flight configurations. The usual notation was used for the various stability derivatives, for example,

$$C_D = C_{D_o} + C_{D_\alpha} [\alpha - \alpha_o] + C_{D_{\delta_e}} [\delta_e] \ . \ . \ .$$

The analysis included two sets of aerodynamic coefficients characteristic of a B-727 on approach, a set of coefficients for a DC-10 on approach, and a set for the DC-10 takeoff.

Distances were obtained by integrating the velocity equations:

$$\dot{x} = V_{ex} \qquad \text{(B-4)}$$

$$\dot{h} = V_{ch} \qquad \text{(B-5)}$$

$$\dot{\theta} = Q \tag{B-6}$$

Equations 1 through 6 were implemented using six state variables, V_{ex}, V_{hx}, Q, x, h, and θ. Three additional state variables (u_T, δ_e, and H_I) were used to implement the thrust control and the pitch control equations:

$$\dot{u}_T = -\frac{u_T}{\tau_T} - \frac{k_T}{\tau_T}(V_a - V_o) \quad , \tag{B-7}$$

and

$$\dot{\delta}_E = -\frac{\delta_e}{\tau_e} - \frac{k_{\Delta h}}{\tau_e}(\Delta h) - \frac{k_{\Delta hi}}{\tau_e}(H_I) + \frac{k_Q}{\tau_e}(Q) - \frac{k_\theta}{\tau_e}(\theta - \theta_o), \tag{B-8}$$

$$\dot{H}_I = \Delta h = h - (-x \tan \gamma_o). \tag{B-9}$$

The system of equations (B-1) through (B-6) was integrated numerically versus time using fourth-order Runge-Kutta approximation. These equations, along with the other equations given above, comprise the aircraft model.

APPENDIX C

WIND PROFILES SELECTED FOR PILOTED SIMULATOR TESTS

Table C-1 summarizes the wind profiles selected for use in piloted simulator tests on wind shear. Since each wind field was examined using a number of runway positions, a number of different wind profiles are available from each wind field. To identify each wind profile, a "derived wind profile number" was assigned.

The wind profiles selected for the piloted simulator tests were also assigned sequential numbers. The wind profiles used in the B-727 simulator tests are prefixed with the letter B, and the wind profiles used in the DC-10 simulator tests are prefixed with the letter D. For example, wind profile numbers N2A, B1, and D1, all represent the wind profile listed first in the table, which was rated "low" in relative severity.

Figures C-1 through C-16 show the three mean wind components, as encountered on a 3-degree glide slope, for the approach wind profiles listed in Table C-1. The takeoff wind profile wind components, as encountered on a 6-degree departure path, are shown in Figures C-17 through C-21.

Table C-1

SUMMARY OF WIND PROFILES USED IN PILOTED SIMULATIONS

Relative Wind Profile Severity	Derived Wind Profile Number	Source of Wind Data	Meteorological Wind Type	B-727 Piloted Simulator Tests, Wind Profile No.	DC-10 Simulator Tests, Wind Profile No.
Approach					
Low	N2A	Meteorological math model	Neutral	B1	D1
	S1A	Meteorological math model	Stable	B2	--
	S2A	Meteorological math model	Stable	B3	--
	S6A	Tower measurements	Stable	B4	--
Moderate	F1A	Logan accident reconstruction	Warm front	B5	D5
	F2A	Same as F1A, rotated 40°	Warm front	B6	--
	T8A	Tower measurements	Thunderstorm	B7	D7
	T9A	Tower measurements	Thunderstorm	B8	D8
	F5A	Tokyo accident reconstruction	Warm front	--	D2
High	F3A	Tower measurements	Cold front	B9	D9
	T24A	Philadelphia accident reconstruction	Thunderstorm	B10	--
	T0A	Kennedy accident reconstruction	Thunderstorm	B11	--
	T0B	Kennedy accident reconstruction	Thunderstorm	B12	D6
	T0C	Kennedy accident reconstruction	Thunderstorm	---	D10
	T25A	Philadelphia accident reconstruction	Thunderstorm	---	D4
	M1A	Mathematical model	Thunderstorm	---	D3
Takeoff					
	T0D	Kennedy accident reconstruction	Thunderstorm	--	D11
	T23A	Philadelphia accident reconstruction	Thunderstorm	--	D12
	T24B	Philadelphia accident reconstruction	Thunderstorm	--	D13
	T25B	Philadelphia accident reconstruction	Thunderstorm	--	D14
	F3B	Tower measurements	Cold front	--	D15

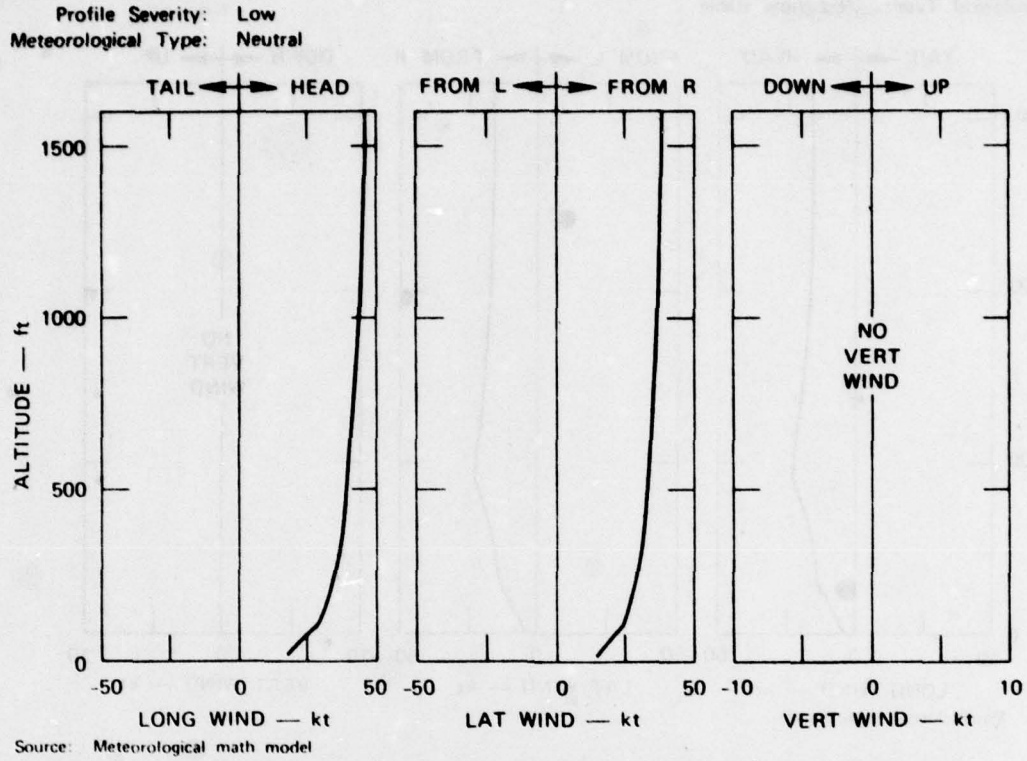

FIGURE C-1 WIND PROFILE N2A, APPROACH ON 3° GLIDE PATH

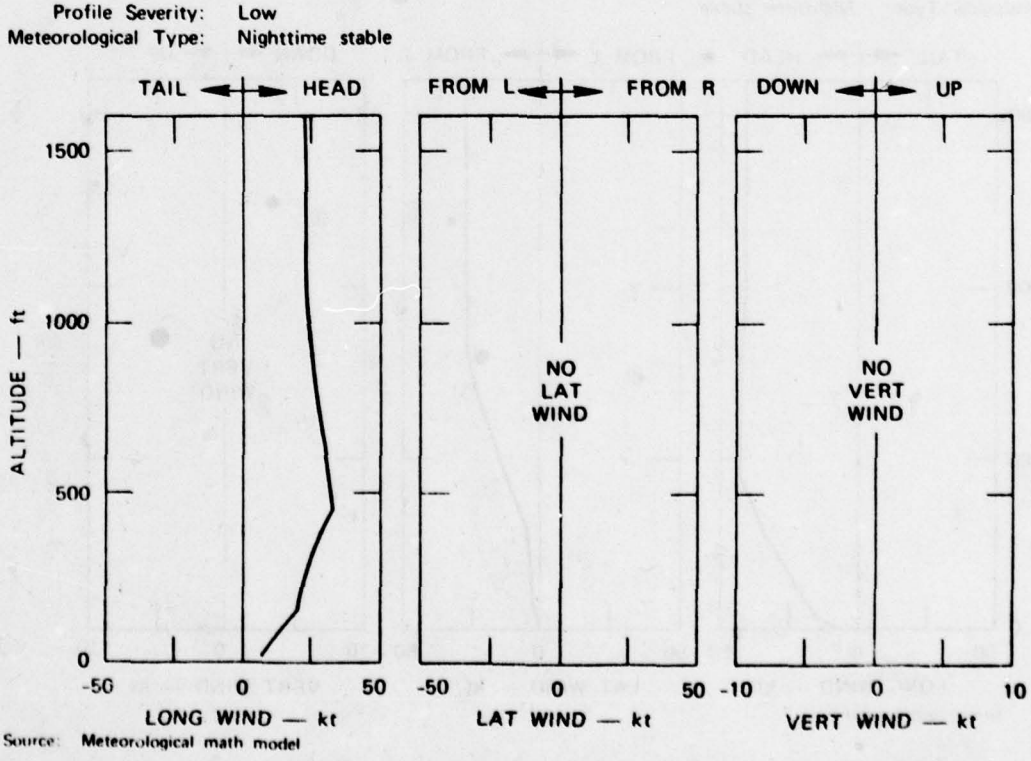

FIGURE C-2 WIND PROFILE S1A, APPROACH ON 3° GLIDE PATH

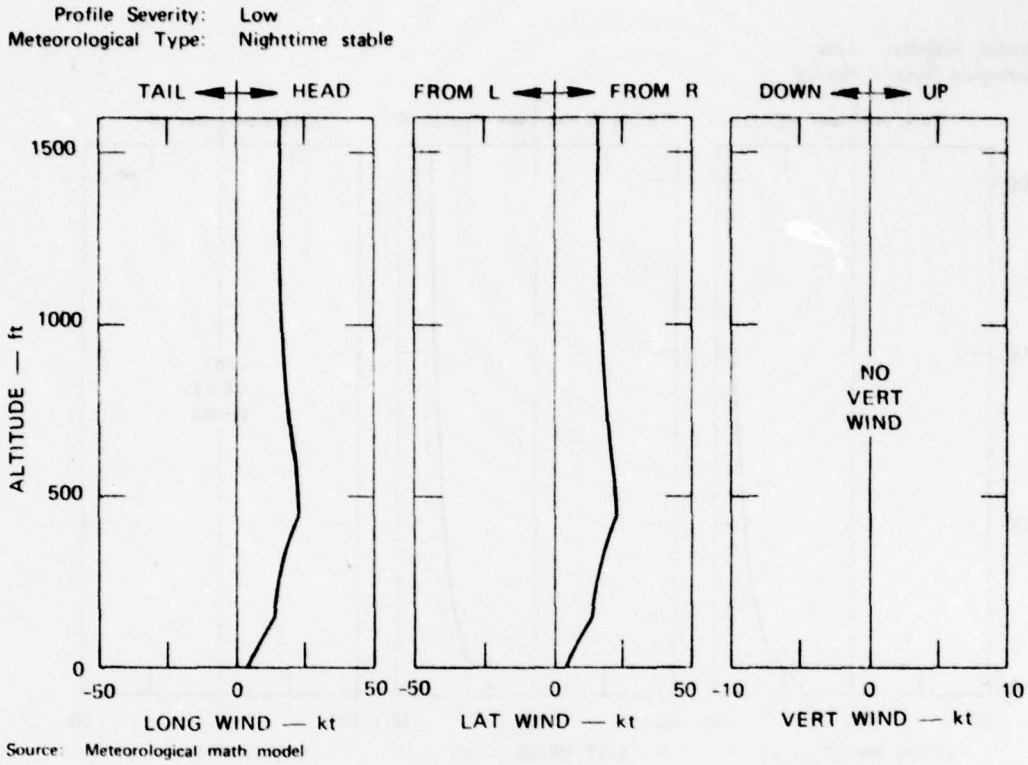

FIGURE C-3 WIND PROFILE S2A, APPROACH ON 3° GLIDE PATH

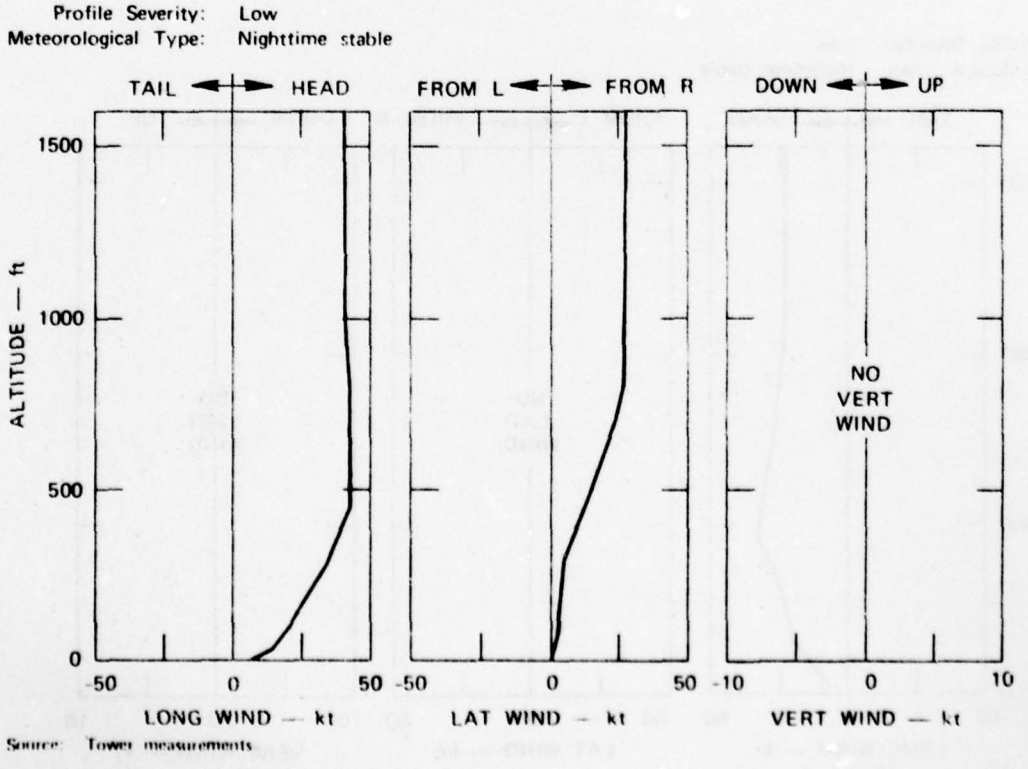

FIGURE C-4 WIND PROFILE S6A, APPROACH ON 3° GLIDE PATH

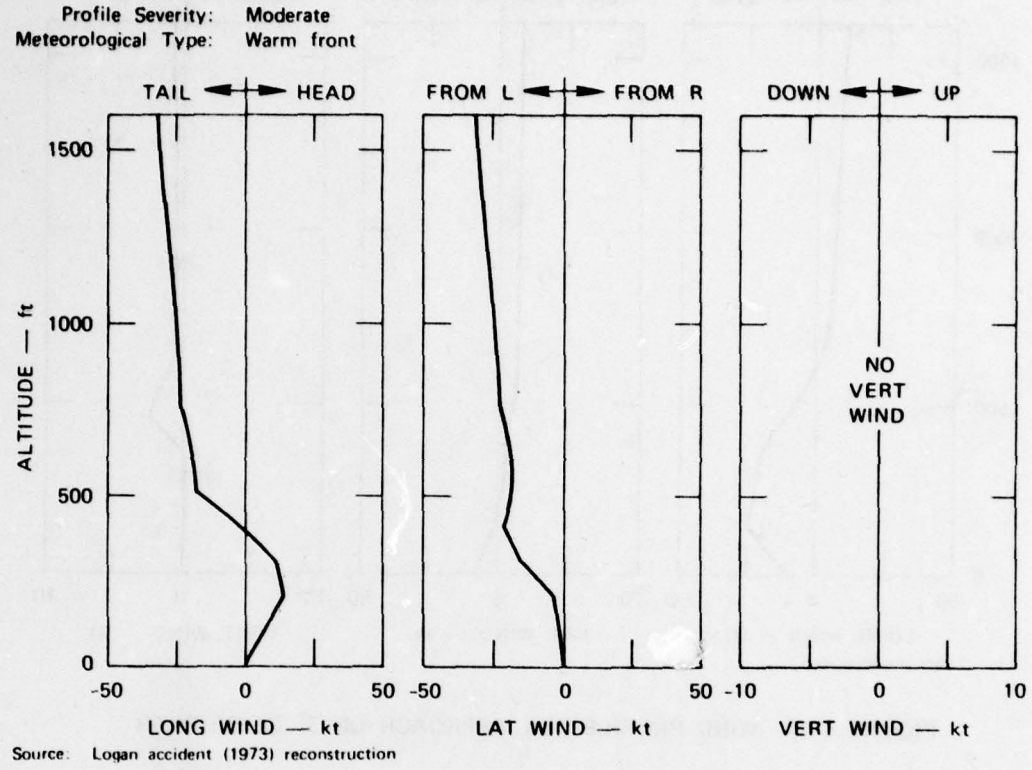

FIGURE C-5 WIND PROFILE F1A, APPROACH ON 3° GLIDE PATH

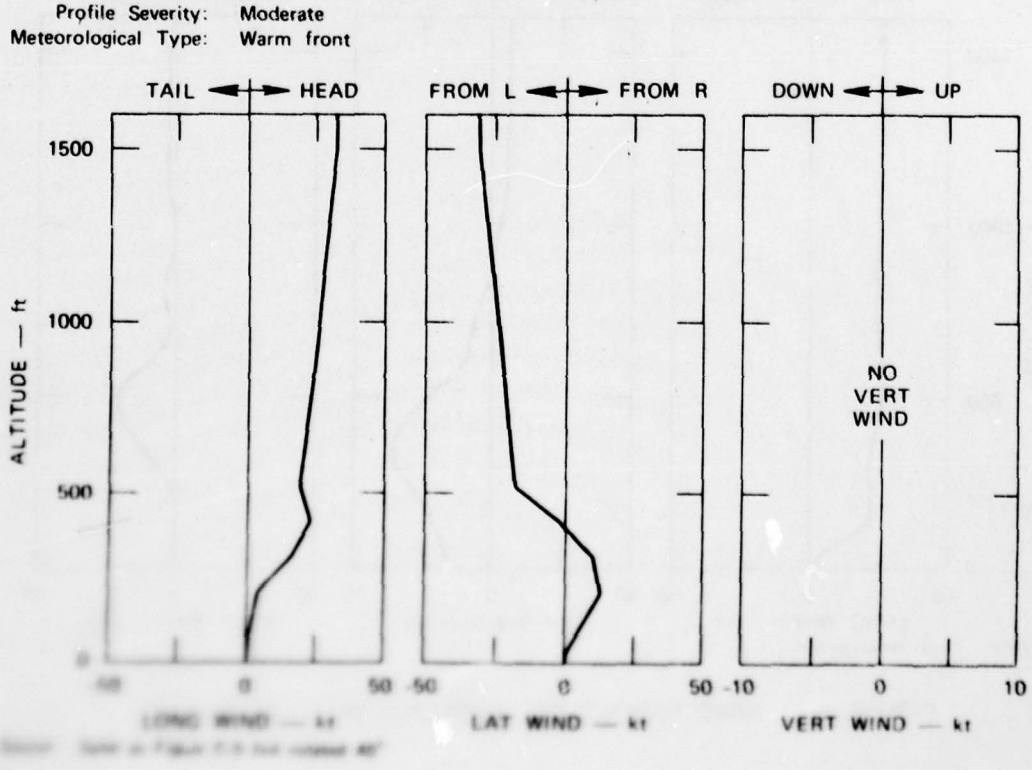

FIGURE C-6 WIND PROFILE F2A, APPROACH ON 3° GLIDE PATH

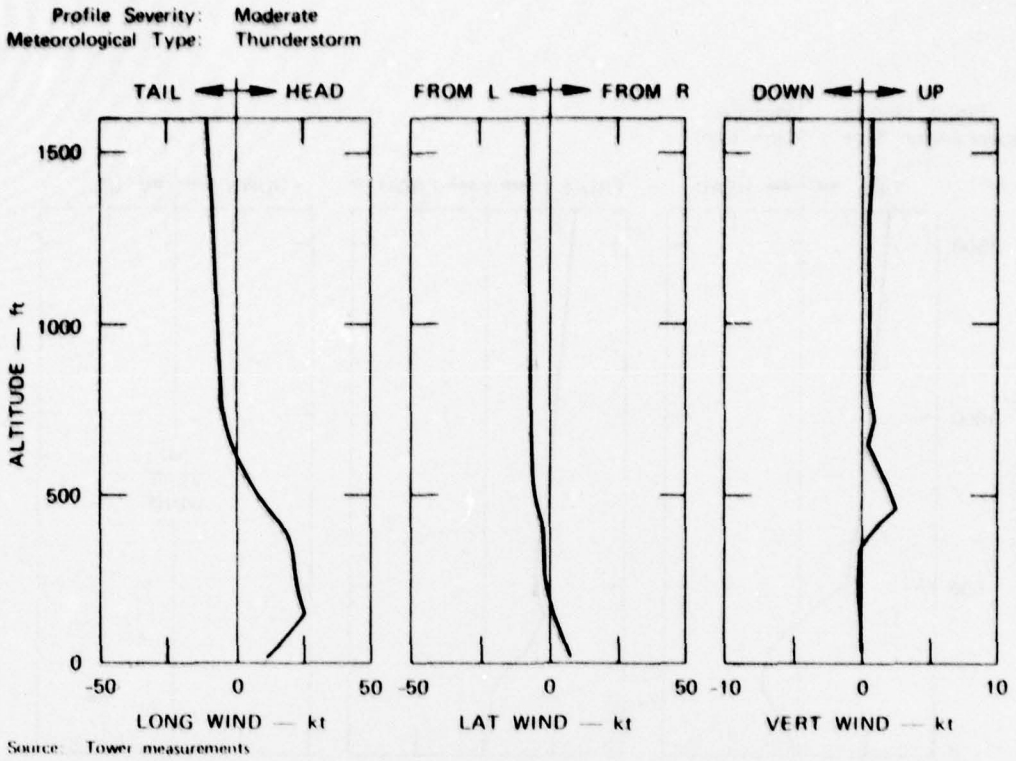

FIGURE C-7 WIND PROFILE T8A, APPROACH ON 3° GLIDE PATH

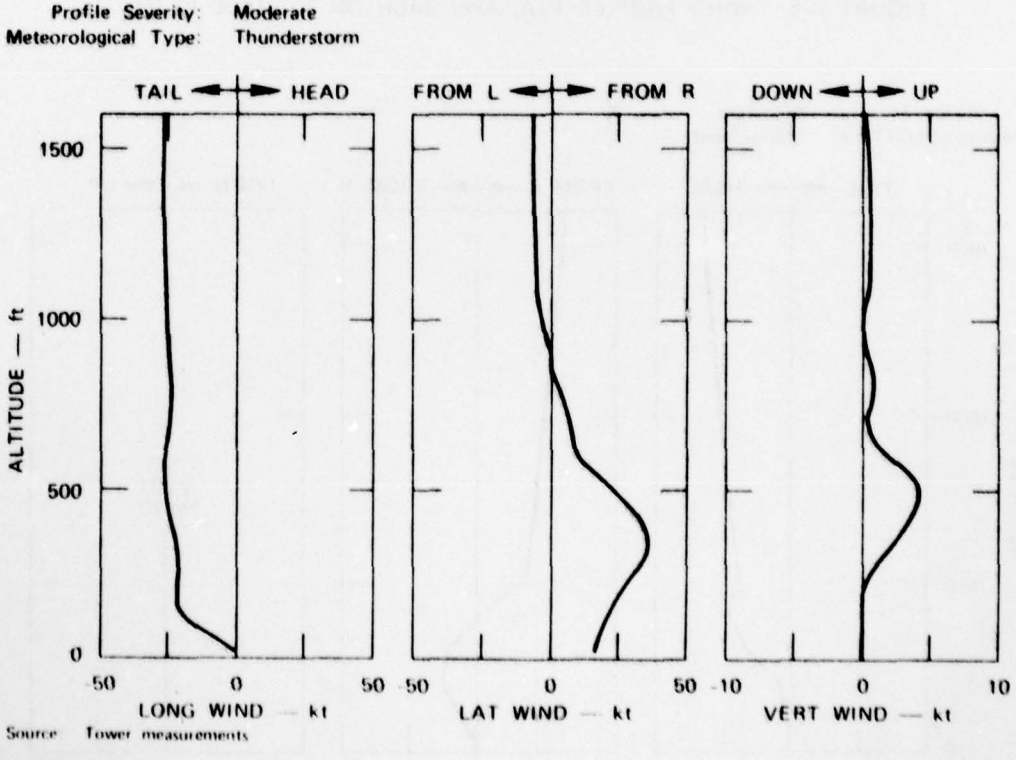

FIGURE C-8 WIND PROFILE T9A, APPROACH ON 3° GLIDE PATH

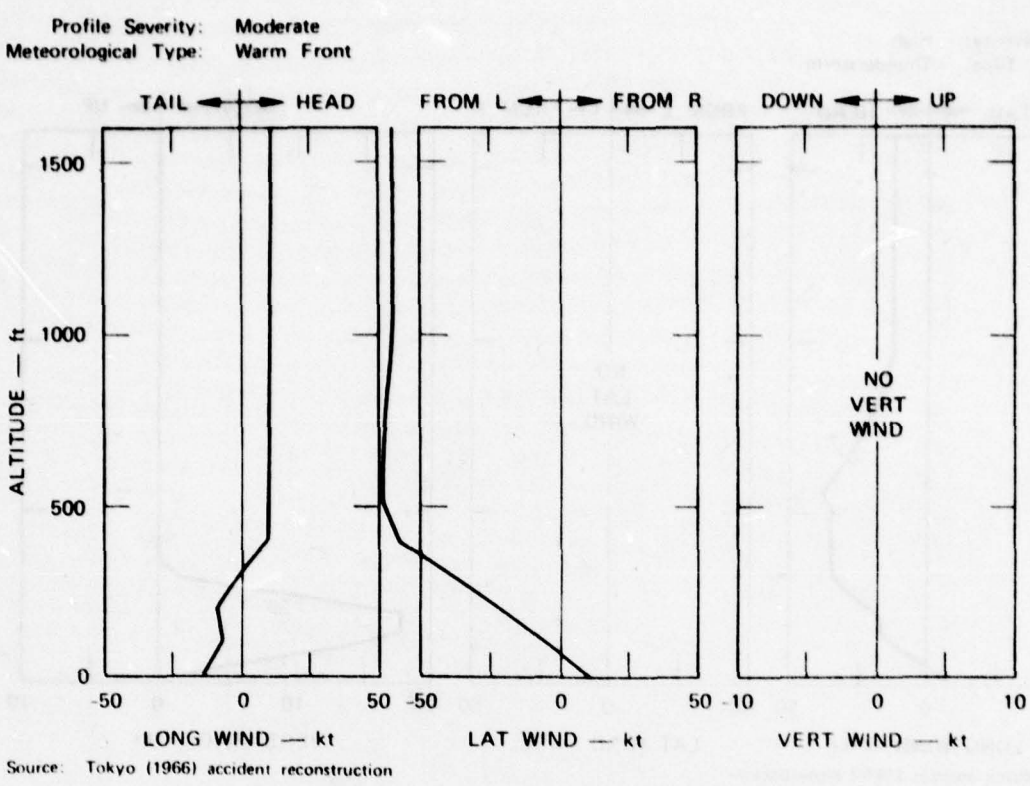

FIGURE C-9 WIND PROFILE F5A, APPROACH ON 3° GLIDE PATH

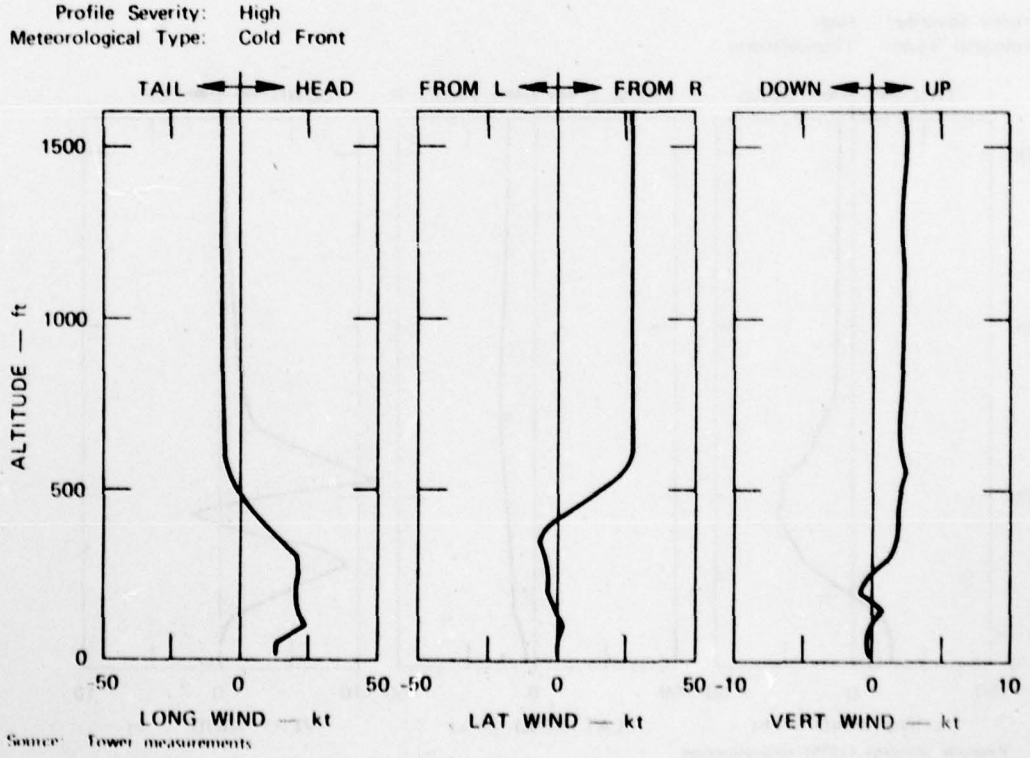

FIGURE C-10 WIND PROFILE F3A, APPROACH ON 3° GLIDE PATH

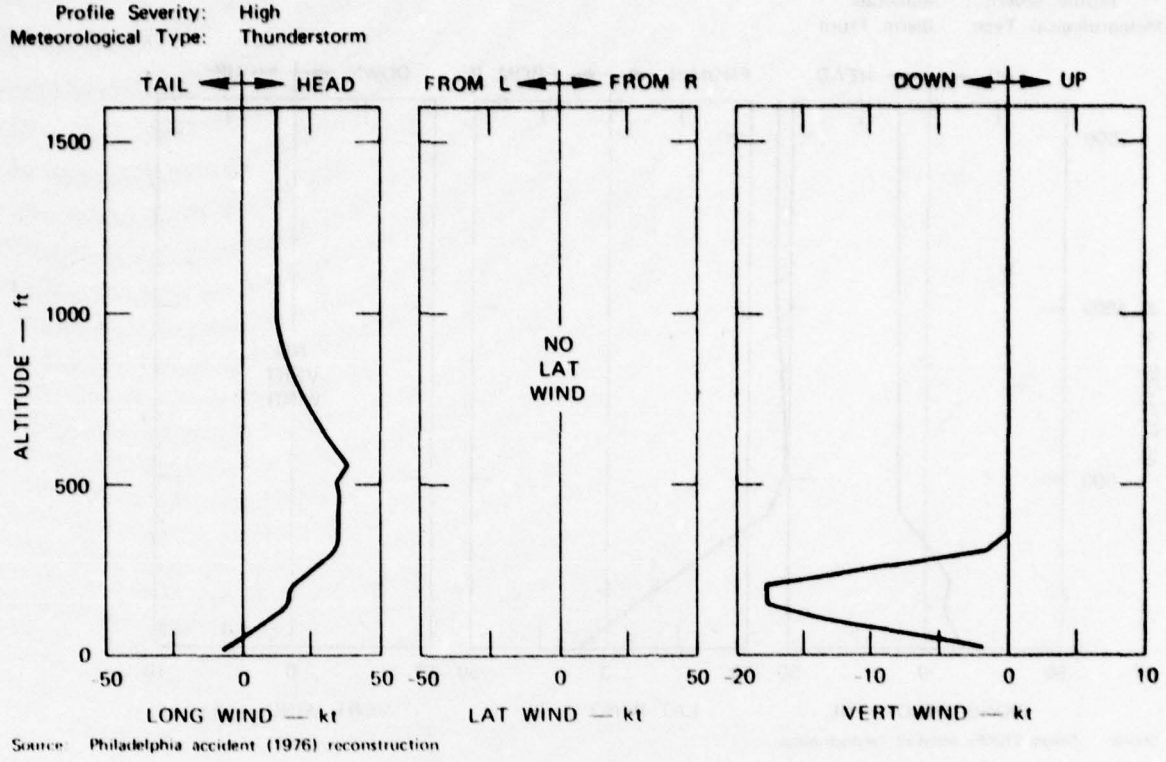

FIGURE C-11 WIND PROFILE T24A, APPROACH ON 3° GLIDE PATH

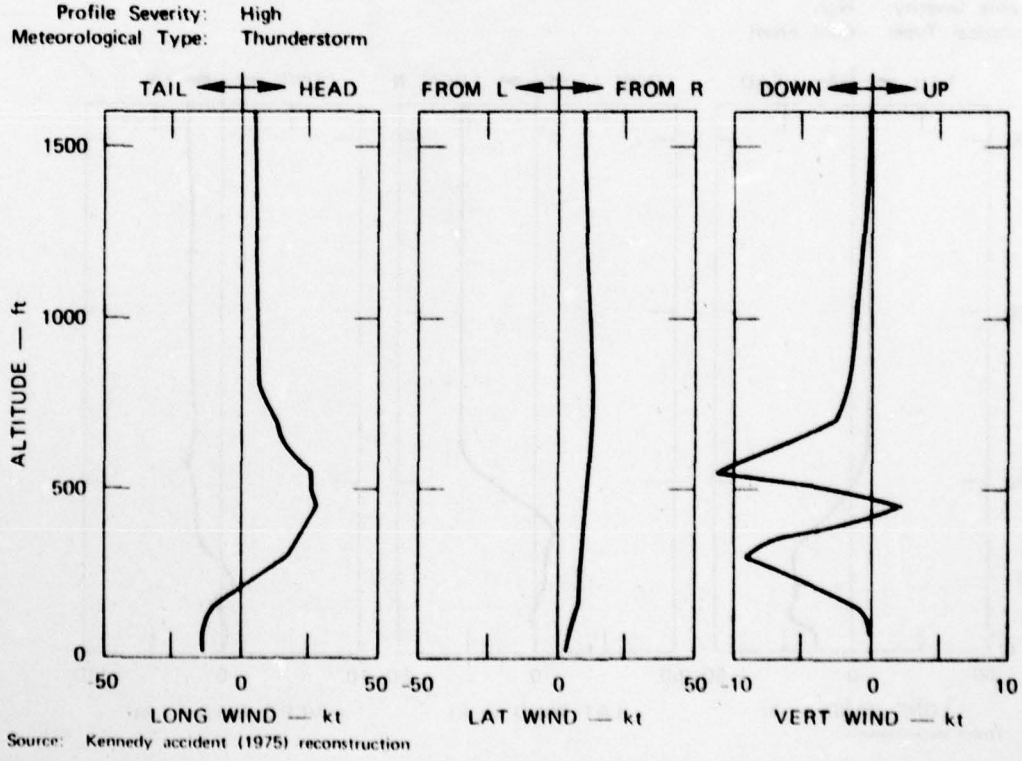

FIGURE C-12 WIND PROFILE T0A, APPROACH ON 3° GLIDE PATH

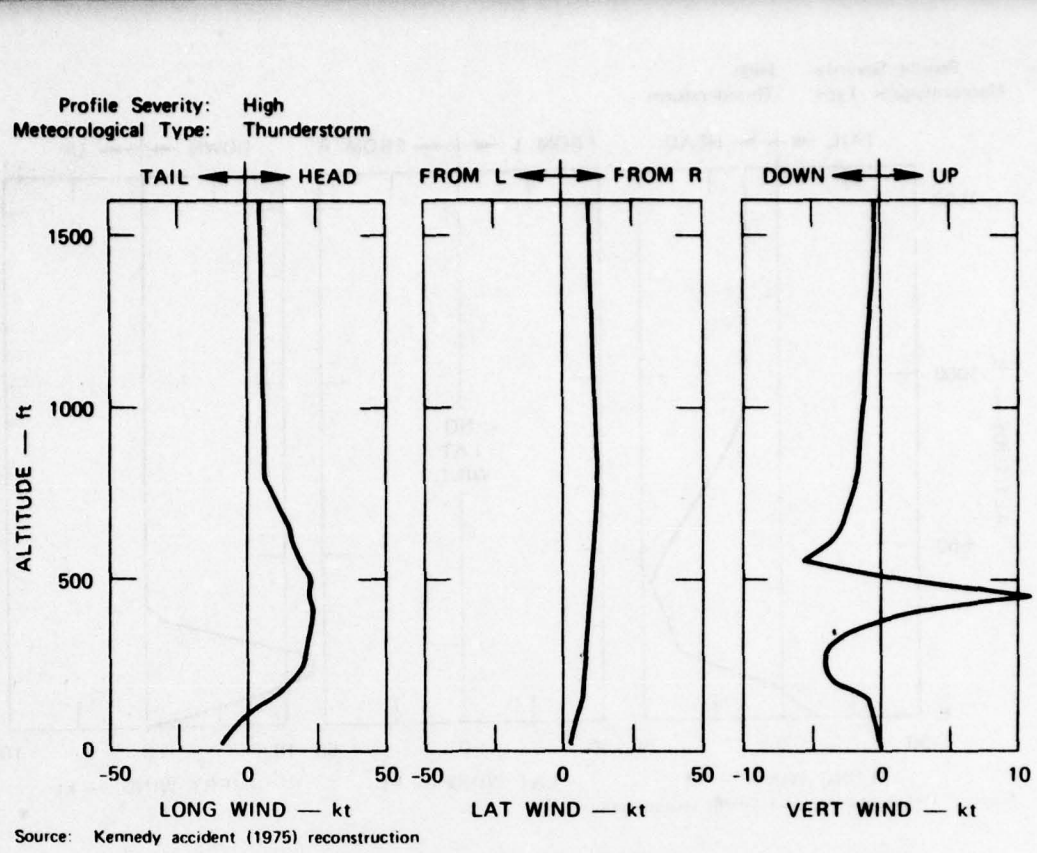

FIGURE C-13 WIND PROFILE T0B, APPROACH ON 3° GLIDE PATH

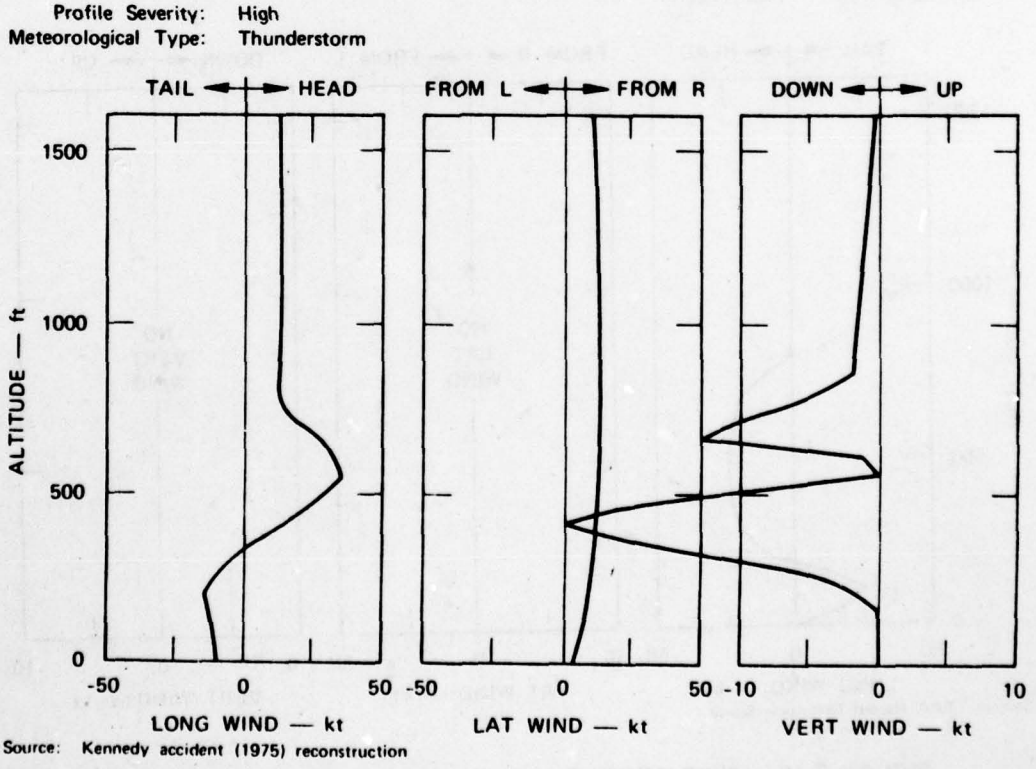

FIGURE C-14 WIND PROFILE T0C, APPROACH ON 3° GLIDE PATH

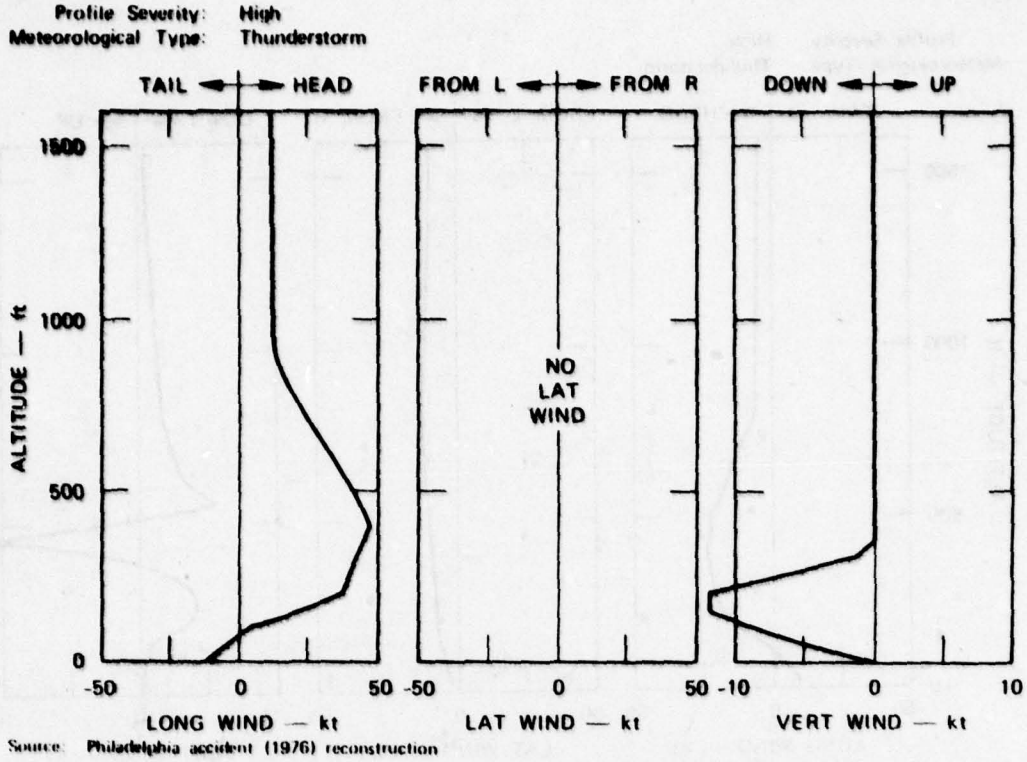

FIGURE C-15 WIND PROFILE T25A, APPROACH ON 3° GLIDE PATH

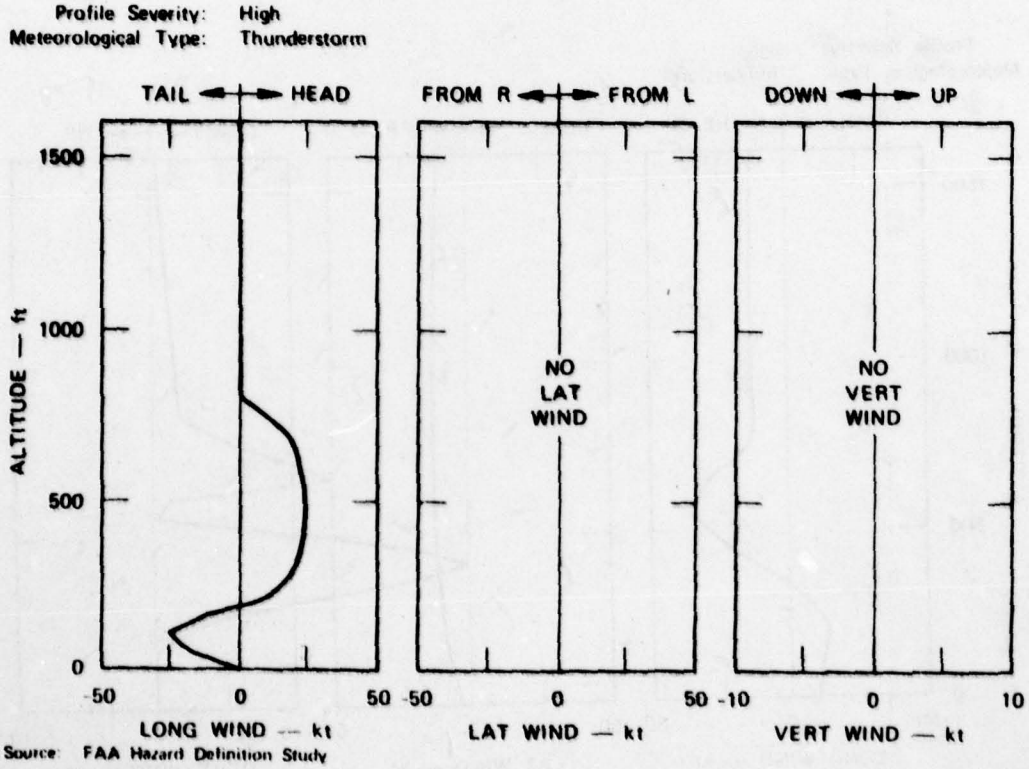

FIGURE C-16 WIND PROFILE M1A, APPROACH ON 3° GLIDE PATH

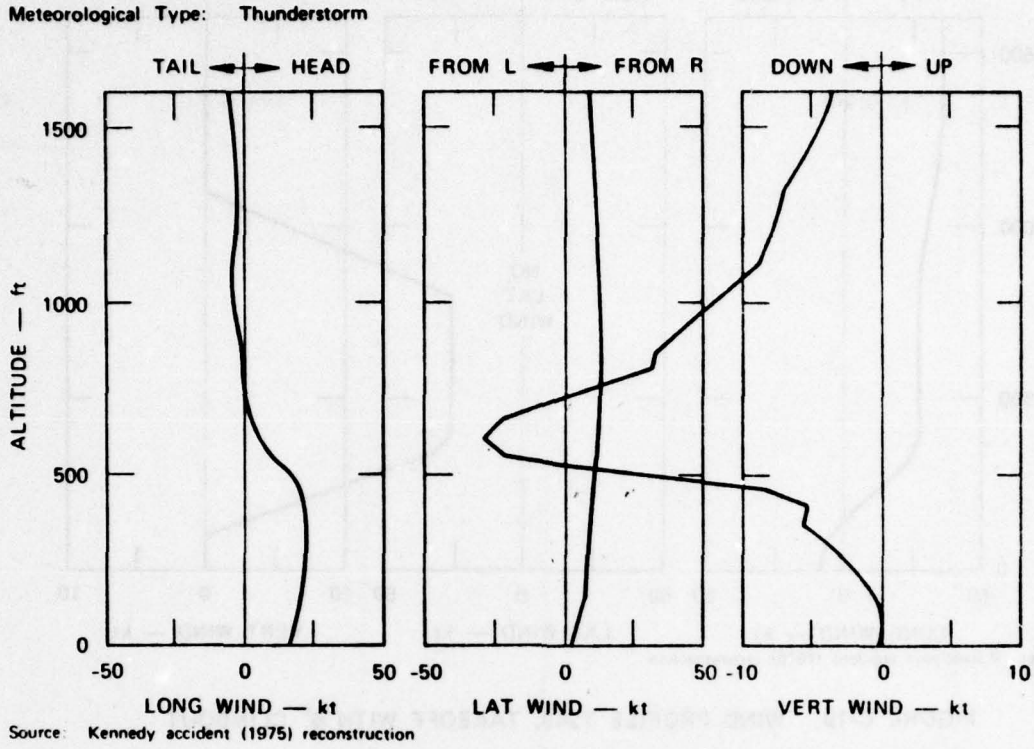

FIGURE C-17 WIND PROFILE T0D, TAKEOFF WITH 6° CLIMBOUT

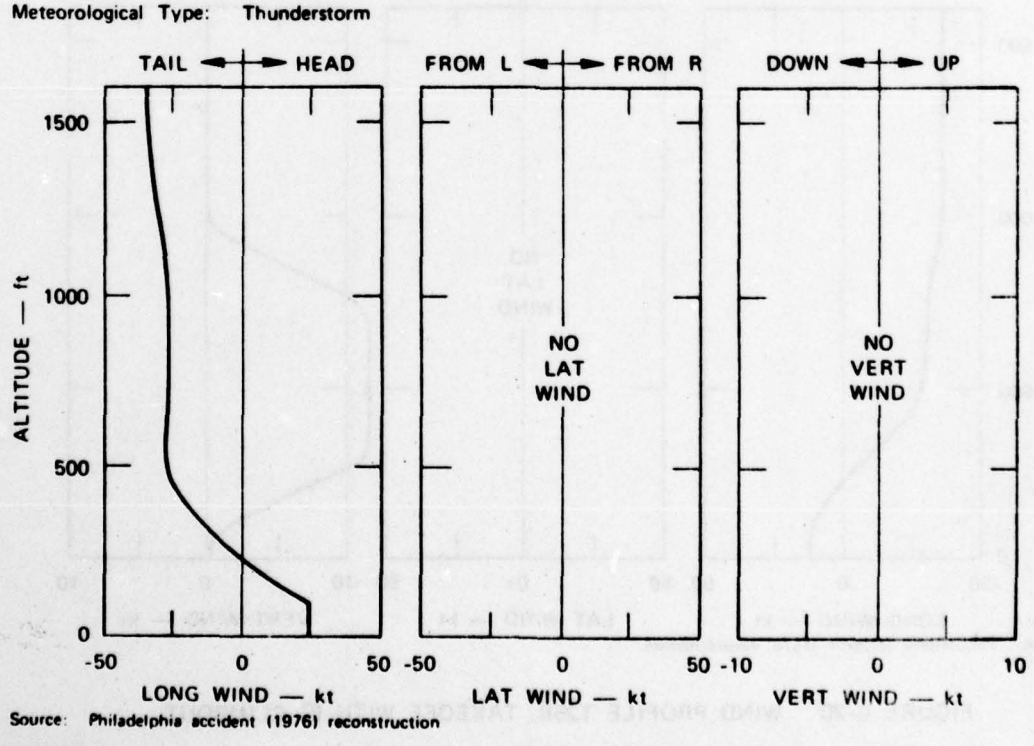

FIGURE C-18 WIND PROFILE T23A, TAKEOFF WITH 6° CLIMBOUT

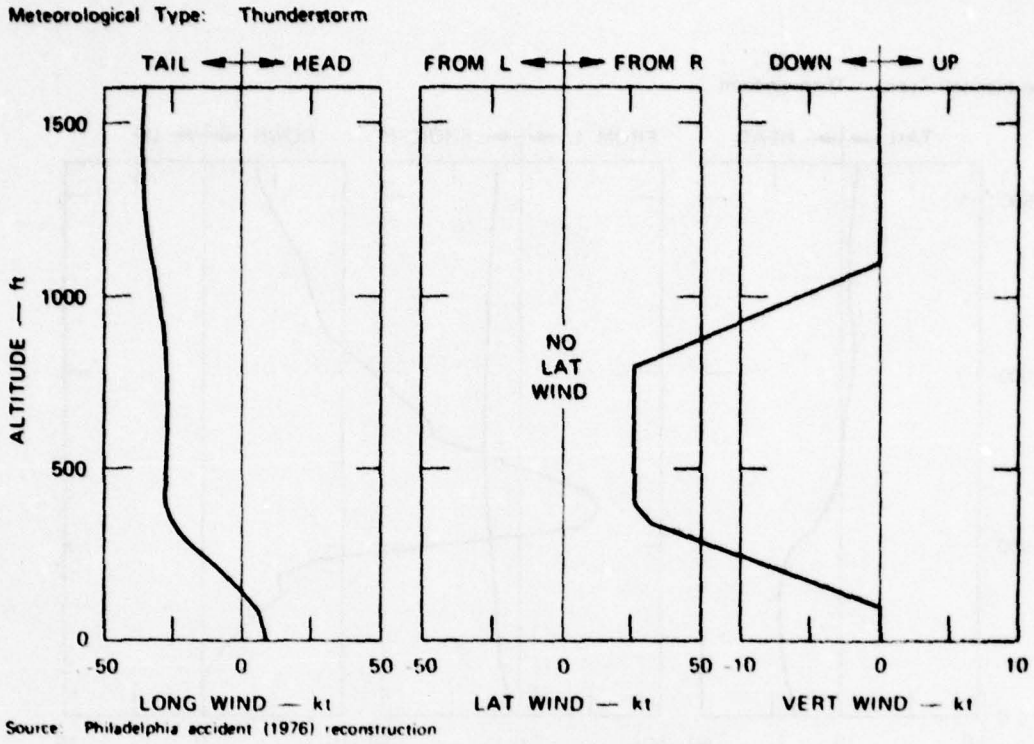

FIGURE C-19 WIND PROFILE T24B, TAKEOFF WITH 6° CLIMBOUT

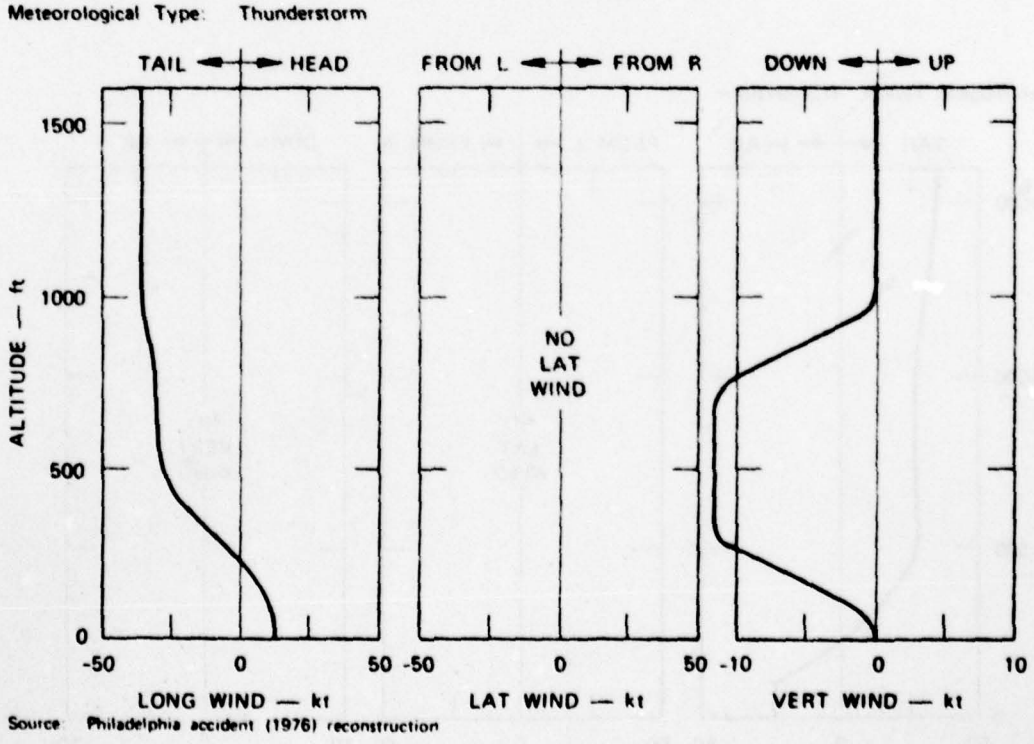

FIGURE C-20 WIND PROFILE T25B, TAKEOFF WITH 6° CLIMBOUT

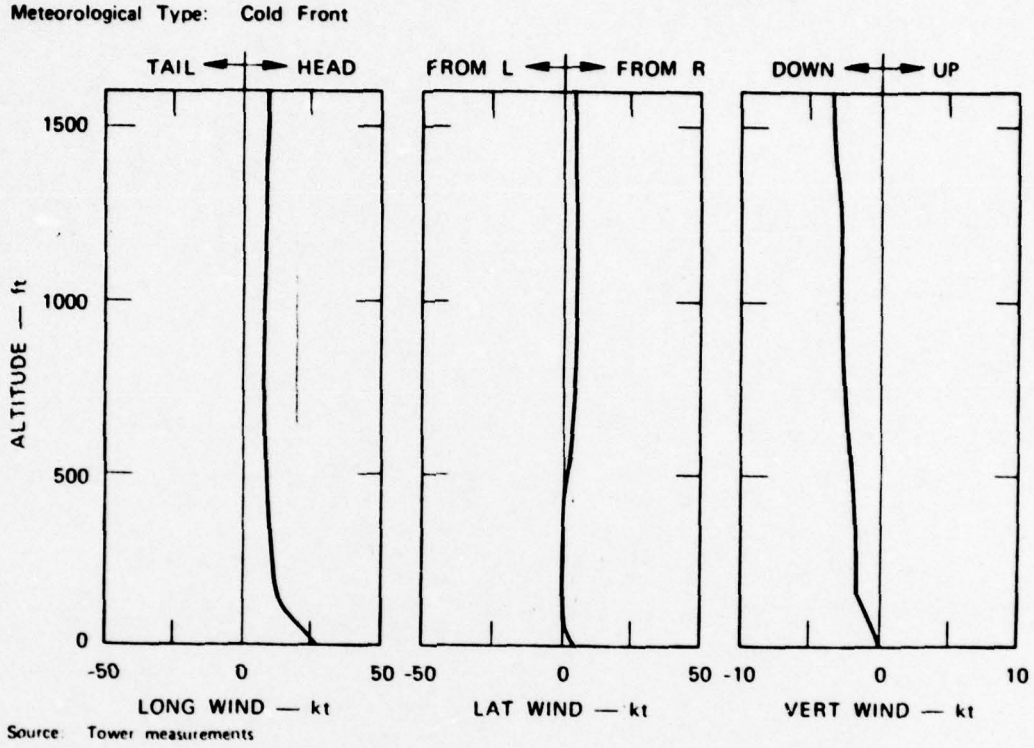

FIGURE C-21 WIND PROFILE F3B, TAKEOFF WITH 6° CLIMBOUT

APPENDIX D

CANDIDATE STANDARD WIND PROFILES

Recommended candidate standard wind profiles for system qualification are given in Table D-1. The intended use of the wind profiles is to demonstrate the ability of methods and systems that will enable the pilot to cope successfully with wind shear. Since the ability to detect and avoid potentially hazardous wind shear is essential, it is necessary to discriminate between relatively mild wind shear, which can be safely negotiated, and potentially hazardous wind shear, which should be avoided. Therefore, the candidate standard wind profiles have been selected to include a wide range of wind shear severity.

High severity wind profiles may be used to test the ability to detect and safely avoid hazardous wind conditions. The expected outcome of an approach under these conditions would be a timely and safely executed go-around, although advanced systems may also be capable of demonstrating consistent, safely negotiated landings in high-severity wind profiles. Low-severity wind profiles are relatively mild. Although some wind shear is present, it lies within the capabilities of the aircraft models tested, and can be safely negotiated. In most instances, the expected outcome of an approach in low-severity wind profiles would be a safe landing. Moderate-severity wind profiles probably represent the most dangerous wind shear conditions for the pilot because they will tempt him to land, when the most prudent choice might be to execute a go-around. The successful outcome of the approach would be either a safe landing or a well-executed go-around.

Table D-1

RECOMMENDED CANDIDATE STANDARD WIND PROFILES

Relative Wind Profile Severity	Derived Wind Profile No.	Source of Wind Data	Meteorological Wind Type
Low	N2A	Meteorological math model	Neutral Stable
	S6A	Tower measurements	
Moderate	F1A	Logan accident reconstruction	Warm Front
	T8A	Tower measurements	Thunderstorm
	T9A	Tower measurements	Thunderstorm
High	T0C	Kennedy accident reconstruction	Thunderstorm
	T25A	Philadelphia accident reconstruction	Thunderstorm

REFERENCES

1. J. K. Luers and J. B. Reeves, "Effect of Shear on Aircraft Landing," NASA CR-2287, National Aeronautics and Space Administration, Washington D.C. (1973).

2. J. R. Gerhardt, "An Example of a Nocturnal Low-level Jet Stream," Journal of the Atmospheric Sciences, Volume 19, pp. 116-118, (January 1962).

3. D. Sowa, "Low-level Wind Shear Effects on Approach and Climbout," DC Flight Approach No. 20, McDonnell Douglas Corporation, 10-7, St. Louis, Missouri (1974).

4. W. Frost and D. W. Camp, "Wind Shear Modeling for Aircraft Hazard Definition," DOT Report FAA-RD-77-36, Federal Aviation Administration, Washington D.C. (1977).

5. R. C. Goff, "Thunderstorm--Outflow Kinetics and Dynamics," NOAA Technical Memo ERL-NSSL-75, National Severe Storms Laboratory, Norman, Oklahoma (1975).

6. T. Fujita and F. Caracena, "An Analysis of Three Weather-Related Aircraft Accidents," SMRP Research Paper 145, Department of Geophysical Sciences, University of Chicago, Chicago, Illinois (1977).

7. J. T. Fujita, "Spearhead Echo and Downburst near the Approach End of a John F. Kennedy Airport Runway, New York City," SMRP Research Paper 137, Department of Geophysical Sciences, University of Chicago, Chicago, Illinois (1976).

8. N. M. Barr, D. Gangass, and D. R. Schaeffer, "Wind Models for Flight Simulation and Certification of Landing and Approach Guidance and Control Systems," Report No. FAA-RD-74-206, Contract DOT-FA72WA-2934, Boeing Commercial Airplance Co., Seattle, Washington (1974).

9. W. B. Gartner et al., "Piloted Flight Simulation Study of Low-level Wind Shear, Phase 2," Interim Report prepared for DOT by SRI International, Report No. FAA-RD-77-157, Federal Aviation Administration, Washington D.C. (March 1977).

10. "Inertially Augmented Approach Couplers--A Review of Previous Work," Prepared for SRI International Project 4364, Contract DOT-FA75WA-3650, by Collins Radio Group, Rockwell International, Cedar Rapids, Iowa (March 17, 1976).

11. R. J. Bleeg et al., "Inertially Augmented Automatic Landing System: Autopilot Performance with Imperfect ILS Beams," prepared for DOT by the Boeing Company, Report No. FAA-RD-72-22, Federal Aviation Administration, Washington D.C. (April 1972).

12. B. J. Winer, Statistical Principles in Experimental Design (McGraw-Hill Book Co., Inc., New York, New York, 1962).

13. W. B. Gartner and A. C. McTee, "Piloted Flight Simulator Study of Low-level Wind Shear, Phase 1," Intertim Report prepared for DOT by SRI International, Report No. FAA-RD-77-166, Federal Aviation Administration, Washington D.C. (May 1977).

14. K. E. Mitchell, "A Numerical Investigation of Severe Thunderstorm Gust Fronts," NASA CR-2635, National Aeronautics and Space Administration, Washington, D.C. (December 1975).

BIBLIOGRAPHY

Barad, M. L., "Low-level Jet Streams," Science American, Vol. 205, pp. 120-131 (Aug. 1961).

Blackadar, A. K., "Boundary Layer Wind Maxima and Their Significance for the Growth of Nocturnal Inversions," Bull. Am. Meteor. Soc., Vol. 38, No. 5 (May 1957).

Fichtl, G., and W. Frost, "Sources of Low-level Wind Shear Around Airports," Journal of Aircraft, Vol. 15, No. 1, pp. 5-14 (January 1977).

Gifford, F. Jr., "The Breakdown of a Low-level Inversion Studied by Means of Detailed Soundings with a Modified Radiosonde," Bull. Am. Meteor. Soc., Vol. 33, No. 9 (November 1952).

Green, G. E., et al., "Windshear Characterization," DOT Report FAA-RD-77-33, Federal Aviation Administration, Washington D.C. (1977).

"Iberia Lineas Aereas de Espana (Iberian Airlines), McDonnell-Douglas DC-10-30, EC CBN, Logan International Airport, Boston, Massachusetts, December 17, 1973," Aircraft Accident, report No. NTSB-AAR-74-14, National Transportation Safety Board.

Izumi, Y., "The Evolution of Temperature and Velocity Profiles During Breakdown of a Nocturnal Inversion and Low-level Jet," J. Appl. Meteor., Vol. 3, pp. 70-82 (February 1964).

Izumi, Y., and M. Barad, "Wind and Temperature Variations During Development of a Low-level Jet," J. Appl. Meteor., Vol. 2, pp. 668-673 (October 1963).

Izumi, Y., and H. A. Brown, "Temperature, Humidity, and Wind Variations During Dissipation of a Low-level Jet," J. Appl. Meteor., Vol. 5, pp. 36-42 (February 1966).

Kaimal, J. C., and Y. Izumi, "Vertical Velocity Fluctuations in a Nocturnal Low-level Jet," J. Appl. Meteor., Vol. 4, pp. 576-584 (October 1965).

Rider, L. T., "Low-level Jet at White Sands Missile Range," J. Appl. Meteor., Vol. 5, pp. 283-287 (June 1960).

Rider, L. T., and M. Armedariz, "Low-level Jet Winds at Green River, Utah," J. Appl. Meteor., Vol. 5, pp. 733-736 (October 1966).

Thuillier, R. H., and U. O. Lappe, "Wind and Temperature Profile Characteristics from Observations on a 1400 Foot Tower," J. Appl. Meteor., Vol. 3, pp. 299-306 (June 1964).

END